BUDAPEST UNIVERSITY OF
TECHNOLOGY AND ECONOMICS

MODELS OF NUCLEAR ALPHA CLUSTER INTERACTING WITH SUPER-INTENSE LASER FIELDS

PH.D. THESIS

AUTHOR

RÉKA SZILVÁSI

Doctoral School of Physical Sciences

BME Faculty of Natural Sciences

BUDAPEST, JANUARY 2025

This page intentionally left blank.

BUDAPEST UNIVERSITY OF
TECHNOLOGY AND ECONOMICS

MODELS OF NUCLEAR ALPHA CLUSTER INTERACTING WITH SUPER-INTENSE LASER FIELDS

PH.D. THESIS

AUTHOR

RÉKA SZILVÁSI

SUPERVISOR

DÁNIEL PÉTER KIS, PHD

BUDAPEST, JANUARY 2025

This page intentionally left blank.

Köszönetnyilvánítás

Mindenekelőtt szeretném megköszönni témavezetőmnek és mentoromnak, Dr. Kis Dániel Péternek a hét éve tartó harmonikus közös munkát, a kutatási pályám példátlan igazgatását, az értékes tanácsait, bölcs meglátásait, melyek nélkül a dolgozat a jelen formájában nem jöhetett volna létre.

Végül szeretnék köszönetet mondani édesanyámnak, édesapámnak és nagymamámnak az egyetemi hallgatói éveim alatt is szüntelen és páratlan támogatásukért és gondoskodásukért, mely lehetővé tette, hogy nyugodt körülmények mellett fókuszáljak a kutatásomra. Külön szeretném megköszönni párom szerető támogatását és kitartását.

Az erő legyen veletek!

Acknowledgements

First and foremost, I wish to thank my supervisor and mentor, Dr. Dániel Péter Kis, for seven years of cohesive collaboration, his exceptional guidance in my research career, and his invaluable advice and wise insights, without which this thesis would not have taken its present form.

Finally, I would like to express my gratitude to my beloved mother, father, and grandmother for their unwavering and unparalleled support and care throughout my university years. Their dedication made it possible for me to focus on my research in calm and stable conditions. I would also like to extend special thanks to my dearest partner for his loving support and perseverance.

May the Force be with you!

This page intentionally left blank.

Contents

This page intentionally left blank.

List of Figures

This page intentionally left blank.

List of Tables

This page intentionally left blank.

1 Introduction

Theoretical nuclear physics has witnessed substantial progress in understanding alpha decay. This process is fundamental to the study of nuclear stability and structural properties, and may have profound implications across various scientific and potentially technological domains. Theoretical models aim to refine the prediction of alpha decay half-lives, in order to facilitate a more nuanced comprehension of nuclear forces and the inter-nucleon interactions [Delion, 2010 ; Poenaru et al., 2011 ; C. Qi et al., 2009 ; Lovas et al., 1998 ; Xu et al., 2006].

Thus far, traditional Hermitian quantum mechanics has been the cornerstone of nuclear decay models [Gamow, 1928 ; Kalbermann, 2008 ; Gurvitz et al., 1987 ; Buck et al., 1992 ; Dumitrescu et al., 2023], explaining the decay by quantum tunneling, using the Gamow factor for the characterization and applying perturbative models to derive the decay width.

In their recent papers based on the monograph [N. Moiseyev, 2011] and the studies [Myo et al., 2020a ; Peskin et al., 1993], the authors suggest an alternative framework for the proper description of decaying states [Szilvasi et al., 2022] that could also apply for the study of the Coulomb tunneling of an already preformed alpha cluster (not covering nuclear structure effects) [Szilvasi et al., 2024]. In this framework, considering a two-body problem of the cluster-remaining nucleus set-up with mean-field nuclear potential, the preformed alpha cluster of the nucleus is considered to occupy a special quasi-stationary state (alpha cluster state) that is associated with the appropriate complex eigenenergy of a non-hermitian Hamiltonian. The imaginary part of the complex energy corresponds to the width and lifetime of the quasi-stationary state, the real part is associated with the alpha-energy, hence the tunneling part of the decay is characterized by a single quantity that is extracted directly and non-perturbatively from the spectrum of the non-hermitian Hamilton operator.

This peculiar method to derive the width and lifetime of alpha tunneling is also

proved to serve valuable ground for the description of laser-assisted alpha decay [Szilvasi et al., 2024]. This process has been widely investigated lately due to the Nuclear Physics division of the Extreme Light Infrastructure (ELI) project that is a promising research facility for the experimental dimension of understanding the elementary properties of nuclear processes via their interaction with some sufficiently high-intensity laser field [*Extreme Light Infrastructure (ELI)* 2011]. In view of the possible experimental actuality, there is practical ground for the theoretical investigation of laser-nuclei interactions.

Thus far, extensive literature covers the field of the theory of laser-influenced molecular and atomic systems, and certain aspects of nuclear processes in intense laser field are also studied such as, multi-photon ionization (MPI) [Wickenhauser et al., 2006 ; Wiehle et al., 2003 ; Moshammer, 2003], strong laser-induced tunneling [Wickenhauser et al., 2006 ; Faisal et al., 2005 ; Faisal et al., 2006], electron bridge processes [Kalman, 1991], internal conversion (IC) [D. Kis et al., 2010 ; Kalman et al., 1986] and nuclear alpha tunneling [Kalbermann, 2008 ; Misicu et al., 2016 ; Delion et al., 2017 ; D. Kis et al., 2018].

In [Szilvasi et al., 2024] the authors explain that the key aspect of laser-assisted alpha decay is expected to be the sole tunneling process: to leading order, the most pronounced effect of the laser field is expected in the modification of the Coulomb barrier, primarily influencing the tunneling process; the nuclear forces are not modified by the typical photon energies and intensities of such laser fields. Indeed, the issue of laser-assisted nuclear alpha decay is commonly investigated using the tunneling picture [Gamow, 1928] in the frame of the Wentzel-Kramers-Brillouin (WKB) approximation, by which a semi-classical expression of the decay width can be derived for the alpha tunneling, relying on standard (hermitian) quantum mechanics. In this case the effect of the external laser field is calculated either by time-dependent perturbation theory [Misicu et al., 2016], or is encoded in the deformations of the Coulomb potential through the Henneberger frame [Delion et al., 2017 ; D. Kis et al., 2018]. Most of the examples predict rather significant alterations in the lifetime of alpha tunneling, which gives a motivation to investigate the issue through different theoretical approaches. One such approach is the non-hermitian formalism of quantum mechanics which allows for wavefunction-centered, analytical computation techniques such as the (t,t')-perturbation calculation of time-dependent potentials affecting decaying systems.

In this thesis a specific mean-field-based, cluster-plus-remaining-nucleus model is presented, which focuses on the Coulomb-barrier-generated quasi-stationary state occupied by a singular, preformed alpha cluster with complex energy, the imaginary part of which expresses the lifetime of the state. The quasi-

stationary state is identified as an eigenstate of a non-hermitian Hamiltonian operator which possesses a complex spectrum, and the complex eigenenergy is determined through diagonalization. For the purpose of validating the computational scheme, specific isotonic chains are under investigation mainly due to the observed systematic trends and variances in their alpha decay properties that regard them as interesting material for studying the Coulomb tunneling phase of the alpha decay process.

In this study I present a theoretical model to demonstrate, through a specific calculation, how a laser pulse with extreme high peak-intensity might alter the decay width of the alpha cluster in a mean-field nuclear potential. I implement the (t,t')-perturbation theory and the non-hermitian complex spectral calculation technique to compute the laser-induced, first-order complex energy correction to the lifetime of the preformed alpha cluster in specific heavy, even-even isotonic nuclei, and analyze the sensitivity of the complex energy-shift to the parameters of the laser pulse, additionally exploring the special electrodynamic properties arising in the description of the interaction between the super-intense laser and the alpha-decaying nucleus, which become pronounced in the non-hermitian quantum mechanical model and within the non-relativistic approximation.

2

Description of decaying states by non-hermitian quantum theory

In this chapter, I present my results and conclusions about the calculation of the complex-energy shift of decaying states upon interacting with some external, time-dependent but perturbative potential. I approach this problem within the non-hermitian quantum mechanical framework and show that the change of the lifetime of various decaying states can be calculated directly from the non-Hermitian spectrum of the Hamiltonian operator describing the system.

In order to establish the context, first, I briefly review the basic ideas and principles of non-hermitian quantum mechanics regarding quasi-stationary states in the subsequent sections (Section 2.1 and Section 2.2). Section 2.3 concerns the question of time-dependent perturbations driving decaying systems. In Subsection, 2.3.1 I discuss the main aspects of the (t,t')-formalism, the method I apply in my calculations with time-dependent potentials. Subsection 2.3.2 and Section 2.4 contains the author's own results and corollaries regarding an alternative description of quasi-stationary states interacting with external, time-dependent potentials via deriving a complex-energy correction formula and exploring the properties by executing calculations on a model system.

2.1 The lifetime of quasi-stationary states

What is a quasi-stationary state? In relation to open quantum systems and specifically decay (that is purely quantum-mechanical) in which situation a system falls apart to its counterparts, one ultimately faces a non-stationary behaviour and must find a suitable quantum-mechanical method to solve the dynamical problem. A straightforward way to describe such systems is by considering the wave-pocket solutions of the time-dependent Schrödinger

equation, that is numerically quite involved most of the time. However, quantum-mechanical decay generally and naturally concerns complex energy eigenvalues.

In the next sections, in order to describe quantum-mechanical decay, I would like to discuss the peculiarities of special states that arise from solving the stationary Schrödinger equation, despite their non-stationary nature. These quasi-stationary states can be found as possible states of systems described by individual potentials (to be detailed later) which in some cases regard them as decaying systems. The potentials that are of our interest support a continuous spectrum and possess a sector of their domain that is outside the Hermitian sector. This domain is most easily reached upon assigning the appropriate boundary conditions to obtain the solutions of the stationary Srchödinger equation. It can be shown that these solutions of the non-hermitian sector are associated with complex eigenvalues. As a result one is faced with complex-energy states which requires the extension of the conventional quantum mechanical formalism to the non-hermitian approach.

The following section (Section 2.2) sets the theoretical background for the quasi-stationary description of decaying systems, discussing the related aspects of non-hermitian quantum mechanics.

2.2 The principals and aspects of non-hermitian quantum-mechanics

Quantum mechanics has quite a few postulates that were established at the dawn of the revolutionizing theory. Without listing all of them, I would like to discuss one fundamental postulate that is in the core of the non-hermitian extension of quantum mechanics.

> Any measurable dynamical quantities that are observed are the eigenvalues of operators representing the measurable quantities. Since the measurable quantities are real quantities, the representing operators should be Hermitian operators.

According to this postulate, the hermiticity requirement is imposed only in relation to real eigenvalues representing the measurables. For example, in accordance with classical mechanics, also in quantum physics the energy of a closed system is conserved thus it exhibits real eigenenergies (this energy conservation, following from Noether's theorem, refers to the time-translation invariance of such systems); in the original formalism of quantum mechanics the

energy eigenvalues of the *stationary Hamiltonian* of such a system are real, hence the Hamiltonian is regarded Hermitian. The original formulation of quantum mechanics - on the basis of the *time-independent* Schrödinger equation - is not extended to cover the problem of open quantum systems and decaying systems.

A noteworthy detail could be that the requirement for real energy eigenvalues can be fulfilled in special cases without the hermiticity of the Hamiltonian. Such a non-hermitian system possesses PT-symmetry, implying that it is robust under the parity and time-reversal transformation of the Hamiltonian[El-Ganainy et al., 2018]. The existence of this type of quantum systems underlies the hermiticity postulate of quantum-mechanics.

Furthermore, one must remember that the hermitian property of an operator is heavily dependent on the functions they operate on. If functions $u_i, u_j \in \mathcal{L}_2(\mathbb{R})$, as in they are square-integrable functions, or asymptotically periodic functions, the operator $\hat{H}$ is hermitian if the equality

$$\langle u_i|\hat{H}|u_j\rangle = \langle u_j|\hat{H}|u_i\rangle^* \tag{2.1}$$

is fulfilled (or in an equivalent form: $\langle u_i|\hat{H}|u_j\rangle = \langle \hat{H}u_i|u_j\rangle$). Hence, square-integrability is another crucial condition.

There are several possible circumstances that could render a Hamiltonian non-hermitian. One obvious case is when the Hamiltonian contains a complex local potential. The inclusion of complex potentials might arise in optical problems or in quantum field theory even when a purely imaginary external field is considered. From the viewpoint of this thesis, however, different sort of special potentials are interesting, that generate non-hermiticity in a distinct way and indirectly. These are the non-hermitian potentials that *support a continuous spectrum*. These type of potentials are crucial signatures of meta-stable, or in other words, decaying systems, as in systems that are able to break up into subsystems and hence exist for a finite amount of time. These systems are, in a sense, open systems. Several physical phenomena are characterized by meta-stable states, such as resonances, ionized states, atomic-molecular-solid state systems subjected to external fields, or radioactive alpha-decay, spontaneous fission and generally the compound nuclear reactions. Of all such phenomena those which happen via quantum-mechanical tunneling are purely quantum-mechanical. Tunneling is characteristic of subsystems that are trapped in special potentials (potential barriers) but do not have enough energy to break free. The typical trapping potential energy well is higher than the (real) energy of the subsystem but decay happens despite of that, hence are they considered in a meta-stable state. The theoretical study and description of such systems is the core subject of this thesis, particularly focusing on the description of radioactive alpha decay;

however, most considerations are also valid for resonance phenomena.

By solving the eigenvalue problem with such (non-hermitian) potentials that support a continuous spectrum, one is able to find complex-energy meta-stable states. These meta-stable states can be associated with the complex poles of the S-matrix (scattering matrix) where it is well-defined, hence they can be treated by conventional hermitian quantum mechanics, although such calculations are quite complicated, furthermore in this case the eigenfunctions associated with the complex resonance poles are embedded within the continuum solutions.

In the next subsection, however, I discuss how to associate these metastable states with special *stationary* solutions of the *time-independent* Schrödinger equation. These are obtained by imposing purely outgoing boundary conditions on the eigenfunctions of Hamiltonians with an appropriate non-hermitian potential supporting a continuous spectrum. These special solutions are meant to represent the *quasi-stationary* states. From now on, I will correspond decaying states with quasi-stationary states. The presence of quasi-stationary solutions naturally requires the extension of the hermitian quantum-mechanical formalism to a non-hermitian one, since these solutions are divergent functions of the spatial coordinate indicating they are not square-integrable functions, thus they reside beyond the hermitian sector of the domain of the Hamiltonian operator. In addition these solutions are associated with complex eigenvalues. Furthermore, it is not only conceptually required to extend quantum mechanics to a non-hermitian formulation when describing quasi-stationary states, but it is also practical especially when one attempts to perform calculations involving the wave-function of the system.

Generally, in non-hermitian quantum mechanics expectation values, such as the energy of the system, might be complex scalars. One example, apart from the energy, is the complex probability density. It is shown in the next subsection that for a quasi-stationary (decaying) state the square of the absolute value of the wave-function is a decaying function of the imaginary part of the complex energy of the state (the dynamical phase factor is complex). The imaginary part of the complex energy is associated with the decay width of the state, hence itself is a measurable quantity.

One can conclude that *by imposing special boundary conditions on the solutions of the time-independent Schrödinger equation with a non-explicitly non-hermitian Hamiltonian, one obtains extra information about the system which is not available when conventional boundary conditions are applied.* However, in Subsection 2.2.1 it is detailed that upon a special unitary transformation (Complex Scaling) the Hamiltonian of such systems can be transformed to display explicit non-hermiticity possessing a complex spectrum that can always be obtained by

diagonalization.

Two aspects are important and must be distinguished: by assigning outgoing boundary conditions the latent non-hermiticity of the Hamiltonian is uncovered; while, the non-hermiticity is an inherent property of systems with distinct potential energy terms (those supporting a continuous spectrum) that can also be invoked by transforming the problem to a different "coordinate system" by applying a Complex Scaling unitary transformation.

Nevertheless, the proper treatment of the divergence of quasi-stationary solutions is indispensable upon building models residing on expressing the wave-function of systems.

2.2.1 Wavefunction-centered description of quasi-stationary states

In this subsection I aim to particularize the nature of the wave-functions of systems in quasi-stationary states, states that are obtained by solving the time-independent Schrödinger equation by imposing outgoing boundary conditions (OBC). It is important for the purpose of performing analytical calculations covering the interaction of decaying sates with external time-dependent, perturbing potentials.

Generally, the wave-function of a quantum-mechanical system depends on some general coordinates (representing any variables belonging to physical quantities) contingent upon the degrees of freedom of the system, and it could also depend on the *time* parameter. The wave-function of a non-hermitian quasi-stationary system shall be investigated from the viewpoint of its behaviour in coordinate space and in time mainly due to the system's energy being complex.

The probability density function

The time-dependence of complex-energy systems, or as in decaying systems is an intriguing topic. One interesting aspect is the action of the time-reversal operator. The time-reversal operator is a special anti-linear operator. Since the time-reversal operation means complex conjugation and the negations of time t, the Schrödinger-equation for a state and for its time-reversed partner is the same if the Hamiltonian $\hat{H}$ commutes with the time-reversal operator $\hat{T}$. Although, due to the fact that $\hat{T}$ is anti-linear, despite commuting with $\hat{H}$ they do not necessarily share common eigenstates. Only if the energy eigenvalue (E) is *real* do the two operators share the corresponding eigenstate ($|\Phi\rangle$), as is seen by the stationary Schrödinger eigenvalue equation:

$$\hat{H}\,|\Phi\rangle = E\,|\Phi\rangle\,, \tag{2.2}$$

$$\hat{T}\hat{H}\,|\Phi\rangle = \hat{H}(\hat{T}\,|\Phi\rangle) = E^*(\hat{T}\,|\Phi\rangle). \tag{2.3}$$

From the second equation it is clearly seen that when E is complex, the eigenstate $|\Phi\rangle$ is not time-reversal symmetric, because the time-reversed partner has a different eigenvalue. But this eigenvalue only differs by complex conjugation, which suggests that for an eigenstate of the Hamiltonian having a complex eigenvalue there exists a time-reversed partner with complex conjugate eigenvalue. Altogether we might conclude that the eigenstate with complex energy breaks the time-reversal symmetry. For non-hermitian, non-PT-symmetric systems there are complex eigenvalues, and even though the Schrödinger equation has time-reversal symmetry, the complex-energy eigenstates do not respect this symmetry. There are cases when the TRS-breaking eigenstates appear together with their time-reversed (complex-conjugate energy) partner, hence restoring the time-reversal symmetry of the problem. In the literature they are conventionally called *resonance* and *anti-resonance* states with complex energy $E_{\text{res}} = \mathfrak{R}(E_{\text{res}}) + \mathrm{i}\mathfrak{I}(E_{\text{res}}) = E_{\text{r}} - \frac{\mathrm{i}}{2}\Gamma$, and its complex conjugate energy $E_{\text{anti}} = \mathfrak{R}(E_{\text{anti}}) + \mathrm{i}\mathfrak{I}(E_{\text{anti}}) = E_{\text{ar}} + \frac{\mathrm{i}}{2}\Gamma$. By this expression it is clear that the pair possesses complex conjugate energies, however Γ denotes the width of resonance-type states (or the width of quasi-stationary states) that is going to be explored later.

Writing the probability density of the system (assuming the separability of the spatial and time-dependent parts), one finds the followings for the resonant solutions:

$$\|\Phi(\mathbf{q},t)\|^2 = \|\phi(\mathbf{q})\|^2 \mathrm{e}^{(-\mathrm{i}E_{\text{res}} + \mathrm{i}E^*_{\text{res}})t} = \|\phi(\mathbf{q})\|^2 \mathrm{e}^{-\Gamma t}, \tag{2.4}$$

while for the anti-resonant solutions

$$\|\Phi(\mathbf{q},t)\|^2 = \phi(\mathbf{q})\|^2 \mathrm{e}^{(-\mathrm{i}E_{\text{anti}} + \mathrm{i}E^*_{\text{anti}})t} = \|\phi(\mathbf{q})\|^2 \mathrm{e}^{+\Gamma t}. \tag{2.5}$$

The form of the probability density function indicates the non-stationary nature of both states. In equation (2.4) the factor $\mathrm{e}^{-\Gamma t}$ grants that the probability of finding the state at time t in $\mathbf{q}$ exponentially decreases, referring to decay. These type of solutions are interesting in the context of the kind of hermiticity discussed in this thesis, namely when the non-hermitian domain is approached by assigning the special boundary conditions to our problems. The two different situations of complex-energy states (resonance-type and anti-resonance-type) can be obtained by imposing two different boundary conditions on the solutions of the time-independent Schrödinger-equation. Anti-resonances are present

when incoming boundary conditions are imposed, resonance-type or decaying states are obtained upon assigning outgoing boundary conditions. I consider the latter case, and refer to these states as quasi-stationary states (or decaying states interchangeably), as mentioned previously.

Outgoing boundary conditions

The assignment of the boundary conditions strongly relates to the properties of the spatial part of the eigenfunction of a non-hermitian system having complex eigenenergy. From the perspective of the spatial coordinate-dependence, due to the complex nature of the energy eigenvalues corresponding to decaying states, these states, in coordinate representation, are asymptotically divergent functions of the spatial coordinate.

To perform calculations with the quasi-stationary states, one has to cure the divergence that occur in the coordinates. The occurrence of the asymptotic divergence of resonance states is a general trait of a quantum system that is subject to outgoing boundary conditions. Since the bounded state will in finite time leave the physical space where the bounding potential dominates, and it can always be represented at large distances from the center of the bounded system by outgoing plane waves. This is clearly seen on a one dimensional example of a particle temporarily trapped in a finite potential barrier and subjected to outgoing boundary conditions. It decays with a lifetime encoded in the corresponding complex energy:

$$E_1 = E_{1\mathrm{r}} + \mathrm{i}\Im(E_1) = E_{1\mathrm{r}} - \frac{\mathrm{i}}{2}\Gamma, \tag{2.6}$$

Γ is the width of the resonance state, which is related to the life-time of the particle. This E_1 complex energy shall be expressed with the corresponding complex argument (arctan $\left(\frac{-\Im(E_1)}{\Re(E_1)}\right)$), that shall be called the *resonance angle* θ_{res} for resonances and decaying states, that is:

$$\theta_{\mathrm{res}} = \arctan\left(\frac{-\Gamma}{2E_{1\mathrm{r}}}\right). \tag{2.7}$$

One can see that this is a negative quantity. The corresponding asymptotic wavefunction is expressed with the energy through the wavenumber (k), which also becomes complex:

$$k \in \mathfrak{R} \longrightarrow k_{\mathrm{res}} = |k|\mathrm{e}^{\mathrm{i}\theta^k_{\mathrm{res}}} \in \mathbb{C}, \tag{2.8}$$

where the θ^k_{res} is the complex argument of the resonance wavenumber, that is $\theta^k_{\mathrm{res}} = \frac{\theta_{\mathrm{res}}}{2}$.

If one takes a look at the asymptotic solution with a boundary constant (C), one finds that it is no longer a plane wave but becomes a divergent function, the so called Gamow-Siegert function [Siegert, 1939]:

$$\varphi_{\text{res}} = Ce^{\mathrm{i}k_{\text{res}}x} = C\mathrm{e}^{\mathrm{i}|k|\mathrm{e}^{\mathrm{i}\theta^k_{\text{res}}}x}. \tag{2.9}$$

Taking into account the argument about the expression of the resonance angle, the divergent nature of the asymptotic wavefunction is clearly seen:

$$C\mathrm{e}^{\mathrm{i}k_{\text{res}}x} = C\mathrm{e}^{\mathrm{i}|k|\mathrm{e}^{\mathrm{i}\theta^k_{\text{res}}}x} = C\mathrm{e}^{\mathrm{i}k\cos(\theta^k_{\text{res}})x}\mathrm{e}^{\mathrm{i}k\mathrm{i}\sin(\theta^k_{\text{res}})x} = C\mathrm{e}^{\mathrm{i}k\zeta x}\mathrm{e}^{k\eta x}, \tag{2.10}$$

where $\zeta \equiv \cos(\theta^k_{\text{res}}) > 0$ and $\eta \equiv -\sin(\theta^k_{\text{res}}) > 0$. Clearly, the first term stands for the plane wave part and the second term, in fact, diverges.

Complex scaling and the c-product

There can be found a thorough study with regard to the possible treatments of the asymptotically divergent Gamow-Siegert functions (for instance by complex absorbing potentials [Jolicard et al., 1985 ; Muga, 2004]), that arise in atomic and molecular physics, in the monograph by [N. Moiseyev, 2011].

In this study, however, the Complex Scaling (CS) transformation is applied to handle the divergence of the quasi-stationary solutions. This is a global coordinate (q) transformation of the form :

$$\mathbf{q} \rightarrow \mathbf{q}e^{i\theta}, \tag{2.11}$$

that for real θ (θ is considered a rotational angle), esentially rotates the complex plane of wavenumbers by a global phase θ (although this interpretation is not entirely accurate, see [Csótó et al., 1990]). This transformation is a type of special similarity transformations serving to regularize the divergent wavefunctions ($\hat{S}$). The new coordinates obtained by the CS-transformation could be considered as the natural coordinate system of non-Hermitian problems. This technique is extensively elaborated in several articles related to molecular physical calculations [Chu et al., 2004b ; Elander et al., 1998 ; Morales et al., 2006 ; McCurdy et al., 1997 ; Rescigno et al., 1997 ; Bengtsson et al., 2008a ; Horner et al., 2007]. The nuanced mathematical background of complex scaling is discussed in [N. Moiseyev, 2011] and is over-viewed in Appendix A. The complex-scaling operator is generally defined as

$$\hat{S} = \mathrm{e}^{\mathrm{i}\theta q\frac{\partial}{\partial q}}, \tag{2.12}$$

and has the simple effect on any function f of the coordinate q:

$$\hat{S}f(q) = f(q\mathrm{e}^{\mathrm{i}\theta}). \tag{2.13}$$

According to this, it is easy to see that the divergent Gamow-Siegert functions become bounded (and square integrable) due to the effect of the complex scaling transformation. The action of the complex scaling transformation on the φ_{res} Gamow-Siegert function is the following:

$$\hat{S}\varphi_{\text{res}} = C\mathrm{e}^{\mathrm{i}k\mathrm{e}^{\mathrm{i}\theta^k_{\text{res}}}q\mathrm{e}^{\mathrm{i}\theta}} = C\mathrm{e}^{\mathrm{i}kq\mathrm{e}^{\mathrm{i}(\theta^k_{\text{res}}+\theta)}} = C\mathrm{e}^{\mathrm{i}kq\mathrm{e}^{\mathrm{i}(\theta-|\theta^k_{\text{res}}|)}} = C\mathrm{e}^{\mathrm{i}kq\mathrm{i}\tilde{\zeta}}\cdot\mathrm{e}^{\mathrm{i}kq\tilde{\eta}} = C\mathrm{e}^{-k\tilde{\zeta}q}\cdot\mathrm{e}^{\mathrm{i}k\tilde{\eta}q}, \tag{2.14}$$

where the variables $\tilde{\zeta}$ and $\tilde{\eta}$ are defined as:

$$\sin(\theta - |\theta^k_{\text{res}}|) \equiv \tilde{\zeta}, \tag{2.15}$$

$$\cos(\theta - |\theta^k_{\text{res}}|) \equiv \tilde{\eta}. \tag{2.16}$$

In the expression above k is a real quantity (the absolute value of the wavenumber), therefore the second term in the last line of (2.14) represents a plane wave, while the first term is of decaying nature (for $x \to \infty$) if and only if $\tilde{\zeta} > 0$. The last condition is crucial, since it defines a lower bound for the complex-scaling angle (remember that $\theta^k_{\text{res}} = \frac{\theta_{\text{res}}}{2}$):

$$2\theta > |\theta_{\text{res}}|. \tag{2.17}$$

By the CS transformation of the Gamow-Siegert function with the appropriate scaling angle θ, it becomes a bounded and square-integrable function. By wrods, only those complex-energy states that belong to resonance angles smaller than 2θ in the complex-energy plane get regularized and, simultaneously, get uncovered in the complex discrete spectrum. Illustratively, by rotating the 2θ-line one essentially "dust-off" the complex-energy plane to reveal the discrete resonance energies and erase the divergence of the solutions.

In addition to cure the divergence of the asymptotic wave-function, the essence of the CS-transformation carried out on the original time-independent Schrödinger equation is that the non-Hermiticity of the decaying problem is captured in such a way, that the spectrum of the complex scaled non-Hermitian Hamiltonian is complemented by discrete resonances with complex eigenenergies. As it was meticulously proven in the work of Moiseyev [N. Moiseyev, 2011] in regards of molecular physics, in the non-Hermitian quantum framework these resonances are allowed to be treated in a mathematically equivalent way as the bound states are - for example using the complex variational principle or spectral calculations - , one only needs to solve the complex-scaled Schrödinger-equation (for the three different types of eigenvalues: the complex resonances (E_r), the bound state energies (E_b) or the continuous scattering energies (E_c)):

$$\hat{H}^\theta\Phi^\theta(\mathbf{r}) = E_{\text{r,b,c}}\Phi^\theta(\mathbf{r}), \tag{2.18}$$

where $\hat{H}^\theta = \hat{S}\hat{H}\hat{S}^{-1}$ is the complex scaled Hamiltonian and $\Phi^\theta(\mathbf{r}) = \hat{S}\Phi(\mathbf{r}) = \Phi(\mathbf{r}e^{i\theta})$ is the complex scaled wavefunction in coordinate representation.

According to the Aguilar–Balslev–Combes (ABC) theorem [Balslev et al., 1971 ; Aguilar et al., 1971], the complete spectrum of the complex scaled non-Hermitian Hamiltonian contains the bound state energies of the original unscaled Hamiltonian, that are - in an ideal case - independent of the choice of θ (they are robust against the transformation, this set retains unchanged in the spectrum). The continuum state energies, although, gets rotated by 2θ in the complex energy plane. The theorem says that the continuum energies define a 2θ line, they have a complex argument of 2θ, but the physical resonances might appear in the spectrum above the 2θ line. By an appropriate choice of θ the resonances get uncovered, hence the number of resonances depends on the scaling angle. However, as we will show by numerical examples in Section 2.4, these statements hold exactly only when one is able to find the exact solutions to the time-independent complex-scaled Schrödinger equation, and if the potential is dilation-analytic which is not always guaranteed even for the simplest cases.

Since the complex scaling of the Schrödinger equation results in a non-Hermitian eigenvalue problem, the standard scalar product definition does not hold anymore. To ensure square integrability, it requires the introduction of a generalized inner product of a non-Hermitian theory, the *c-product*. The c-product is defined through the eigenstates of a non-Hermitian operator in a similar way as the standard scalar product is defined with the bra and ket states of a Hermitian operator. The properties of this inner product are discussed in detail in the relevant chapters of the book of Moiseyev [Nimrod Moiseyev, 2011]. Here, we only mention that the c-product is defined through the left and right eigenvectors of the non-Hermitian operator in its matrix representation. Although, the decaying problems considered here are special eigenvalue problems, the corresponding Hamiltonian operators are represented by complex symmetric matrices for which the left and right eigenvectors are the same. With respect to the c-product the resonance eigenfunctions of the complex scaled non-Hermitian Hamiltonian of the decaying system are square-integrable, hence the norm *can* be defined:

$$\int_{allspace} dV\Phi(q)\Phi(q) = \big(\Phi(q)|\Phi(q)\big)\,. \tag{2.19}$$

The ultimate purpose of this study is to precisely investigate three dimensional nuclear decay problems with rather complicated nuclear potentials by the method of complex scaling. Generally for these nuclear potentials of more complicated structure, the Schrödinger equation (with or without complex scaling) cannot be solved exactly. Although, these could be investigated numerically with

discretization methods by implementing the *complex spectral calculation scheme* instead of assigning boundary conditions.

Complex spectral calculation: discretization of the problem

After complex scaling the time-independent Schrödinger equation:

$$\hat{H}_0^\theta \Phi^\theta(\mathbf{r}) = E_0 \Phi^\theta(\mathbf{r}) \tag{2.20}$$

is now defined to include quasi-stationary states as singular and non-divergent eigenstates of $\hat{H}_0^\theta$ with complex eigenvalues. The spectrum of the complex-scaled Hamiltonian contains bound states, complex-energy resonance-type states and the "θ-rotated" continuum. How to obtain these solutions and the total complex-energy spectra?

Generally, finding the exact solution to equation (2.20) for arbitrary non-Hermitian $V(\mathbf{r})$ potentials is not possible, but it can be approximated, for instance by discretization methods, numerically. By the complex spectral calculation, after complex scaling, with an appropriate (not necessarily orthonormal) set of square-integrable basis functions one might find the discretized *total* spectrum of the non-Hermitian operator containing bound-state energies, complex resonance energies and the rotated discretized continuum energies. This method is also beneficial for determining nuclear resonances as it is discussed in [Myo et al., 2020a ; Myo et al., 2020b]. The expanded wave-function is the following with the number of basis functions N, the θ-dependent expansion coefficients c_j^θ and the square-integrable basis functions denoted by $w_j(r)$:

$$\Phi^\theta(\mathbf{r}) \approx \sum_{j=1}^{N} c_j^\theta w_j(\mathbf{r}). \tag{2.21}$$

The Hamiltonian matrix elements are expressed with the basis functions:

$$H_{ij}^\theta = \langle w_i | \hat{H}^\theta | w_j \rangle \,. \tag{2.22}$$

We emphasize, that if we were able to find the exact solutions, the ABC theorem [Aguilar et al., 1971 ; Balslev et al., 1971] would hold exactly and the bound energies would be independent of θ and only the *number* of resonances would depend on the scaling angle, while the continuum energies would fit exactly a line rotated by 2θ. The convergence of the approximate solution to the exact one depends on the number of basis functions, as a matter of fact. The eigenvalues of equation (2.20) are approximately given by the spectra of the Hamiltonian matrix H_{ij}^θ, furthermore the eigenvectors of H_{ij}^θ give the expansion coefficients c_j^θ in formula (2.21).

To conclude, the singular-state decay problem is non-hermitian due to the specific (real) potential energy supporting a continuous spectrum for which proper boundary conditions can be imposed to find diverging quasi-stationary solutions and to move the dynamical problem to the non-hermitian domain, but the interesting properties, stemming from this type of non-hermiticity, are exposed by the complex scaling transformation of the stationary Schrödinger equation. This renders the Hamiltonian operator of the system explicitly non-hermitian and allows for the identification of the quasi-stationary solution with a singular, square-integrable eigenfunction of the complex-scaled Hamiltonian, the complex eigenenergy of which can be found by conventional discretization methods.

2.3 Quasi-stationary states driven by time-dependent perturbative potentials

Above, I explained the need for the non-hermitian treatment of decay phenomena and introduced the essential concepts regarding the wavefunction-centered description of quasi-stationary states. Up until now, I considered spontaneous decay without explicit time-dependence of the Schrödinger equation of the decaying system. This section is concerned with the proper practice of describing the interaction of some time-dependent potential with decaying systems in the non-hermitian frame, by discussing one specific direction to solve the time-dependent problem, that is the novel (t,t')-formalism.

2.3.1 The (t,t')-formalism

One particular *analytical* approach to investigate - in a wavefunction-centered way - specific time-dependent potential-driven decays is the (t,t')-formalism. By this novel method one diverts the time-dependent problem to a "time"-independent one in a generalized, extended Hilbert space, hence allowing for the mathematical tools of perturbation calculations formulated for time-independent cases. This formalism can be generalized for non-Hermitian cases [Bengtsson et al., 2008b]. The formalism was originally developed for time-periodic problems in scattering theory (Floquet-formalism) but it was generalized for arbitrary time-dependence also [Chu et al., 2004a]. In this subsection I attempt to briefly summarize the main aspect of the (t,t')-method.

In essence, the formalism puts the time *parameter* of the evolution equation to a different role in a generalized Hilbert space (extended Hilbert space $\mathcal{H}_{ext}$) by

regarding it as an extra *coordinate* there. The extended Hilbert space is the tensor product space of the original Hilbert space $\mathcal{H}$ of square integrable functions with respect to the spatial variable and an extra Hilbert space $\mathcal{H}_t$ containing square integrable functions with respect to a *coordinate* t:

$$\mathcal{H}_{ext} = \mathcal{H} \otimes \mathcal{H}_{t'}, \tag{2.23}$$

where the t symbol stands for the *time coordinate*.

In this extended Hilbert space the original time-dependent Schrödinger-equation could be viewed as a 'time'-independent one, considering 'time' (t') as the evolution parameter in the extended Hilbert space, hence producing us the required stationary formulas. This idea is in the spirit of the method.

For a given element of the extended Hilbert space in coordinate representation $\tilde{\Phi}(q,t)$ the square integrability with respect to all the coordinates (the general coordinates q and t), in the standard norm sense:

$$\langle\langle\tilde{\Phi}_\alpha|\tilde{\Phi}_\beta\rangle\rangle = \int_{-\infty}^{\infty} \mathrm{d}t \int_{allspace} \mathrm{d}V \tilde{\Phi}^*_\alpha(q,t)\tilde{\Phi}_\beta(q,t) < \infty. \tag{2.24}$$

This is, of course, can be formulated with respect to the c-norm when dealing with the eigenfunctions of non-Hermitian operators (with left and right eigenfunctions $\tilde{\Phi}^{L\theta}_\alpha(q,t)$, $\tilde{\Phi}^{R\theta}_\beta(q,t)$):

$$((\tilde{\Phi}^\theta_\alpha|\tilde{\Phi}^\theta_\beta)) = \int_{-\infty}^{\infty} \mathrm{d}t \int_{allspace} \mathrm{d}V \tilde{\Phi}^{L\theta}_\alpha(q,t)\tilde{\Phi}^{R\theta}_\beta(q,t) = \delta_{\alpha\beta}. \tag{2.25}$$

Such doubly square-integrable functions from the extended Hilbert space are, for instance, the eigenfunctions of the Floquet-type operator $\hat{H}_F$:

$$\hat{H}_F(q,t) = \hat{H}(q,t) - i\hbar\frac{\partial}{\partial t} \tag{2.26}$$

which is now considered t'-independent [Pfeifer et al., 1983], where t' is the *evolution parameter* on the extended Hilbert space. The corresponding Floquet-type eigenvalue equation with the ε Floquet-type eigenenergy:

$$\hat{H}_F(q,t)\tilde{\Phi}(q,t) = \varepsilon\tilde{\Phi}(q,t). \tag{2.27}$$

$\hat{H}(q,t)$ is the original Hamiltonian of the original Schrödinger equation with the progress parameter t (that is regarded as a coordinate in $\mathcal{H}_{ext}$)

$$i\hbar\frac{\partial}{\partial t}\Psi^\theta(q,t) = \hat{H}(q,t)\Psi(q,t). \tag{2.28}$$

where $\Psi(q,t) \in \mathcal{H}$ is the solution of the original problem that we would like to obtain.

$\hat{H}_F(q,t)$ is the generator of the t' (quantum) time evolution in the extended Hilbert space:

$$i\hbar\frac{\partial}{\partial t'}\chi(t';q,t) = \hat{H}_F\chi^\theta(t';q,t), \tag{2.29}$$

As it was proved in [Pfeifer et al., 1983], *if* the stationary ($t' = 0$) solutions of this equation (the Floquet-type eigenfunctions $\tilde{\Phi}(q,t)$) exactly satisfy the original t-dependent Schrödinger equation, then upon the projection $t' \equiv t$ $\chi^\theta(t';q,t)$ yields the solution $\Psi(q,t)$ of the original problem [Peskin et al., 1993]. As it is anticipated, for $\varepsilon = 0$ it gives the same result as the solution of the t'-progress equation in the extended Hilbert space when projected to the original Hilbert space ($t' \equiv t$).

Altogether, to obtain the time-dependent solutions of the original problem, one should solve the Floquet-type eigenvalue equation. However, it was found, that this gives the *exact* time-dependent solutions *if and only if* the original Hamiltonian is time-independent, otherwise it is an approximation. Hereby, it must be emphasized that the advantage of this formalism is that approximation tools of time-independent problems, such as the time-independent perturbation theory, can be utilized *formally* to solve time-dependent ones thus reducing the strong dependence of the results on numerical solvers needed for calculating the dynamics. In the next subsection the formally time-independent (first-order) perturbation calculation will be presented in regards of the Floquet-type eigenenergy.

A remarkable property of the (t,t')-perturbation calculation is that it is exclusively applicable for quasi-stationary states, as in states which decay in time.

2.3.2 Derivation of the complex energy-correction formula

This subsection is dedicated to present the author's analytical result concerning the first-order (t,t')-perturbative complex energy-correction formula for time-dependently perturbed decaying systems. This formula is the fundamental original result of this thesis.

Take a specific time-independent non-Hermitian Hamiltonian $\hat{H}_0$ representing the decaying system which is perturbed by a time-dependent potential $\hat{H}_I(\mathrm{t})$, the time evolution of the whole system is described by the general Schrödinger equation:

$$\mathrm{i}\hbar\frac{\partial}{\partial t}\Psi(\mathbf{r},t) = \hat{H}(\mathrm{t})\Psi(\mathbf{r},t), \tag{2.30}$$

where the total Hamiltonian is $\hat{H}(\mathrm{t}) = \hat{H}_0 + \hat{H}_I(\mathrm{t})$. The non-perturbed system includes a spherical potential $V(\mathrm{r})$ with characteristic properties that makes $\hat{H}_0$ non-Hermitian, therefore the spectrum of the Hamiltonian contains complex eigenvalues, as mentioned above. The corresponding states are quasi-stationary states of the basic non-perturbed system, we will address these in the following way:

$$\hat{H}_0\Phi(\mathbf{r}) = E_0\Phi(\mathbf{r}), \tag{2.31}$$

where $E_0 = E_{0r} - \frac{\mathrm{i}}{2}\Gamma$ is the complex eigenenergy. One of the interesting questions is how the complex energy eigenvalues might be altered in the presence of a time-dependent external potential $\hat{H}_I(\mathrm{t})$?

After solving the eigenvalue problem of the time-independent system by the Complex Scaling transformation and the complex spectral calculation scheme, as it is thoroughly explored in Subsection 2.2.1, and obtaining the stationary solutions, the focus shall be placed on acquiring the full time-dependent solution of (2.30). As we focus only on the quasi-stationary states one shall apply the CS-transformation on equation (2.30) also in order to keep the states regularized:

$$\mathrm{i}\hbar\frac{\partial}{\partial t}\Psi^\theta(\mathbf{r},t) = \hat{H}^\theta(\mathbf{r},t)\Psi^\theta(\mathbf{r},t), \tag{2.32}$$

where the CS-transformed Hamiltonian is $\hat{H}^\theta(t) = \hat{H}_0^\theta + \hat{H}_I^\theta(\mathrm{t})$. An additional increment of situations with regard to quasi-stationary states (non-Hermitian problems), is the applicability of the (t,t')-formalism, which diverts the time-dependent problem to a 'time'-independent one in a generalized, extended Hilbert space, hence allowing for the mathematical tools of perturbation calculations formulated for time-independent cases. If the wave function $\Psi^\theta(\mathbf{r},t)$ describes a quasi-stationary state then the time dependent part of $\Psi^\theta(\mathbf{r},t)$ is regularized and could indeed be normalized, because in this case the energy is complex. Therefore the Hilbert space of the non-Hermitian system can be extended with the time parameter t by regarding it as an extra coordinate there. The expanded Hilbert space is a tensor product space of the original Hilbert space $\mathcal{H}$ of square-integrable functions with respect to the spatial variable and an extra Hilbert space $\mathcal{H}_\mathrm{t}$ containing square-integrable functions with respect to a coordinate t.

The CS-transformed Schrödinger equation (2.32) can be rearranged according to the (t,t')-formalism:

$$0 = [\hat{H}_\mathrm{F}^\theta(t) + \hat{H}_I^\theta(\mathbf{r},t)]\Psi^\theta(\mathbf{r},t), \tag{2.33}$$

where

$$\hat{H}_\mathrm{F}^\theta(t) = \hat{H}_0^\theta(\mathbf{r}) - \mathrm{i}\hbar\frac{\partial}{\partial t} \tag{2.34}$$

is the Floquet-type operator of a complex symmetric Hamiltonian in the expanded Hilbert space. Now $\hat{H}_I^\theta(\mathbf{r}, t)$ is considered as a perturbation, hence in leading order equation (2.33) corresponds to the eigenvalue equation of the $\hat{H}_F^\theta(t)$ operator when the Floquet-type eigenvalue is equal to zero ($\varepsilon = 0$):

$$\hat{H}_F^\theta(t)\tilde{\Phi}^\theta(\mathbf{r}, t) = \varepsilon\tilde{\Phi}^\theta(\mathbf{r}, t). \tag{2.35}$$

The eigenvalue equation (2.35) can be solved by the Fourier-method combined with the complex spectral calculation. Equation (2.35) can be separated with respect to the coordinates $\mathbf{r}$, t:

$$\frac{1}{\Phi^\theta(\mathbf{r})}\hat{H}_0^\theta(\mathbf{r})\Phi^\theta(\mathbf{r}) - \frac{1}{\varphi(t)}i\hbar\frac{\partial}{\partial t}\varphi(t) = \varepsilon, \tag{2.36}$$

which can only be satisfied if the two terms on the left equal the constants $E_0 - E_2$, respectively, giving two solvable differential equations. The choice of the constant E_0 is, of course, due to the fact that the first term on the left side of (2.36) is the unperturbed original eigenvalue equation, that has already been solved, while E_2 is just a not necessarily real constant. Hence the Floquet eigenvalue is $\varepsilon = E_0 - E_2$ and the Floquet-type eigenfunction can be written as:

$$\tilde{\Phi}^\theta(\mathbf{r}, t) = \Phi^\theta(\mathbf{r})\varphi(t). \tag{2.37}$$

After substituting the single solutions, one obtains the following expression (with $E_2 = E_0 - \varepsilon$):

$$\begin{aligned}\tilde{\Phi}^\theta(\mathbf{r}, t) &= \mathcal{N}e^{-\frac{i}{\hbar}(E_0-\varepsilon)t}\Phi^\theta(\mathbf{r}) \\ &= \mathcal{N}e^{-\frac{i}{\hbar}(E_{0r}-\varepsilon)t}e^{-\frac{\Gamma}{2\hbar}t'}\Phi^\theta(\mathbf{r}),\end{aligned} \tag{2.38}$$

where $\mathcal{N} = ((\tilde{\Phi}^\theta(\mathbf{r}, t)|\tilde{\Phi}^\theta(\mathbf{r}, t)))$ is the *complex* normalization factor of the complex-scaled eigenfunctions in the extended Hilbert space which comes from equation (2.25), and E_0 corresponds the eigenvalue of $\hat{H}_0^\theta$, in equation (2.20). This one exactly solves the original t-dependent Schrödinger equation for $\varepsilon = 0$. As it is anticipated, for $\varepsilon = 0$ it gives the same result as the solution of the t'-progress equation in the extended Hilbert space when projected to the original Hilbert space ($[t \equiv t']$):

$$\begin{aligned}\chi_0^\theta(t'; \mathbf{r}, t)|_{t'\equiv t} &= \mathcal{N}e^{-\frac{i}{\hbar}}\Phi^\theta(\mathbf{r})\varphi(t) \\ &= \mathcal{N}e^{-\frac{i}{\hbar}(E_0-E_2)[t'\equiv t]}e^{-\frac{i}{\hbar}E_2}\Phi^\theta(\mathbf{r}) \\ &= \mathcal{N}e^{-\frac{i}{\hbar}E_0[t'\equiv t]}\Phi^\theta(\mathbf{r})\end{aligned} \tag{2.39}$$

So, the (t,t')-method is, in fact, exact for the unperturbed problem. The presence of the interaction term alters the Floquet-type eigenenergy and intuitively the

change in the Floquet-type energy gives the shift in the E_0 complex energy. The formally time-independent perturbation calculation is performed with the unperturbed Floquet-type eigenfunction having the variable t as a coordinate.

In the special case when the perturbation only depends on t and not on the position coordinate, the Floquet-type eigenfunction can be expanded in the basis of the time-independent problem. For spherically symmetric problems (for which the time-independent quasi-stationary solution can be separated into radial and angular parts: $\Phi^\theta(\mathbf{r}) = \Phi^\theta(r)Y_{\ell,m}(\Omega)$, where $Y_{\ell,m}(\Omega)$ are the spherical harmonics of order ℓ) and with expression (2.21), the solutions can be written in the following way:

$$\tilde{\Phi}^\theta(\mathbf{r},t) = \mathcal{N}\sum_{j=1}^{N} \mathrm{e}^{-\frac{i}{\hbar}(E_0-\varepsilon)t}\tilde{c}_j^\theta w_j(r)Y_{\ell,m}(\Omega), \tag{2.40}$$

where ε must be zero and $Y_{\ell,m}(\Omega)$ denote the spherical harmonics which are due to the spherical potential $V(r)$ (certainly $Y_{\ell,m}(\Omega)$ is a constant in s-wave approximation).

Finally, as it was mentioned above, $\hat{H}_I^\theta(\mathrm{r},\mathrm{t})$ is considered as a perturbation, the effect of which on the unperturbed system can be formally approximated by time-independent perturbation formalism in the framework of the (t,t')-formalism. Accordingly, the first-order energy correction yields

$$\begin{aligned}\varepsilon^{(1)} &= ((\tilde{\Phi}^\theta(\mathbf{r},t)|\hat{H}_I^\theta|\tilde{\Phi}^\theta(\mathbf{r},t))) = \\ &= \mathcal{N}^2\int_0^\infty \mathrm{d}t\mathrm{e}^{-\frac{\Gamma}{\hbar}t}\left(\Phi^\theta(\mathbf{r})|\hat{H}_I^\theta(\mathbf{r},t)|\Phi^\theta(\mathbf{r})\right),\end{aligned} \tag{2.41}$$

where $\Phi^\theta(\mathbf{r}) = \sum_{j=1}^{N}\tilde{c}_j^\theta u_j(r)Y_{\ell,m}(\Omega)$. The derived equation (2.41) is one of the most important results of the thesis where the real and imaginary parts of $\varepsilon^{(1)}$ divided by E_{0r} or Γ yield the relative change caused by the time-dependent perturbation in the real eigenenergy shift and essentially in the shift of the width of the decaying state.

2.4 Model calculation for a particle trapped in a Gaussian potential well subjected to pulse-type drivings

This section is concerned with the aim to emphasize the generality of the merged formalism of non-Hermitian quantum theory and the (t,t')-formalism. This section conatains the author's own numerical results. In the followings a toy model is presented to demonstrate how the above formulated theoretical considerations shall be applied in practical calculations. Nevertheless, ultimately this methodology is proved to be applicable for suitably chosen mean field potentials which could describe alpha-decay processes in nuclei, that is the fundamental purpose of this thesis.

Now, let us consider a time-independent Hamiltonian that represents a spherically symmetric bound system with a Gaussian potential well. Due to the potential, the system could possess quasi-stationary states, one of which is occupied by a particle of reduced mass m. The time-independent, unperturbed, complex-scaled Hamiltonian takes the following form:

$$\hat{H}_0^\theta(r) = \frac{-\hbar^2}{2m} \mathrm{e}^{-2i\theta} \left(\frac{1}{r} \frac{\mathrm{d}^2}{\mathrm{d}r^2} r \right) + V_{\mathrm{kG}}(r\mathrm{e}^{i\theta}), \tag{2.42}$$

where $\frac{\hbar^2}{2m} = \frac{1}{2}$ MeVfm^2, the potential $V_{k\mathrm{G}}(r)$ is a Gaussian potential with arbitrary parameters $A_k, B_k, C_k, D_k, (k = 1, 2)$ introduced in [Csótó et al., 1990]:

$$V_{k\mathrm{G}}(r) = -A_k e^{-C_k e^{2i\theta} r^2} + B_k e^{-D_k e^{2i\theta} r^2}. \tag{2.43}$$

At first, the $\theta = 0$ case is considered, which, in fact, is the original Hamiltonian that represents the physical system before complex scaling. The discretized spectrum of the unperturbed time-independent Hamiltonian is obtained by diagonalization (2.22). The radial part of the wavefunction $u^\theta(r)$ is expanded in terms of a harmonic oscillator basis (Csótó et al., 1990) with oscillator parameter b, for the $l = 0$ case:

$$u^\theta(r) = \sum_{j=0}^{N} c_j^\theta \frac{1}{r} e^{-\frac{r^2}{2b^2}} \mathcal{L}_j^{1/2}(r^2/b^2) \frac{1}{b^{3/2}} \left[\frac{2\Gamma(j+1)}{\Gamma(j+3/2)} \right]^{1/2}, \tag{2.44}$$

where N is the number of basis functions used, $\mathcal{L}_j^{1/2}$ is the j-th Laguerre polynomial and Γ is the gamma function. The θ-dependent expansion coefficients c_j are determined by complex variational calculations. The unscaled spectrum is depicted in the underlying Figure 2.1.

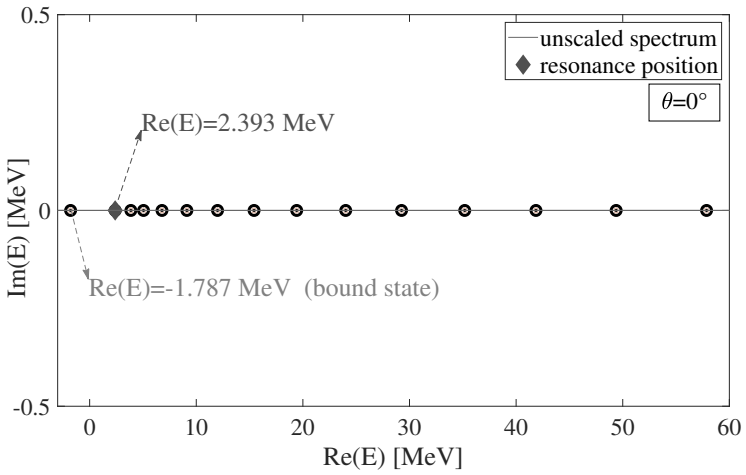

Figure 2.1: *Real spectrum of the Hamiltonian with potential $V_{2G}(r)$ with $\theta = 0°$ and $b = 0.51$. The specific parameters of potential $V_{2G}(r)$ are the followings: $A_2 = 15$, $B_2 = 12$, $C_2 = 0.3$ and $D_2 = 0.1$.*

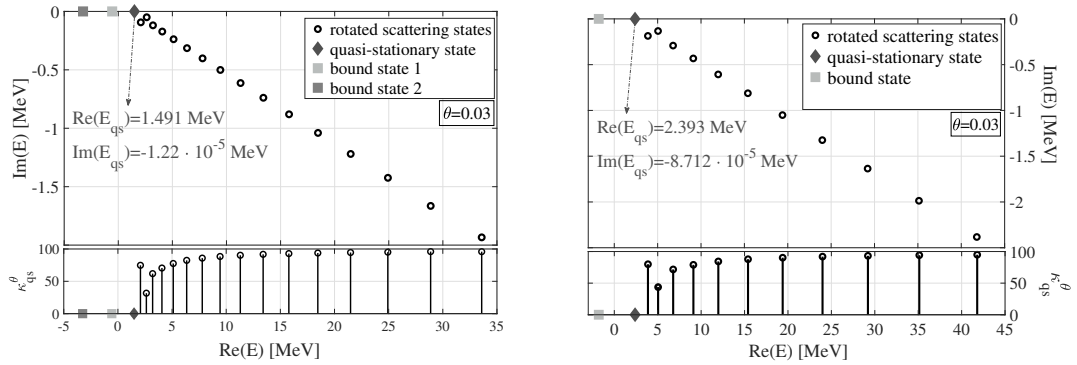

Figure 2.2: *Complex non-Hermitian spectra of the Hamiltonian with potential $V_{1G}(r)$ (a) and $V_{2G}(r)$ (b) choosing the scaling angle as $\theta = 0.03$, the number of basis functions as $N = 20$, while the oscillator parameters are $b = 0.9$ for potential $V_{1G}(r)$ (the specific parameters for potential $V_{1G}(r)$ are: $A_1 = 8$, $B_1 = 4$, $C_1 = 0.16$ and $D_1 = 0.02$.) and $b = 0.51$ for potential $V_{2G}(r)$. The lower subfigures emphasize the relative deviation of the discrete eigenvalues from the 2θ-line $\kappa_\theta^{qs} = \left(\frac{-\theta_{qs}}{\theta} \cdot 100\right)$.*

We find, that the spectrum of the unscaled operator possesses one bound state and discretized continuum states with real, positive energy eigenvalues. One particular positive eigenvalue is highlighted in Figure 2.1 at real energy $\mathrm{Re}(E) = 2.393$ MeV. In the followings we will show that this eigenenergy corresponds to a quasi-stationary state of the system, after the problem is rotated to its natural coordinate system upon performing the complex scaling transformation. This procedure uncovers the imaginary part of the eigenenergy in the spectrum which corresponds to the finite lifetime of the state.

After the CS-transformation, applying the complex spectral calculus, the complete spectrum of the non-Hermitian Hamiltonian is achieved as it is shown in Figure 2.2 for the two different potential models in equation (2.43). In the subfigures, the $\kappa_\theta^{\mathrm{qs}} = \left(\frac{-\theta_{\mathrm{qs}}}{\theta} \cdot 100\right)$ ratio indicates the necessary deviations of the complex-scaled (rotated) continuum energies from the 2θ-line. This discrepancy is due to the finite basis the wavefunction is expanded on. The spectra in Figure 2.2 are achieved by setting the number of basis functions $N = 20$, as the results already show convergence for such amount of basis functions. As it is anticipated, the convergence fastens by using larger scaling parameters θ, although for potentials containing exponential functions θ should be chosen carefully in order to avoid oscillations appearing in the transformed potential. For our purpose, a relatively small scaling angle is sufficient, since we are looking for quasi-stationary states with widths (Γ) many orders of magnitude smaller than those of molecular resonances. For $\theta = 0.03$ the convergence is fast enough for both potential shapes however, the unwanted oscillations are not yet present. Nevertheless, the bound-state energies and the energies corresponding to quasi-stationary states are robust to the choice of θ as long as it does not exceed the critical range ($\theta < \frac{\pi}{4}$) [Myo et al., 2020b] and so long as the harmonic oscillator basis function expansion coefficient b is chosen appropriately. By relatively higher values of b the lower-energy spectrum is obtained with higher accuracy, although for smaller values of b the high-energy part is described well and the basis functions are not adequate to approximate sufficiently the quasi-stationary solutions that should appear at lower energies.

After the quasi-stationary states and the complex eigenvalues of the decaying system are obtained by the CS-transformation and the complex spectral calculus, the situation when the system is coupled to an external time-dependent potential field can be investigated properly with the (t,t')-formalism as explained in Subsection 2.3.2. Consider a plain time-dependent potential with Gaussian anharmonic time-dependence:

$$\hat{H}_I^\theta(\mathbf{r}, t) = V_I^\theta(t) = A_0 \cos\left(\frac{\zeta t}{\hbar}\right) \mathrm{e}^{-\left(\frac{\zeta}{\sigma\hbar} t\right)^2}, \tag{2.45}$$

where $\zeta/\hbar$ is the frequency of the potential, A_0 is the amplitude of the external potential and σ is the width of Gaussian envelope function.

When the system is coupled to the external time-dependent potential with Gaussian anharmonic time-dependence, one expects the lifetime of the quasi-stationary state to decrease, so at the same time, the width shall increase. In the followings, we present our first-order perturbative results (applying equation (2.41)) with regard to the modifications the width and the lifetime suffer due to the presence of the perturbative external potential, in the case of the two different potential models. In (2.41) the integration with respect to the *time coordinate* is performed over the whole coordinate space. The normalization factor $\mathcal{N}$ is computed by the use of the spectral calculation method in the extended Hilbert space (applying equation (2.25)). Performing the integration in the energy correction (2.41) for the specific external potential (2.45), one obtains the following analytical closed-form expression (for the physically motivated case of $\frac{\Gamma}{\zeta} << \sigma$):

$$\begin{aligned} \varepsilon^{(1)} &= \frac{\mathcal{N}^2}{4} A_0 \sqrt{\pi} \frac{\sigma}{\zeta} \mathrm{e}^{\frac{1}{4}\left(\frac{\Gamma^2}{\zeta^2}-1\right)\sigma^2} \cdot \\ &\cdot \left[\mathrm{e}^{-\mathrm{i}\frac{\Gamma\sigma^2}{2\zeta}} \left(1 + \mathrm{i} \cdot \mathrm{erfi}\left(\frac{\sigma}{2}\right)\right) + \mathrm{e}^{\mathrm{i}\frac{\Gamma\sigma^2}{2\zeta}} \left(1 - \mathrm{i} \cdot \mathrm{erfi}\left(\frac{\sigma}{2}\right)\right) \right], \end{aligned} \tag{2.46}$$

where $\mathrm{erfi}(x)$ denotes the imaginary error function. In order to emphasize that the time-dependent, interactive potential could indeed be considered as a perturbation, the relative change of the real part of the energy eigenvalues are depicted in Figure 2.4 and Figure 2.5. Since the ratio of the perturbed and unperturbed lifetimes serves as an appropriate measure of the effect of the external potential, some numerical values of the relative change of the widths are summarized in Table 2.1 and Table 2.2 for three different external control parameters.

A remarkable trait of the problem is that even though the external potential could only slightly alter the discrete real energies of bound and quasi-stationary states, the imaginary part (the width) might change with several orders of magnitude.

It shall be stressed that, although the real continuum energies might become moderately altered at some energy region, they cannot be treated sufficiently by the presented calculation method and they are not in the focus of our analysis. This substantial trait is highlighted in the above mentioned figures and tables, where Γ^{pert} stands for the modified width. It is found that the value of the

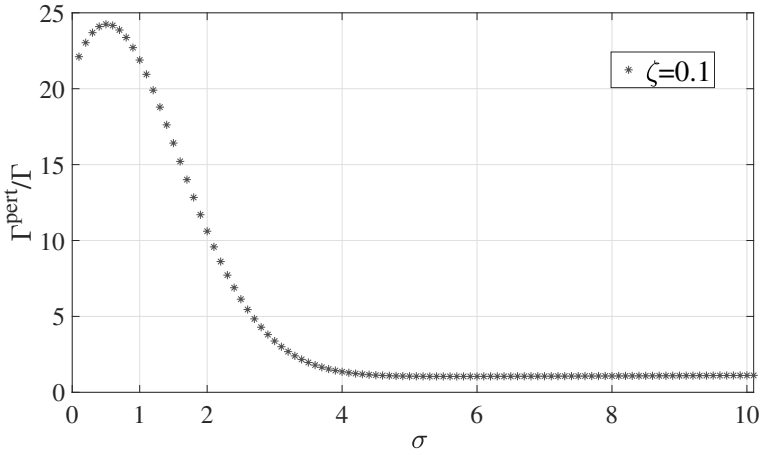

Figure 2.3: *The relative change of the width* $\frac{\Gamma^{\text{pert}}}{\Gamma}$*, in the case of potential* $V_{1\text{G}}(r)$*, as a function of the width of the Gaussian envelope function, for fixed* $\zeta = 0.1$.

ζ	$\text{Re}(E_{\text{qs}})$	Γ	$\Gamma^{\text{pert}}_{\sigma=1}$	$\frac{\Gamma^{\text{pert}}_{\sigma=1}}{\Gamma}$
0.01	1.491	$6.09 \cdot 10^{-6}$	$6.50 \cdot 10^{-4}$	106.5
0.1	1.491	$6.09 \cdot 10^{-6}$	$7.05 \cdot 10^{-5}$	11.5
1	1.491	$6.09 \cdot 10^{-6}$	$1.25 \cdot 10^{-5}$	2.05

Table 2.1: *The widths corresponding to the quasi-stationary states at real energy* $\text{Re}(E) = 1.491$ MeV *in the case of the potential model* $V_{1\text{G}}(r)$*. The modified widths* Γ^{pert} *and the relative changes of the width* $\frac{\Gamma^{\text{pert}}}{\Gamma}$ *are calculated with three different frequency parameters (*ζ*) of the external potential and with* $\sigma = 1$*. The parameter* A_0 *is set arbitrarily as* $A_0 = 10000$ *throughout the computations. All the quantities are measured in MeV.*

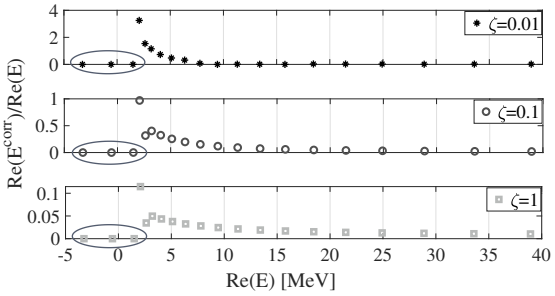

Figure 2.4: *The relative change of the real part of the energy eigenvalues corresponding to the potential model* $V_{1\text{G}}(r)$ *for three different frequency parameters* ζ *with* $\sigma = 1$*. The bound and quasi-stationary energy corrections are highlighted by an ellipse.*

modified width depends on the frequency parameter of the external potential (2.45). Also, one might want to check how the ratio of the lifetimes depends on the width of the Gaussian envelope function (σ). This σ-dependency is depicted in Figure 2.3 for a fixed frequency parameter $\zeta = 0.1$. We observe that, after a peak-like change, the effect vigorously decreases as the width σ increases, as anticipated, since as $\sigma \to \infty$ the Gaussian envelope potential converges to

ζ	$\mathrm{Re}(E_{\mathrm{qs}})$	Γ	$\Gamma^{\mathrm{pert}}_{\sigma=1}$	$\frac{\Gamma^{\mathrm{pert}}_{\sigma=1}}{\Gamma}$
0.01	2.393	$4.36 \cdot 10^{-5}$	$9.36 \cdot 10^{-5}$	2.15
0.1	2.393	$4.36 \cdot 10^{-5}$	$4.49 \cdot 10^{-5}$	1.11
1	2.393	$4.36 \cdot 10^{-5}$	$4.41 \cdot 10^{-5}$	1.01

Table 2.2: *The widths corresponding to the quasi-stationary states at real energy* $\mathrm{Re}(E) = 2.393$ MeV *in the case of the potential model* $V_{2\mathrm{G}}(r)$. *The modified widths* Γ^{pert} *and the relative changes of the width* $\frac{\Gamma^{\mathrm{pert}}}{\Gamma}$ *are calculated with three different frequency parameters* (ζ) *of the external potential and with* $\sigma = 1$. *The parameter* A_0 *is taken as* $A_0 = 10000$ *throughout the computations. All the quantities are measured in MeV.*

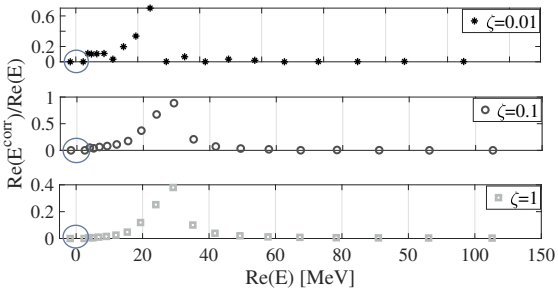

Figure 2.5: *The relative change of the real part of the energy eigenvalues corresponding to the potential model* $V_{2\mathrm{G}}(r)$ *for three different frequency parameters* ζ *with* $\sigma = 1$.

a plane-wave form. This behaviour is in accordance with the conclusion of previous computations with respect to laser pulse-assisted internal conversion processes [D. Kis et al., 2010]. Nevertheless, we conclude that by this theoretical method, one is able to find plausible, finite corrections to the width of the quasi-stationary states. A notable increment of the the presented computational method is obtaining the perturbative corrections to the lifetimes directly from the non-Hermitian spectrum of the Hamiltonian operator representing the decaying system.

3

Properties of super-intense laser-assisted decay within the non-hermitian formalism

In this chapter, I introduce and explain my own results concerning the coherent electromagnetic field-induced shift of the complex energy of single quasi-stationary states, elaborating thoroughly the special situation of gauge-transformations within the non-hermitian frame and in relation to strong-field laser fields. This chapter sets ground for an alternative, strongly analytical description of laser-assisted alpha decay to be presented in the next chapters. This chapter contains the author's own analytical and numerical results and corollaries.

3.1 Applicability of the classical description of the coherent electromagnetic field

When the interaction of a physical system with a coherent electromagnetic field (laser field) is considered, one must involve the eigenstates of the Hamiltonian of the electromagnetic field into the total state of the interacting system. When the interaction happens with a laser field then the state of the electromagnetic field must be described by a *coherent state*, that is by definition the eigenstate of the photon-annihilation operator:

$$a_k \left|\lambda_k\right\rangle = \lambda_k \left|\lambda_k\right\rangle , \tag{3.1}$$

with k denoting all the possible mode indices of the photon. The free Hamiltonian of a coherent electromagnetic field requires the second-quantized description, accordingly any interaction with the laser field contains the scalar and vector

potential of the quantized electromagnetic field built up by creation and annihilation operators. However, a special transformation can be constructed [D. P. Kis, 2013 ,] which transfers the coherent state to vacuum! This (time-dependent) transformation reads

$$\hat{T}_k(t) = \exp\left(\lambda_k e^{i\omega_k t}\hat{a}_k - \lambda_k^* e^{-i\omega_k t}\hat{a}_k^+\right), \tag{3.2}$$

where ω_k stands for the frequency of the laser. In addition, when considering the interaction of laser fields with a (in our case a non-relativistic) system, the interaction Hamiltonian is complemented by a new term, that is the classical vector potential determined by the well-defined eigenvalue λ_k and polarization (ϵ_k) of the coherent state:

$$\hat{\mathbf{A}}(k, \mathbf{r}, t) = A_0\left(\lambda_k \epsilon_k e^{i(\mathbf{k}_k\mathbf{r}-\omega_k t)} + \lambda_k^* \epsilon_k e^{-i(\mathbf{k}_k\mathbf{r}-\omega_k t)}\right), \tag{3.3}$$

where A_0 is an amplitude depending on the frequency and intensity of the field. One must note that this transformation remains valid only if the system does not undergo such transformations that could transform the coherent state back from vacuum. In this thesis we do not engage in such transformations. Henceforth, one creates the terms in the interaction Hamiltonian that describes the interaction of the system with a classical vector potential that appropriately represents the laser field since it is only evoked by the effect of a transformation operator. This interaction Hamiltonian is specified in the next section.

3.2 The interaction Hamiltonian

Now, we consider a coherent electromagnetic field characterized by a classical vector potential ($\mathbf{A}(\mathbf{r}, t)$) that is taken into account by minimally coupling the vector potential to the kinetic part of the Hamiltonian operator describing a non-relativistic system characterized by a reduced mass M. Thus, in Coulomb gauge ($\nabla\mathbf{A} = 0$) where the scalar potential is omitted, the total and already complex-scaled Hamiltonian of the laser-assisted decaying system yields:

$$\hat{H}^\theta(\mathbf{r}, t) = \frac{1}{2M}\left(\mathbf{p}^\theta - \frac{e}{c}\mathbf{A}^\theta(\mathbf{r}, t)\right)^2 + V(re^{i\theta}), \tag{3.4}$$

where e is the elementary charge and c is the speed of light. Due to the gauge choice the squared term in equation (5.33) gets simplified, hence we get the commonly known *velocity gauge* formula where the remaining terms containing the vector potential determine the interaction Hamiltonian $\hat{H}_I^\theta(\mathbf{r}, t)$ as follows:

$$\hat{H}_I^\theta(\mathbf{r}, t) = \frac{-e}{Mc}\mathbf{p}^\theta\mathbf{A}^\theta(\mathbf{r}, t) + \frac{e^2}{2Mc^2}\left(\mathbf{A}^\theta(\mathbf{r}, t)\right)^2. \tag{3.5}$$

This form can be further reduced by applying the dipole approximation or long-wave approximation (LWA), which converts the vector potential as $\mathbf{A}^{\theta}(\mathbf{r}, t) \rightarrow \mathbf{A}^{\theta}(t)$, thereby eliminating the spatial dependence of the vector potential. One shall note that this approximation is automatically valid in the case of the interaction with nuclear systems, since the characteristic wave-length of typical lasers (1-1000 eV) is at least five orders of magnitude larger than the nuclear size.

We use here the velocity gauge formula, although there are multiple examples in literature in relation to laser-matter interactions where this form is substituted with ease by an expression containing the electric field, referring to it as a special type of gauge-choice: the length gauge (also referred to as rE-gauge). In the next subsections the question of the gauge-choice, especially with regard to complex-scaling and the description of high-intensity *laser* fields is thoroughly discussed, for the derivation of the laser-induced complex-energy correction formula we adopt the velocity-gauge expression of the interaction Hamiltonian.

3.3 Derivation of the first-order, (t,t')-perturbative laser-induced complex-energy correction function

Now considering the above-specified interaction Hamiltonian, in this subsection I intend to discuss the calculation of the correction to the complex energy of the quasi-stationary state due to the presence of the vector potential representing the external laser field.

The parametrization of the vector potential depends on the polarization. In this study calculations are presented for both linearly and circularly polarized laser fields, in LWA. The concrete form of the vector potential is specified later. In order to stress the generality of the formalism, I take as the basic non-perturbative system the already presented toy model 2.4 where a particle of reduced mass m is trapped inside a Gaussian-type potential barrier.

In the interaction Hamiltonian in equation (3.5) there are two terms containing the vector potential on different powers. We are looking for the following matrix element ((t,t')-expectation value rather) to obtain the first-order perturbative correction to the complex energies of the quasi-stationary states:

$$((\tilde{\Phi}^{\theta}(\mathbf{r}, t)|\hat{H}_I^{\theta}|\tilde{\Phi}^{\theta}(\mathbf{r}, t))). \tag{3.6}$$

Note that one must consider the spatial integrals also which, in this case, are separated to integrals over radial and spherical angular coordinates, due to the system possessing spherical symmetry. Generally, it is found that considering

this spherically symmetric problem, independently of the polarization direction the perturbative complex-energy correction (2.41)

$$((\tilde{\Phi}^{\theta}(\mathbf{r},t)|\hat{H}^{\theta}_{I,1}|\tilde{\Phi}^{\theta}(\mathbf{r},t))) = 0 \tag{3.7}$$

for the first term in (3.5) $\hat{H}^{\theta}_{I,1} = \frac{-e}{Mc}\mathbf{p}^{\theta}\mathbf{A}^{\theta}(\mathbf{r},t)$, as a result of the integrals over spherical angular coordinates ($\Omega = \phi, \Theta$) with the spherical harmonics $Y_{\ell,m}(\Omega)$ appearing in the spatial part of the wave-function $\Phi^{\theta}(\mathbf{r}) = \sum_{j=1}^{N} \tilde{c}^{\theta}_{j} u_j(r) Y_{\ell,m}(\Omega)$. It is an essential distinct property of the non-hermitian treatment of the problem, that will be elaborated later on. It is important to note that this trait might be a consequence of calculating an *expectation value*, in other words with the initial and final states being equal, rather than a transition matrix element typically applied in calculations concerning laser-assisted nuclear processes. This is validated if the Keldysh-Gamma parameter is much smaller than one $\gamma_{\mathrm{KG}} << 1$ (see for example [Reiss, 2008]), furthermore when the external laser field cannot alter significantly the real part of the complex energy, as in, the perturbation does not transfer the system to a different energy level. This will be the case for laser-nuclei interactions.

To obtain the matrix element for the second term $\hat{H}^{\theta}_{I,2} = \frac{e^2}{2Mc^2}\left(\mathbf{A}^{\theta}(\mathbf{r},t)\right)^2$, one is allowed to calculate the integrals over spherical coordinates and the time coordinate of the extended Hilbert space separately. Differently from the frequently applied theoretical frameworks, in this case the $\left(\mathbf{A}^{\theta}(\mathbf{r},t)\right)^2$ matrix element gives non-zero contribution; moreover, due to the use of the c-product, in the calculation of matrix elements (expectation values) the phase symmetry of the system is not present, therefore the phase transformation of the eigenfunction between the different gauges cannot be performed.

As a direct consequence of these, it must be pointed out here that in the case of quasi-stationary states, described within the framework of non-Hermitian quantum theory, the (pA) and (rE) gauges are unsuitable and insufficient because the quadratic term of the vector potential is non-vanishing in the interaction Hamiltonian [M. Sargent et al., 1974] which in Coulomb gauge includes only the $\mathbf{pA}$ and the $\mathbf{A}^2$ components. In the presented calculation scheme, since the $\mathbf{A}^2(\mathbf{r},t)$ term gives the non-zero contribution, the unitary transformation that connects the (pA) and (rE) gauges is not justified, hence it is not appropriate to regard our Schrödinger equation in either one of those (sub-) gauges but in the standard Coulomb gauge. This circumstance is detailed and clarified in the next subsection.

Analytical closed formulas are obtained with the following specification of

the vector potential. For linear polarization the vector potential is built up as

$$\mathbf{A}(\mathbf{r},t) = A_0\mathbf{e}_z\cos\left(\frac{\zeta}{\hbar}t+\alpha\right)\mathrm{e}^{\left(-\frac{\zeta t}{\hbar\sigma}\right)^2}, \tag{3.8}$$

while for circular polarization $\mathbf{A}(\mathbf{r},t)$ is expressed as

$$\mathbf{A}(\mathbf{r},t) = A_0\left(\mathbf{e}_x\cos\left(\frac{\zeta}{\hbar}t+\alpha\right)+\mathbf{e}_y\sin\left(\frac{\zeta}{\hbar}t+\alpha\right)\right)\mathrm{e}^{\left(-\frac{\zeta t}{\hbar\sigma}\right)^2}, \tag{3.9}$$

where $\mathbf{e}_x$, $\mathbf{e}_y$, $\mathbf{e}_z$ are the unit vectors in Cartesian coordinate system, $\frac{\zeta}{\hbar}$, α are the frequency and the phase of the laser field, respectively and σ is the width of the Gaussian envelope function. A_0 can be expressed with the amplitude of the corresponding electric field $E_0 = \frac{\zeta}{\hbar c}A_0$, where $E_0 = \sqrt{\frac{4\pi}{c}}\sqrt{I}$ with I denoting the intensity of the laser field.

Performing the integration over the whole coordinate space in $\varepsilon^{(1,\mathrm{l})} = ((\tilde{\Phi}^{\theta}(\mathbf{r},t)|\hat{H}^{\theta}_{I,2}|\tilde{\Phi}^{\theta}(\mathbf{r},t)))$, the following closed-form expressions are achieved for the energy correction, for the physically motivated limit of $\frac{\Gamma}{\zeta} << \sigma$. The latter condition refers to the situation of actual nuclear physical systems. In the interesting case of alpha decay the typical order of magnitude of the decay width is smaller than 10^{-14} MeV and the mean-field widths (to be specified later) are also at most 10^{-7} MeV, which trait justifies the condition $\frac{\Gamma}{\zeta} << \sigma$ for a certain range of ζ values (ζ accounts for the photon energy in physical processes: typically $1-1000$ eV for super-intense lasers). It shall be noted here that the value of the photon energy cannot be arbitrarily small for a given intensity due to possible relativistic effects, see [Reiss, 2008] and Subsection 5.1.3 for further clarifications. As a result, in the case of linear polarization the energy correction yields:

$$\begin{aligned}\varepsilon^{(1,\mathrm{l})} &= \mathcal{N}^2\mathcal{K}\frac{I\hbar}{\zeta^3}\sqrt{\frac{\pi}{2}}\Bigg(\frac{1}{4\sigma}\mathrm{e}^{\frac{\Gamma^2}{8\zeta^2\sigma^2}}f(\sigma,\Gamma,\zeta)+ \\ &+ h(\sigma)\left[\mathrm{e}^{-2\mathrm{i}\frac{\Gamma\sigma^2}{8\zeta}}\mathrm{e}^{2\mathrm{i}\alpha}g(\sigma)+\mathrm{e}^{2\mathrm{i}\frac{\Gamma\sigma^2}{8\zeta}}\mathrm{e}^{-2\mathrm{i}\alpha}g^*(\sigma)\right]\Bigg),\end{aligned} \tag{3.10}$$

where the function $g(\sigma) = \left(1+\mathrm{i}\cdot\mathrm{erfi}\left(\frac{\sigma}{\sqrt{2}}\right)\right)$ and $g^*(\sigma)$ is its complex conjugate, as well as $f(\sigma,\Gamma,\zeta) = \left[1-\mathrm{erf}\left(\frac{\Gamma}{\sqrt{8}\zeta\sigma}\right)\right]$, and function $h(\sigma) = \frac{\sigma}{16}\mathrm{e}^{\left(\frac{\Gamma^2}{\zeta^2}-4\right)\frac{\sigma^2}{8}}$. The energy correction for circular polarization is determined as:

$$\varepsilon^{(1,\mathrm{c})} = \mathcal{N}^2\mathcal{K}\frac{I\hbar}{\zeta^3}\sqrt{\frac{\pi}{8}}\frac{1}{\sigma}\mathrm{e}^{\frac{\Gamma^2}{8\zeta^2\sigma^2}}f(\sigma,\Gamma,\zeta). \tag{3.11}$$

Note that the norm factor $\mathcal{N}^2$ is a complex quantity (as c-norm) and depends on the width of the quasi-stationary state Γ [Szilvasi et al., 2022]. The

constant $\mathcal{K}$ includes the followings: $\mathcal{K} = \frac{\alpha_{\mathrm{EM}} 2\pi(\hbar c)^3}{\mu c}$, where $\mu = Mc^2$ and α_{EM} is the electromagnetic fine structure constant (remember that in the previously introduced Gaussian model system the following parameterization is used: $\frac{\hbar^2}{2M} \equiv \frac{1}{2}$).

It is clearly seen from equations (3.10) and (3.11) that the energy correction formulas are roughly inversely proportional to the photon energy ζ, although one must bare in mind that this non-relativistic model is not predictive for arbitrary $I - \zeta$ values, rather for certain intensity and photon energy pairs which ensure that one does not cross the limit of the non-relativistic approximation [Reiss, 2008]. This particular ζ-dependency behavior is also a characteristic trait of certain laser-assisted nuclear processes [Kalman et al., 1986 ; D. Kis et al., 2010], in addition to laser-electron interactions described by the ponderomotive potential energy U_{pon}, which grows with ζ^{-2} in the case of continuous plane weave lasers [**Reiss**]. Although, in the matter of laser pulses one has the freedom to parameterize the pulse length T with the photon energy through introducing a dimensionless pulse width σ. In this study the following pulse length parameterization is used: $T = \frac{\hbar\sigma}{\zeta}$ which produces an additional ζ^{-1} in the energy correction. The signature characteristic of the control-parameter dependence of superintense-laser and alpha cluster interaction in this framework might only be investigated in the context of the non-relativistic limit that is quantified by the ponderomotive potential of the alpha cluster (Subsection 5.1.2) that is presented in Section 5.4.

It shall be mentioned that a significant trait of the closed forms $\varepsilon^{(1,\mathrm{p})}$, where the superscript p denotes the two possible polarization states, is that it is a general formula in the sense that it yields the complex energy correction to any suitably chosen decaying system subjected to the above-specified laser field. To quantify the measure of effect the external laser field has on the complex energy of the quasi-stationary state, typical values of the external control parameters (I, ζ, σ) are adopted from studies concerning the non-relativistic description of laser-matter interactions [D. Kis et al., 2018], see Subsection 5.1.3.

3.4 The question and discussion of the gauge-choice

Whenever one is faced with problems involving - in a broader sense - the fundamental interactions of particle physics (the currently state-of-the-art framework of nuclear physics also) such as the strong interaction and the electroweak interaction, given these are exquisitely described today by gauge theories, it is indispensable to regard the question of the gauge choice of the gauge fields or potentials. In this thesis I consider laser-matter interaction in

a non-relativistic aspect - for which the theoretical background is introduced in Section 3.2 -, hence from the viewpoint of the gauge choice the classical electromagnetic vector-potential must be examined.

After the development of quantum mechanics, it became clear that the fundamental quantities of the electromagnetic interaction are not the electric and magnetic fields ($\mathbf{E}, \mathbf{B}$), rather the vector potential $\mathbf{A}(\mathbf{r}, t)$ and the scalar potential ($\phi(\mathbf{r}, t)$). Although, the potentials inherently have the property to be indefinite upon a total time derivative; the set of potentials to represent the fields is not unique. Hence, there should exist special transformations (unitary transformations) that intend to map between different sets of potentials; these transformations are called *gauge* transformations. Practical purposes decide, in general, which gauge-fixing is suitable for a given problem. For the description of a non-relativistic electromagnetic interaction a commonly used gauge is the Coulomb-gauge ($\nabla\mathbf{A} = 0$) that is usually complemented by fixing $\phi(\mathbf{r}, t) = 0$ when the problem is investigated far from any sources (it is always true for a plane-wave).

However, in the context of electromagnetic fields interacting with matter there exists several *approximate*-gauges that can be applied in special situations and intend to simplify the computations of, for example, transition matrix elements. Such gauges are the length gauge or (rE)-gauge; and the (pA)-gauge. Those gauges are both obtained by the "simplification" of the velocity-gauge Hamiltonian considered in the *dipole-approximation*

$$\hat{H}_I(\mathbf{r}, t) = \frac{-e}{Mc}\mathbf{p}\mathbf{A}(t) + \frac{e^2}{2Mc^2}\left(\mathbf{A}(t)\right)^2. \tag{3.12}$$

The (pA)-gauge emerges straightforwardly when transition matrix elements are calculated with plane-waves in the *hermitian* formalism of quantum mechanics, since in this case the $(\mathbf{A}(t))^2$ term does not contribute to the transition, it is only a number multiplying an orthogonal inner product ($\mathbf{A}^2 \langle\Phi_i|\Phi_k\rangle$) (it is very important here that this inner product is the hermitian one!):

$$\hat{H}_I^{\mathrm{pA}}(\mathbf{r}, t) = \frac{-e}{Mc}\mathbf{p}\mathbf{A}. \tag{3.13}$$

The (rE)-gauge is a result of the electric dipole approximation and is physically motivated for longitudinal electromagnetic fields (the laser field is not such a field). It has the form

$$\hat{H}_I^{\mathrm{rE}}(\mathbf{r}, t) = \frac{-e}{Mc}\mathbf{r}\mathbf{E}, \tag{3.14}$$

where $\mathbf{E}$ is the electric field. The (rE)-gauge Schrödinger equation emerges mathematically, by a special unitary transformation, from the (pA)-gauge Schrödinger equation, but this transformation can only be applied when the $(\mathbf{A}(t))^2$ term is

already transformed out by a unitary transformation, otherwise these gauges cannot be considered. Three conditions are necessary for this: dipole approximation, transition matrix elements and the phase symmetry of the eigenfunctions. In the calculation scheme for the complex-energy shift in non-hermitian quantum mechanics we calculate an expectation value in c-product, hence not fulfilling the phase-symmetry requirement. This major difference is accentuated in the next subsection.

Gauge-transformations in Hermitian and non-hermitian systems

The non-hermitian quantum-mechanical framework includes several differences compared to the Hermitian formulation. A pivotal difference lies in the definition of the scalar product and norm on the Hilbert space. The conventional definitions are not valid in the non-Hermitian picture, rather a special c-product and c-norm must be used, see Subsection 2.2.1. This has serious consequences for the solution of the Schrödinger equation: the most crucial one is that the wave function loses the phase symmetry (due to the properties of the c-product, which does not contain the complex conjugate of the eigenfunction) which is present in the Hermitian case. It is in relation with the fact that when dealing with decaying systems there is no time reversal symmetry anymore (just as for open quantum systems). This results in the circumstance that in the calculation scheme that is presented above the usual phase change transformation, that is valid for hermitian systems, cannot be executed, hence the $\mathbf{A}^2$ term remains in the Hamiltonian. As a consequence of this the gauge-invariance issue must be revised when calculating quasi-stationary states (decaying states), especially in perturbation theory.

To further emphasise my point, I collected the possible cases of the interaction of some external laser field with Hermitian and non-Hermitian quantum systems with regard to the matrix elements:

1. Case 1: Hermitian system and external electromagnetic field:
   (a) 1a: with transition between two levels, nonzero c_{fi} transition amplitude:
      - $\langle \mathrm{f}|\mathbf{rE}|\mathrm{i}\rangle \neq 0$;
      - $\langle \mathrm{f}|\mathbf{pA}|\mathrm{i}\rangle \neq 0$;
      - $\langle \mathrm{f}|\mathbf{pA} + \mathbf{A}^2|\mathrm{i}\rangle = \langle \mathrm{f}|\mathbf{pA}|\mathrm{i}\rangle \neq 0$;
   (b) 1b: without transition between two levels, just small energy perturbations
      - $\langle \mathrm{f}|\mathbf{rE}|\mathrm{i}\rangle = 0$;
      - $\langle \mathrm{f}|\mathbf{pA}|\mathrm{i}\rangle = 0$;

- $\langle f|\mathbf{pA} + \mathbf{A}^2|i\rangle = 0$;

2. Case 2: non-Hermitian system and external electromagnetic field (using the c-product $(.|.|.)$):
   (a) 2a: with transition between two levels, nonzero c_{fi} transition amplitude:
      - $(f|\mathbf{rE}|i) \neq 0$;
      - $(f|\mathbf{pA}|i) \neq 0$;
      - $(f|\mathbf{pA} + \mathbf{A}^2|i) \neq 0$;
   (b) 2b: without transition between two levels, just small energy perturbations
      - $(f|\mathbf{rE}|i) = 0$;
      - $(f|\mathbf{pA}|i) = 0$;
      - But $(f|\mathbf{pA} + \mathbf{A}^2|i) = (f|\mathbf{A}^2|i) \neq 0$;

In Case 1a and 1b (hermitian systems), the gauge invariance is exact. In case 1a, $\mathbf{A}^2$ term can be transformed out or cannot lead to transition. In Case 1b, $\mathbf{A}^2$ term *can also be* transformed out, although in such a situation there is no energy correction to the real eigenergy due to the lack of transition. In contrast to Case 1, in the non-hermitian cases (2a, 2b) the gauge transformation cannot be performed due to the properties of the c-product, in other words, $\mathbf{A}^2$ term cannot be transformed out.

In the last case (Case 2b) although the real energy correction is zero (the Keldysh parameter$\ll 1$, the energy level cannot be changed), due to the non-Hermitian nature of the problem, there is an *additional degree of freedom* that is the imaginary part of the complex energy which is proportional to the width of the quasi-stationary state (Γ). The external electromagnetic field might change this quantity without altering the real part of the energy. This cannot be observed in Hermitian systems.

The peculiarity of super-intense laser fields with regard to the gauge choice

In his several articles, H. R. Reiss discusses the special situation of ultra-high intensity coherent electromagnetic fields interacting with matter. In this subsection I aim to summarize his most essential findings and conclusions in relation to the proper approach of high-intensity laser and matter interaction on the basis of gauges, that is in accordance with the conclusions of the non-hermitian, complex-energy shift calculation method I presented in Section 3.3.

From the viewpoint of this thesis, the laser-nucleus interaction is central. For this reason, when one observes the literature covering the field of laser-nucleus

interaction (see for example [J. Qi et al., 2019 ; Pálffy et al., 2020 ; Rehman et al., 2022]), evidently a great number of studies operate with the length gauge that is conventionally used in electrodynamics, and it originates from the traditional treatment of electromagnetic interactions with matter when no high-intensity lasers were considered. It is argued in this thesis and also in the work of Reiss that the question of gauge-invariance involving special gauges frequently used in, for example, the description of laser-matter interactions (the gauges discussed in Section 3.4) shall be revisited and treated carefully.

In [Reiss, 2008 ; Reiss, 2002 ; Reiss, 2014] Reiss explores the question of gauge-invariance in special situations involving typically strong-field lasers; as well as emphasises and contrasts the two fundamentally different cases of electromagnetic interactions with matter: the longitudinal quasi-constant electric field versus the laser field that is a transverse coherent electromagnetic *plane-wave* field.

Reiss concludes that the length gauge is fine for problems that address the interaction of matter with such electromagnetic field that can be considered longitudinal but for transverse fields such as an intense laser field the total, velocity gauge shall be applied. It is also examined in [Reiss, 2014] that when an electron exists in a strong plane-wave field (propagating field) it necessarily acquires a ponderomotive 4-potential energy that appears in the mass-shell condition in a dimensionless way via the intensity-dependent strong-field coupling (the intensity-dependent strong-field coupling z_f is introduced in Subsection 5.1.2). The main conclusion of the author's reasoning is that the ponderomotive potential energy is an inherent property of propagating laser fields that is only manifested in the velocity gauge, not in the length gauge. I will return to the relevance of the ponderomotive potential energy when discussing the approximation limits (non-relativistic limit) of strong-field interactions with an alpha cluster.

Based on the above, when describing the perturbative interaction of non-hermitian systems with some external coherent electromagnetic field, the usual gauge transformation between the gauges (r.E, or p.A or p.A + A^2) is not valid. It is argued that there exists a physical gauge (which is the velocity gauge), which is in accordance with the conclusion of H. Reiss [Reiss, 2002 ; Reiss, 2008 ; Reiss, 2014 ; Reiss, 2019 ; Reiss, 2021]: for the description of the interaction between ultrahigh-intensity laser fields and matter the velocity gauge is adequate.

4

Theoretical description of alpha decay

The field of theoretical nuclear physics has made significant advancements in comprehending alpha decay, which is regarded as a critical process for studying nuclear stability and structural characteristics. Theoretical models strive to improve the accuracy of alpha decay half-life predictions, enhancing our grasp of nuclear forces and interactions among nucleons. These studies [Varga et al., 1992 ; Rowley et al., 1992 ; Mohr, 2006 ; Duarte et al., 2002 ; Brown, 1992 ; Royer, 2000 ; Royer et al., 2002 ; Basu, 2003 ; Gambhir et al., 2005 ; Gupta et al., 2002] focus on either the proposition of a *universal decay law* partly in order to explain decay properties and enhance the effectiveness of predicting decay rates of a broad number of isotopes for practical purposes, or the *microscopic theories* governing cluster radioactivity and nuclear structural properties for theoretical advancements and precision calculations. For the latter purpose nowadays high-performance computational techniques are incapacitated due to the complexity of the underlying nuclear interactions originating from the in itself perplexing theory of strong interactions. However these microscopic computations are proved to be efficient in simulations and predictions of single nuclei, these do not necessarily advance the general knowledge about the processes occurring in the atomic nucleus.

During my own theoretical research, I intended to turn the focus on building analytically more controllable and quantum mechanically vigorous models which naturally could give more insight into the general phenomenon of alpha decay. In this section, I endeavor to give a brief summary of the current understanding of alpha decay both on theoretical and empirical divisions, especially reviewing the common theoretical frameworks and models, commonly applied in recent studies, emphasizing the properties relevant for the description of laser-assisted nuclear alpha decay considering this constitutes the core subject of this thesis.

From this point of view, the general mean-field framework of atomic nuclei and the conventional quantum-mechanical description of alpha tunneling is reviewed in this and the following sections, supplemented by the novel non-hermitian quantum-mechanical approach for the description of tunneling proposed in the author's recent studies [Szilvasi et al., 2022 ; Szilvasi et al., 2024] and explained thoroughly in Chapter 2. For this purpose, I incorporated as the basis of my study the specific frame that characterizes alpha decay as a two-step process involving the cluster formation and cluster tunneling phases, that will be elaborated in Section 4.2. In this section, I attempt to review the basic ideas and theoretical frameworks regarding the process of alpha decay, while in the next section I oppose the conventional descriptions of tunneling to the novel non-hermitian quantum-mechanical approach and finally present my own results with the purpose of elucidating the essential signatures of the non-hermitian quantum-mechanical, mean-field cluster model of alpha tunneling by investigating special heavy, alpha-decaying isotonic chains.

4.1 Properties of alpha-decay

In this section I only address the properties of alpha decay that are crucial for my investigation. I also introduce some rather important knowledge about alpha decay derived upon early quantum-mechanical theories or empirical grounds.

In an alpha-decaying isotope with mass number A_1 and atomic number Z_1, we consider a subsystem consisting of two bound protons and neutrons (this is the alpha cluster), which is observed to be emitted from the nucleus in a form of an alpha particle, hence due to the emission an $A = A_1 - 2, Z = Z_1 - 2$ nucleus is created that is referred to the daughter nucleus in the literature. The alpha particle radioactivity was first observed by Ernest Rutherford in 1899.

Alpha decay is a probabilistic process which is usually described by the energy of the alpha particle emitted and a quantity depicting the probability of the emission. The specification of this quantity depends on the type of description one chooses to characterize alpha decay. For a statistical (and also practical) purpose, one shall operate with the exponential decay law and define quantities such as the decay rate λ and the half-life $T = \frac{\ln 2}{\lambda}$ which are assigned, measurable quantities of every decaying isotope. However, from the point of view of theoretical purposes, one ought to investigate the fundamental process of the alpha decay phenomenon that is found to be a purely quantum-mechanical problem. The possibility of tunneling was first explained mathematically by George Gamow in 1928 [Gamow, 1928] by the notion of quantum-mechanical tunneling by defining a tunneling probability.

The energy released during alpha decay, known as the Q-value, is the difference between the mass of the parent nucleus (M_P) and the combined masses of the daughter nucleus (M_D) and the alpha particle (M_α):

$$Q_\alpha = (M_P - M_D - M_\alpha)\, c^2$$

Here, c is the speed of light in vacuum. This energy is shared between the alpha particle and the daughter nucleus according to conservation of momentum.

Since the alpha particle is much lighter than the daughter nucleus, the kinetic energy (T_α) of the alpha particle is approximately equal to the Q-value $M_D \gg M_\alpha$:

$$T_\alpha \approx \frac{Q_\alpha M_D}{M_D + M_\alpha} \approx Q_\alpha$$

The interaction between the nucleons inside the nucleus is always a delicate topic, that is why the nuclear interaction between parts of the nucleus is usually approximated by an average potential. Working in the cluster-daughter nucleus model, in the mean-field approximation, the alpha cluster moves in a potential ($V(\mathbf{r})$), shaped by the short-range attractive nuclear force between nucleons and the Coulomb repulsion between protons: at short distances (within the nucleus), the attractive nuclear part of the potential dominates, but as we move away from the nucleus, the Coulomb decay determines its shape, thus creating a potential barrier in front of the particles. From a classical physics perspective, two things can happen to the particles: if their energy (Q_α) is greater than the height of the potential barrier, they can leave the nucleus; if it is lower, they cannot.

From the broader quantum mechanical perspective, the alpha cluster is in a special, so-called quasi-bound (or quasi-stationary) state, meaning it has a finite lifetime, or in other words, it is a decaying state (see Section 2.1). This is due to the nature of the potential felt by the alpha cluster, which can be understood as a potential barrier that "traps" the alpha particle, although the probability of passing through the barrier is finite. This phenomenon can be well understood illustratively with the quantum mechanical concept of tunneling. However, alpha tunneling can be viewed through two different perspectives. The first one involves using the conventional tunneling picture, and an alternative approach is based on the complex energy corresponding to the quasi-stationary state. The latter concept has been introduced in 2 and is also the core subject of this thesis, while the first one is based on the WKB approximation, according to which, traditionally, the tunneling probability p is given by:

$$p = \exp\left(-2\int_{r_1}^{r_2}\sqrt{\frac{2M}{\hbar^2}\left(V(r) - Q\right)}\mathrm{d}r\right) \tag{4.1}$$

where M is the reduced mass of the alpha cluster and the daughter nucleus, r_1 and r_2 are the classical turning points (the points where the energy of the alpha cluster intersects the potential), and $\hbar$ is the reduced Planck constant. It is of paramount importance to emphasise that the potential energy term $V(r)$ present in the formula must necessarily be time-independent, as the formula, in its current form, is defined for a stationary system.

The Geiger-Nuttall law [Biswas, 1949] shall also be mentioned. There is voluminous literature covering the expressions of the Geiger-Nuttall law with several possible experiment-based or theory-based extensions (see [Froman, 1957 ; Wapstra et al., 1959 ; Taagepera et al., 1961 ; Viola et al., 1966 ; Keller et al., 1972 ; Poenaru et al., 1980 ; Hatsukawa et al., 1990 ; Brown, 1992 ; Royer, 2000]). It provides an empirical relation between the half-life and the energy of the emitted alpha particle. It shows that nuclei with higher alpha energies decay more rapidly:

$$\log_{10} T = a\frac{Z}{\sqrt{Q_\alpha}} - b$$

where a and b are empirical constants, Z is the atomic number of the daughter nucleus, and Q_α is the alpha energy. It is important to remark at this point, that the half-life of the alpha-decay process (a statistical quantity) is related to the fundamental quantities essential in the discussion of the quasi-stationary state representing the alpha cluster in an alpha-decaying nucleus: $T = \hbar \cdot \ln 2/\Gamma^{\text{decay}} = \tau/\ln 2$, with Γ^{decay} denoting the decay width and τ denoting the lifetime of the alpha cluster. In Section 4.3.3 I introduce a particular formulation of this law for isotonic series, employing the (mean-field) complex energy of the quasi-stationary state of the alpha cluster.

4.2 Characterization of alpha decay as a resultant of two separate processes

Alpha decay is a complex spontaneous nuclear process which is driven by nuclear forces and electromagnetic interaction. During this research I incorporated an alternative picture to interpret this decay phenomenon, in which alpha decay is regarded as a resultant of two independent processes, which are the alpha cluster preformation due to nuclear structure effects and the interaction between the alpha cluster and the remaining nucleus which leads to tunneling through the Coulomb barrier. This type of depiction of the decay phenomenon also provides the basic framework for the traditional description of alpha decay via the WKB-approximation. Typically, the decay process is characterized by the decay width (Γ^{decay}) which is constructed by quantities that denote the two separate steps of the total decay process. In the followings I would only mention the traditional quantum-mechanical, perturbative approach to derive the total decay width, nevertheless in this chapter I focus essentially on the characterization of the Coulomb tunneling of the preformed alpha cluster. For the description of tunneling the commonly applied mean-field nuclear models are proved to be capable to produce the tunneling width of the decay (Γ), hence in the next section I provide the framework for the cluster-mean-field description.

In this chapter, I would like to introduce a factor that intuitively bears the name of the nuclear structure factor and is denoted by s_0 in the followings.

The tunneling part of the decay process can be characterized by the already preformed alpha cluster occupying a quasi-stationary state with complex eigenenergy. In this study I rely on the approximation that the interaction between the preformed alpha-cluster and the remaining nucleus is considered within the mean-field frame, neglecting any effects stemming from the nuclear structure. Hence, it is important to distinguish between the total width of alpha decay (Γ^{decay}) and the width of the performed alpha cluster (Γ):

$$\Gamma^{\text{decay}} = s_0 \Gamma, \tag{4.2}$$

where we call s_0 the nuclear structure factor, which includes the clustering effects and the possible corrections to the interaction between the alpha cluster and the remaining nucleus (for example pair correlations). In Subsection 4.3.2 I present my computations with regard to the complex energy of an alpha cluster in the mean-field frame, by non-hermitian quantum-mechanical methods. It must be emphasized here, that the model to be presented cannot predict the total width of the alpha decay, rather the mean-field tunneling width can be derived from

the Hamiltonian of the system. In Subsection 4.3.3 I explain the justification for such a model in relation to the subject of Chapter 5 where I show that this type of model is capable to adequately describe the relative change of the lifetime of alpha-decaying nuclei induced by some high-intensity laser.

In addition, it shall be indicated that the traditional description of alpha decay is based on the WKB-approximation which is a quasi-classical treatment. In their article [Gurvitz et al., 1987 ; Buck et al., 1992] the authors derive a perturbative formula to express the decay width of an alpha cluster (a stationary formula)

$$\Gamma_{\alpha}^{\text{decay}} = S_{\alpha} F \frac{\hbar^2}{4\mu} \exp\left[-2\int_{r_2}^{r_3} k(r)dr\right], \tag{4.3}$$

where S_α is the spectroscopic factor (it includes the fine structure information), F is the normalization factor, r_2 and r_3 denote the turning points of the potential and $k(r)$ is the potential and energy-dependent wave-number. One can clearly see that equation (4.2) and (4.3) have the same structure despite having rather different interpretation, the quantities denoting the tunneling properties and the fine-structure characteristics represent independent processes. In contrast to the traditional approach, the model that is in the core of this thesis is based on a non-perturbative approximation, which directly yields the tunneling width from the discretized Hamiltonian spectrum.

4.3 Cluster-mean-field description of the Coulomb-tunneling phase of the decay-process

The interaction between nucleons inside the nucleus is substantially a challenging many-body problem.

Since the birth of nuclear physics, the problem of understanding the force between nucleons has been an ongoing challenge. This understanding is necessary to provide sufficiently precise theoretical calculations and conclusions about the properties of atomic nuclei and various nuclear processes.

To this end, numerous nuclear models have been developed. Most of them are based on initial empirical findings, primarily known through scattering experiments. We can evaluate the success of these models (e.g., the Liquid Drop Model, Fermi Gas Model, Shell Model, and Collective Model) based on the consistency of the measurable quantities calculated with these models and experimental results. In calculations within the framework of the Independent Particle Shell Model, we have freedom in selecting the specific form of the central mean-field potential, defined in the Mean Field approximation to eliminate

pairing interactions. To gain as much information as possible about the nuclear force, it is crucial to accurately understand the pair potential generally involved in the many-body Hamiltonian. Generally, non-relativistically, the many-body Hamiltonian operator for nucleons bound in the nucleus can be written as follows:

$$\hat{H} = \sum_{i=1}^{A} \frac{\mathbf{p}_i^2}{2M} + \sum_{i,j} V_p(\mathbf{r}_i - \mathbf{r}_j), \tag{4.4}$$

where A denotes the number of nucleons in the given nucleus (which is also the mass number), M is the reduced mass of the nucleons, $\mathbf{p}_i$ is the kinetic momentum of each nucleon, and V_p is the pair potential. The second term of the Hamiltonian, the pair potential, is essentially a two-particle operator, while the kinetic term is the sum of one-particle operators. The essence of the Shell Model is that if this pair potential can be approximated with a suitable average-field potential, the many-body operator decomposes into the sum of one-particle operators.

In the mean-field frame the nuclear pair potential is replaced by a pilot potential (mean potential, average-field potential) that includes the average contribution of the interacting nuclear forces acting upon a single particle. The introduction of such a mean potential results in a single-particle Schrödinger equation.

Considering the case of the alpha-cluster the single-particle Hamiltonian $\hat{H}_0(\mathbf{r})$ consists of a kinetic part $\hat{H}_{\text{kin}} = \frac{\mathbf{p}^2}{2M}$ of an alpha cluster of reduced mass $M = \frac{m_\alpha \cdot M_{\text{rn}}}{m_\alpha + M_{\text{rn}}} \approx 4.003 \frac{(A-4.003)}{A} m_{\text{n}}$ with the average nucleon mass m_{n} and mass number A of the remaining nucleus, and the yet-to-be specified mean potential of the nuclei $\hat{V}(\mathbf{r})$:

$$\hat{H}_0(\mathbf{r}) = \frac{\mathbf{p}^2}{2M} + \hat{V}(\mathbf{r}). \tag{4.5}$$

In this study the nuclear mean potential felt by the alpha cluster is represented by a spherically symmetric potential barrier ($V(r)$). There are several ways to construct such a nuclear potential energy term, although I consider here two similar expressions that are illustrated in 4.3.

In both cases the quantum barrier is built up with a uniquely parametrized attractive nuclear potential part along with a repulsive Coulomb potential attached to it. This attachment is realized through the Fermi function.

In the first specific case the attractive part is the commonly considered Woods-Saxon-type interaction. The potential energy term reads:

$$\hat{V}_{\text{WSC}} = -V_0 f(r) + \left(1 - f(r)\right) \frac{c_0}{r}, \tag{4.6}$$

where the constant c_0 of the Coulomb-term $\frac{c_0}{r}$ contains the following quantities and physical parameters: $c_0 = 2 \cdot Z \cdot \alpha\hbar c$ with Z connoting the atomic number of the daughter-nucleus and α denoting the fine-structure constant at vacuum energy. The function $f(r)$ is a Fermi-type function:

$$f(r) = \frac{1 + \mathrm{ch}(R/a)}{\mathrm{ch}(r/a) + \mathrm{ch}(R/a)}, \tag{4.7}$$

where a is the Fermi-function's length-parameter and R is the nuclear radius.

In the second case, the attractive part is complemented with a harmonic oscillator multiplicative factor in order to distort the shape inside the nuclei and only slightly alter the vicinity of the Coulomb barrier. ($\hat{V}_{\mathrm{WOC}}$ abbreviates the combined use of the Woods-Saxon, harmonic oscillator and Coulomb potentials. The total form of the spherical potential generally reads:

$$\hat{V}_{\mathrm{WOC}} = V_0 \left(\frac{K_0}{L^2} r^2 - 2 \right) f(r) + \left(1 - f(r)\right) \frac{c_0}{r}, \tag{4.8}$$

where V_0 is the maximal depth of the attractive potential and L is the length-parameter of the harmonic oscillator potential, while $K_0 = \frac{c_0}{V_0 L} + 2$.

The primary free parameters of the models are those of the Woods-Saxon and harmonic oscillator terms: a, V_0, L. The other two inner parameters can be expressed with them: $K_0 = \frac{c_0}{V_0 L} + 2$ and $R = \frac{\sqrt{2}L}{\sqrt{K_0}}$.

After writing the Schrödinger equation in spherical coordinates, since the problem is spherically symmetric, it can be divided into a radial part and an angular part. Including a centrifugal potential with angular momentum quantum number ℓ, having been obtained from the eigenequation of the angular momentum operator, the radial Schrödinger equation is achieved

$$\hat{H}_0^{\ell} \Phi_0(r) = \left(\frac{-\hbar^2}{2M} \frac{\mathrm{d}^2}{\mathrm{d}r^2} + \hat{V}(r) + \frac{\hbar^2 \ell \left(\ell + 1\right)}{2Mr^2} \right) \Phi_0(r) = E \Phi_0(r), \tag{4.9}$$

where $\hat{V}(r)$ denotes the possible mean-field nuclear potentials (in this study the $\hat{V}_{\mathrm{WOC}}$ and $\hat{V}_{\mathrm{WSC}}$; and where $\Phi_0(r)$ is the time-independent radial wavefunction. In this work explicit calculations are carried out considering only spherically symmetric nuclei with $\ell = 0$, thus allowing for the s-wave approximation and the neglect of the centrifugal potential.

Substituting the $\ell = 0$ order specific nuclear potential $\hat{V}_{\mathrm{WOC}}$ or $\hat{V}_{\mathrm{WSC}}$ to the Hamiltonian in equation (4.9) $\hat{H}_0(r) = \frac{-\hbar^2}{2M} \frac{\mathrm{d}^2}{\mathrm{d}r^2} + \hat{V}(r)$ the $\ell = 0$ time-independent Schrödinger equation of the alpha cluster in the mean-field potential is obtained:

$$\hat{H}_0 \Phi_0(r) = E \Phi_0(r). \tag{4.10}$$

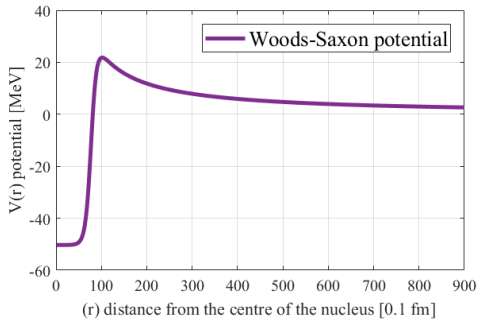

(a) *Coupled Woods-Saxon and Coulomb type mean-field nuclear potential*

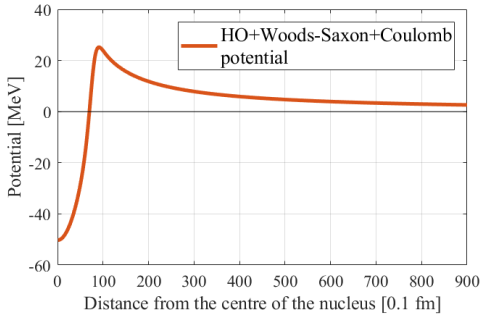

(b) *Coupled Woods-Saxon weighted by harmonic oscillator and Coulomb type mean-field nuclear potential*

Figure 4.1: *Mean-field nuclear potentials*

4.3.1 Quasi-classical derivation of the tunneling width: the conventional tunneling picture and the Gamow factor

Examining the problem of alpha decay, Gamow found that the probability of a particle passing through the potential barrier (the probability of being on the other side of the barrier) is non-zero and can be clearly characterized by the so-called Gamow factor (G), which depends on the potential [Gamow, 1928]: the transition probability (the transmission coefficient) is $T = e^{-2G}$, where G is the integral of the potential-dependent wave number (obtained by solving the time-independent Schrödinger equation) as follows:

$$G = \int_0^L k(\mathbf{r})\mathrm{d}\mathbf{r}, \tag{4.11}$$

where the integration is performed over the region where $Q < V(r)$.

The regular depiction of a cluster state in a typical nuclear (mean-field) potential is shown in Figure 4.2.

The alpha cluster has positive energy, while the energy of the bound states are negative, resulting in a "strange" state that describes the alpha cluster. This is the quasi-stationary (quasi-bound) state, which has a finite lifetime (unlike stationary states).

According to the conventional understanding of decay phenomena, the preformed alpha cluster in the quasi-bound state can escape from the nucleus through quantum mechanical tunneling. It is important to note again that the individual process of alpha-tunneling in the two-step picture can be modelled by the mean-field method. In the following I aim to briefly express the regular mean-field description of alpha tunneling using the traditional hermitian quantum mechanical framework to calculate the transmission coefficient associated with

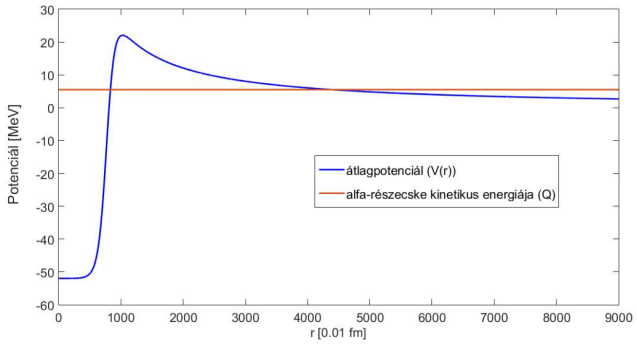

Figure 4.2: *Typical depiction of the alpha-cluster energy level in a quasi-bound state with positive real energy in the Woods-Saxon and Coulomb-type nuclear mean-potential $V(r) = V_{\mathrm{WSC}}$, see equation 4.6.*

the Gamow factor in a quasi-classical picture as the transmission coefficient is proportional to the transition probability per unit time (the decay constant).

In scattering theory, the transmission coefficient (η) is given by the ratio of the transmitted (j_{trans}) and incoming (j_{inc}) currents:

$$\eta = \frac{\left\|\mathbf{j}_{\mathrm{trans}}\right\|}{\left\|\mathbf{j}_{\mathrm{inc}}\right\|}. \tag{4.12}$$

According to elementary Hermitian quantum mechanics, an operator for the current can be derived and defined from the time-independent Schrödinger equation (in the absence of external time-dependent excitation, the problem of alpha decay is described by the non-relativistic, time-independent Schrödinger equation, see 4.3) and its adjoint in accordance with the "quantum-classical" correspondence:

$$\mathbf{j} = \frac{\hbar}{2M\mathrm{i}} \left(\Phi^* \nabla \Phi - \Phi \nabla \Phi^*\right), \tag{4.13}$$

while the ρ probability density emerges as

$$\rho \equiv |\Phi|^2 \tag{4.14}$$

describing the probability of finding a quantum object of mass M, represented by the wave-function Φ, in a given region of phase space. According to the definition of classical current (in the case of plane waves) $\mathbf{j} \approx \rho \mathbf{v}$, where $\mathbf{v}$ can be identified with the object's velocity (or group velocity) that is related to the classical momentum $\mathbf{k} = \mathrm{M}\ \mathbf{v}$. Thus, the expression for the transmission coefficient significantly simplifies to:

$$\eta \approx \frac{|\Phi_{\mathrm{trans}}|^2 k_{\mathrm{trans}}}{|\Phi_{\mathrm{inc}}|^2 k_{\mathrm{inc}}}. \tag{4.15}$$

Let us estimate the transmission probability for the three-dimensional central nuclear potential introduced in 4.3. For a general central potential $V(r)$ being

dependent on a continuous parameter, the transmission coefficient (exploiting isotropy $|\Phi|^2 = |R(r)|^2|Y|^2$) reads:

$$\eta = \frac{\int |R(r)_{\text{trans}}|^2 r^2 k_{\text{trans}} dr \int d\Omega |Y|^2}{\int |R(r)_{\text{inc}}|^2 r^2 k_{\text{inc}} dr \int d\Omega |Y|^2} = \frac{\int |R(r)_{\text{trans}}|^2 r^2 k_{\text{trans}} dr}{\int |R(r)_{\text{inc}}|^2 r^2 k_{\text{inc}} dr}. \tag{4.16}$$

From the viewpoint of tunneling, the Coulomb potential is the interesting part of the nuclear potentials (4.8) and (4.6), hence, for the sake of simplicity, let us consider only the Coulomb potential V_C and the $\ell = 0$ case (the s-wave approximation):

$$V_C(r) = \frac{c_0}{r}, \tag{4.17}$$

where the previously introduced constant c_0 contains the atomic number of the daughter nucleus Z and some typical constants of nuclear physics: $c_0 = 2 \cdot Z \cdot \alpha\hbar c$ with α denoting the fine-structure constant at vacuum energy. The Gamow factor emerges as an integral of $k_0(r)$, where the integration limits (a, b) are determined by the (real) energy (E) of the cluster to be described:

$$G = \int_a^b dr \sqrt{\frac{2m}{\hbar^2}\left(\frac{c_0}{r} - E\right)} = \sqrt{\frac{2m}{\hbar^2 E}} 2Z\alpha\hbar c \left[\arccos\left(\sqrt{\frac{a}{b}} - \sqrt{\frac{a}{b}\left(1 - \frac{a}{b}\right)}\right)\right], \tag{4.18}$$

where the second expression is an approximate analytical closed form, from which the transmission coefficient can be calculated as $\eta \sim e^{-2G}$, and from that, the half-life can also be given according to the aforementioned relationship. This estimated value for ^{212}Po is $T = 3\mu s$ at an energy of $E = 8.77$ MeV. The above formula establishes a mathematical relationship between the half-life of alpha decay and the energy of the alpha cluster. The postulate of early nuclear physics models of alpha decay was that the higher the energy of the cluster, the more likely the decay (in the tunneling picture, we get closer to the height of the potential barrier; thus, with the decrease of the barrier, the decay probability increases, see spontaneous fission), so the shorter the half-life assigned to the decay. This expectation was experimentally supported, by the Geiger-Nuttal law introduced in Section 4.1.

4.3.2 Non-hermitian quantum-mechanical, non-perturbative derivation of the tunneling width: the complex energy picture

In this section the alpha cluster is investigated in the particular frame of quasi-stationary states. In this frame the alpha cluster occupies a special quasi-stationary state that possesses complex energy eigenvalue $E_{\mathrm{qs}} = E_0 - \mathrm{i}\frac{\Gamma}{2}$, the imaginary part of which yields the lifetime $\tau \propto \frac{1}{\Gamma}$ of the state, while the real part E_0 is positive definite. The goals is to determine the mean-field tunneling lifetime of the quasi-stationary state of the alpha cluster through the complex energy.

As it was deeply elaborated in [Szilvasi et al., 2022] and in Chapter 2 and the embedded papers, the inner property of potentials with the characteristics of potential barriers such as $\hat{V}_{\mathrm{WOC}}$ in (4.8) makes the Hamiltonian $\hat{H}_0$ non-Hermitian and naturally allows for the existence of complex energies in the total spectrum. First, the complex part of the spectrum must be uncovered (numerically) and the eigenfunctions must get regularized by non-Hermitian quantum-mechanical techniques.

The peculiarity of the non-Hermitian quantum mechanical description of the alpha-cluster is that the lifetime corresponding to the alpha cluster in the nucleus might be derived directly from the complex spectrum of a non-Hermitian operator. By applying complex scaling on the time-independent radial Schrödinger equation (4.10)

$$\hat{H}_0^{\theta}\Phi_0^{\theta}(r) = E\Phi_0^{\theta}(r), \tag{4.19}$$

where the $\hat{H}_0^{\theta}$ complex-scaled Hamiltonian operator shall be specified with the appropriate mean-field nuclear potentials introduced in 4.3. The possible set of eigenvalues E of the now complex-scaled Hamiltonian operator $\hat{H}_0^{\theta}$ is extended into the complex plane, where the parameter θ is the scaling parameter of the transformation and is presumed to be real throughout this paper [Szilvasi et al., 2022]. The eigenfunctions of $\hat{H}_0^{\theta}$ associated with complex eigenvalues are regularized and square-integrable with respect to the *c-product*, the special inner product of the Hilbert space regarding the transformed Hamiltonian. To achieve the quasi-stationary solutions and discrete eigenenergies of (4.19), generally one shall use numerical discretization techniques. For this purpose, the complex spectral calculation is applied that was introduced in Subsection 2.2.1 Chapter 2. Following the methodology using the expressions (2.21) and (2.22) the Hamiltonian matrix elements are calculated accordingly. For the problem of (4.9) a suitable choice for the basis function set $w_j(r)$ is the following harmonic

oscillator type function

$$w_j(r) = \frac{1}{r} e^{-\frac{r^2}{2b^2}} L_j^{1/2}\left(\frac{r^2}{b^2}\right) \frac{1}{b^{3/2}} \left[\frac{2\tilde{\Gamma}(j+1)}{\tilde{\Gamma}(j+3/2)}\right]^{1/2}, \tag{4.20}$$

with L_j denoting the j-th Laguerre polynomial and $\tilde{\Gamma}$ is the Gamma function. Specifically in the case of 4.8, performing computations with this set is rather favored, since the attractive part of the nuclear potential is built up with a harmonic oscillator-type potential, thus the convergence of the numerical computation is improved.

The relevant properties of discrete complex-scaled spectra regarding quasi-stationary solutions (decaying-states) are thoroughly explored in 2.2.1. As a reminder, the key distinguishing characteristic between bound and quasi-stationary states versus the complex, rotated, discretized continuum lies in the behaviour of their eigenvalues relative to the scaling parameter θ. In theory, the eigenvalues of bound and quasi-stationary states are robust against changes in θ, whereas those of the continuum states vary with it. Additionally, the distinctive features of quasi-stationary energies from the bound-state energies are their complex nature and their positive real part.

From the nuclear theory perspective, the quasi-stationary subset of the discretized spectrum represents the possible energy-levels ($\mathrm{Re}(E_{\mathrm{qs}}) = E_0$) the alpha cluster of the *decaying* radioactive isotope might occupy in the nucleus with the corresponding imaginary part (Γ) yielding the lifetime of that nuclear energy-state.

Complex spectral calculations; demonstration and analyzes of the properties of the numerical method

In practice, by tuning the free parameters of the nuclear potential, for a given isotope with atomic number Z and mass number A, the experimentally known alpha energies (the real part of the complex energy) can be estimated *with* their corresponding lifetime *directly* from the non-Hermitian spectrum, numerically by the complex spectral calculus. For example, for the 4.8 spherical nuclear potential, the complex-scaled Hamiltonian is the following:

$$\hat{H}_0^{\theta} = \frac{-\hbar^2}{2M}\frac{\mathrm{d}^2}{\mathrm{d}r^2}\mathrm{e}^{-2\mathrm{i}\theta} + V_0\left(\frac{K_0}{L^2}r^2\mathrm{e}^{2\mathrm{i}\theta} - 2\right) f(r\mathrm{e}^{\mathrm{i}\theta}) + \left(1 - f(r\mathrm{e}^{\mathrm{i}\theta})\right)\frac{c_0\mathrm{e}^{-\mathrm{i}\theta}}{r}. \tag{4.21}$$

The experimentally known real energy $E_0 = \mathrm{Re}(E_{\mathrm{qs}}) = 8.9$ MeV is found in the spectrum upon setting the Woods-Saxon free parameters (a, V_0) as depicted in Figure 4.3 and fixing the oscillator length parameter L in order to obtain the common value of the nuclear radius R of ^{212}Po. The width Γ corresponding

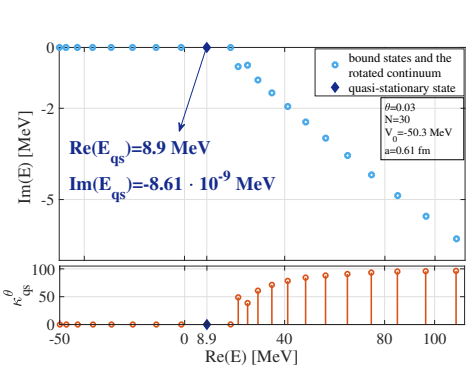

(a) *CS-spectrum produced by the Woods-Saxon type nuclear potential*

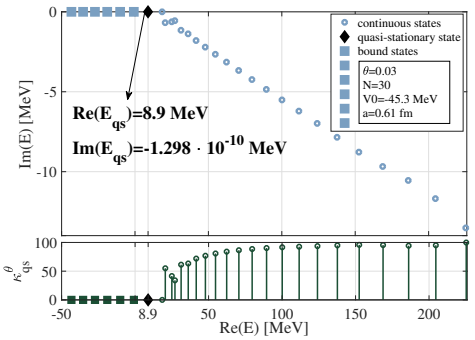

(b) *CS-spectrum produced by the harmonic oscillator-weighted Woods-Saxon type nuclear potential*

Figure 4.3: *Complex spectra achieved by the complex diagonalization procedure*

to the real energy, identified in the figure, is achieved using $N = 30$ basis functions. While the value of the real energy is affected mostly by the choice of the Woods-Saxon free parameters, the numerical value of Γ even more strongly depends on the choice of the basis function parameter b [Szilvasi et al., 2022]. The typical widths of alpha-decaying isotopes are many orders of magnitude smaller than the real energies ($\mathrm{Re}(E_{\mathrm{qs}})$), more specifically are of the $10^{-14} - 10^{-29}$ MeV interval, thus it is numerically challenging to extract the small values of Γ with the expected numerical precision, even with regards to the proper order of magnitude. Generally, the larger the number of basis functions the higher the precision, although it requires greater numerical capacity.

As an example, results for Γ are presented using harmonic oscillator basis functions in Figure 4.3. Computations with $N = 30$ and $b = 1.35$ fm yield $\Gamma = 2.5968 \cdot 10^{-10} \pm 10^{-13}$MeV for the WOC-potential, while a slightly different result is obtained for the WSC-potential (Figure 4.3a) with $b = 1.31$ fm and $N = 30$.

An error of the computation might be attached to Γ from the following considerations: since the imaginary energies of bound states should be zero in principle, their difference from zero due to numerical deviations indicates the magnitude of the error of the computation given that the computed imaginary parts of the bound-state energies are significantly smaller than that of the quasi-stationary energies. It shall be emphasized again that the discrepancy between the numerically calculated value of the lifetime of the alpha cluster of ^{212}Po and the measured value of the lifetime of ^{212}Po is mainly due to the simplified mean field representation of the nuclear interactions which is not sufficient to thoroughly treat the peculiarities of isotopes stemming from the nuclear fine

structure, see equation 4.2. Although, this deficiency of the nuclear model does not affect the to-be-presented description of laser-nuclei interaction, since the external laser field is not expected to alter the structure of the nuclei, as it is explained in [D. Kis et al., 2018] and referred to in [Szilvasi et al., 2022].

The precision of the numerical method was tested. The computations were carried out by the symbolic toolbox of Matlab and by the numerical approximation tools of Python.

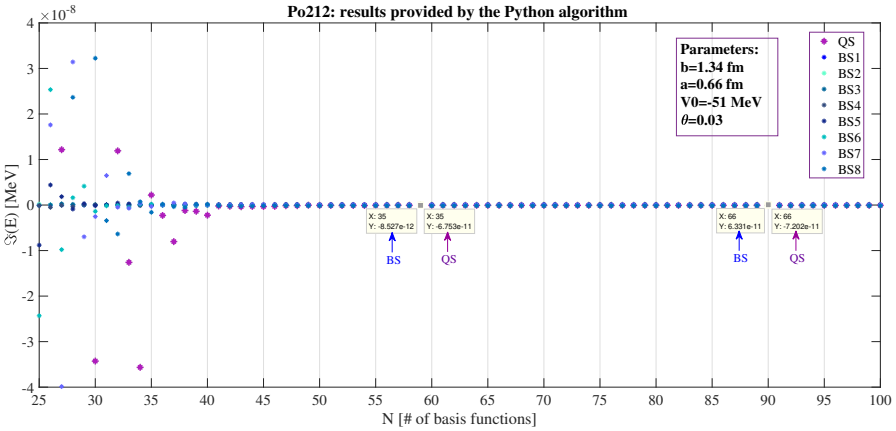

Figure 4.4: *The convergence of the imaginary energies of bound and quasi-stationary states provided by the Python algorithm*

The integrals over the spatial coordinate r in the matrix elements of $\hat{H}^{\theta}$ are generally functions varying according to higher powers of the spatial coordinate. The more basis functions used in the computation, the higher powers appear in the matrix elements. It is due to this, that while increasing the basis number N, it is only up to a certain value of N that the accuracy of the numerical results improve. Beyond a specific N, terms start to appear in the matrix elements that Matlab's symbolic toolbox cannot estimate with sufficient accuracy in numerical calculations, hence the computation stops. Certainly, this depends on the numerical capacity also. This maximal N was found to be $N = 31$, the demonstrative calculations were carried out with $N = 30$ according to the systematic displayed in Figure 4.5, which is supported by the numerical results provided by Python.

The python algorithm uses numerical integration techniques to solve the eigenvalue problem. This purely numerical method enables the computations to go further in N, hence the convergence of the results could be tested. It is indicated in Figure 4.4.

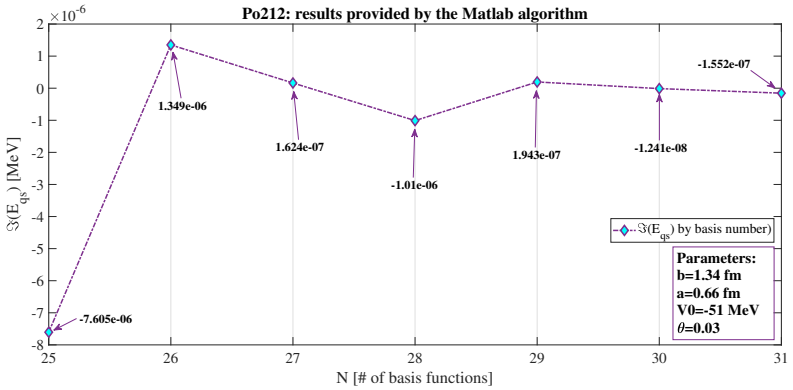

(a) *The imaginary part of the complex energy as a function of the number of basis N provided by Matlab.*

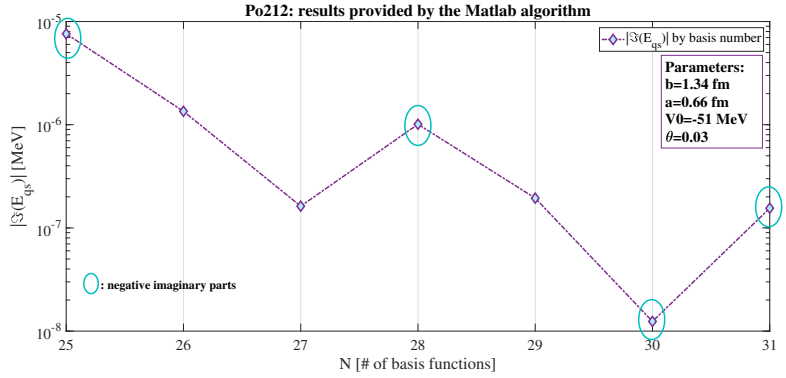

(b) *The absolute value of the imaginary parts on a log-scale graph for a given range of basis number. Similar systematics was achieved by the Python algorithm for the range* $N = 25 - 31$.

Figure 4.5: *Basis-function dependence of the quasi-stationary imaginary parts*

4.3.3 Studying the quasi-stationary alpha-states in even-even heavy isotonic chains with non-hermitian spectral calculations

The non-hermitian approach sets the stage for substituting the usual tunneling picture by a finite-lifetime quasi-stationary cluster-state that naturally possesses a finite (non-zero) decay width in its complex eigenenergy, which is directly elicited by solving the non-hermitian time-independent Schrödinger equation. In this section my goal is to show that such a description is suitable to serve as a feasible approximation for the half-life of special short-lifetime, alpha-decaying isotones. In this section the details of the specific non-hermitian calculation of the "tunneling-lifetime" and how it provides information about the total "decay-lifetime" of isotones in certain isotone-groups is presented.

By the non-hermitian spectral calculation, the mean-field tunneling width can be extracted to a certain accuracy provided by the computational apparatus. Typically small lifetimes (not larger than microseconds) are estimated correctly, since, smaller lifetime is equivalent to larger width that is computationally favorable. In Section 4.2 I proposed that for alpha decay the total decay width Γ^{decay} is manufactured in a way to reflect the two independent processes producing it: $\Gamma^{\text{decay}} = s_0\Gamma$, where Γ is, again, the mean-field tunneling width, while s_0 encodes the nuclear fine-structure information (and also contains the uncertainties arising from the determination of the mean-field tunneling width). Moreover, one can observe certain regularities in some properties of heavy isotones. Particular heavy, alpha-decaying, short-lifetime isotones (the $A \in [210, 224]$ island of the isotope map) are organized into groups by their Q-values as a function of the corresponding Coulomb factors ($\frac{Z^2}{A}$) (see Figure 4.8), and also with respect to the half-lives. It is expected that for one N-isotone chain the s_0 structure factor is near constant, as in, the ratio $\Gamma^{\text{decay}}/\Gamma$ is close to 1 for the members of the given istone group. This postulate is supported by the idea that the Coulomb tunneling process of alpha decay is predominantly affected by the height of the Coulomb barrier that is principally sensitive to the number of protons (Z), while clustering (and all the nuclear structure-based phenomena) is exceedingly influenced by the neutrons. Hence, it is anticipated that by extensively analysing numerically (using the spectral calculation tools on the mean-field Hamiltonian) the small alterations of the Coulomb barrier moving from one element of a given isotone chain to another, one can track down the mean-field tunneling widths of the nuclei. Compering them with the experimental total decay widths, the assumption about the s_0 structure function can in theory be validated.

The main goal is to exploit this special trait in order to prove the applicability of

the aforementioned non-hermitian computational method of the alpha-tunneling lifetime. Another aim is, furthermore, to present a tool to show how the life-time (half-life) of not-yet experimentally detectable nuclei can be estimated from NHQM-type (Non-hermitian quantum-mechanical) spectral calculations.

From now on, let us restrict our attention to even-even isotones in order to be able to regard the problem spherically symmetric and use the exact formulae introduced in the previous subsection 4.3.2. By this philosophy, the even-even nuclei in the $N = 128, 130, 132$ isotone chains are subjected to numerical investigation.The numerical values of the relevant properties of these nuclei are collected in Table 4.1.

N=128				N=130				N=132			
Isotone	Q_α [MeV]	T [μs]	Γ^{decay} [MeV]	**Isotone**	Q_α [MeV]	T [μs]	Γ^{decay} [MeV]	**Isotone**	Q_α [MeV]	T [μs]	Γ^{decay} [MeV]
^{212}Po	8.954	0.2939	$1.552 \cdot 10^{-15}$	^{214}Po	7.833	163.47	$2.79 \cdot 10^{-18}$	^{218}Rn	7.262	33750	$1.35 \cdot 10^{-20}$
^{214}Rn	9.208	0.259	$1.762 \cdot 10^{-15}$	^{216}Rn	8.198	45	$1.014 \cdot 10^{-17}$	^{220}Ra	7.59	18000	$2.53 \cdot 10^{-20}$
^{216}Ra	9.526	0.161	$2.834 \cdot 10^{-15}$	^{218}Ra	8.54	25.91	$1.761 \cdot 10^{-17}$	^{222}Th	8.133	1964	$2.323 \cdot 10^{-19}$
^{218}Th	9.849	0.122	$3.740 \cdot 10^{-15}$	^{220}Th	8.973	10.4	$4.387 \cdot 10^{-17}$	^{224}U	8.6228	840	$5.431 \cdot 10^{-19}$
				^{222}U	9.48	4.7	$9.707 \cdot 10^{-17}$				

Table 4.1: *The experimental data of the isotones [jnds2020]*

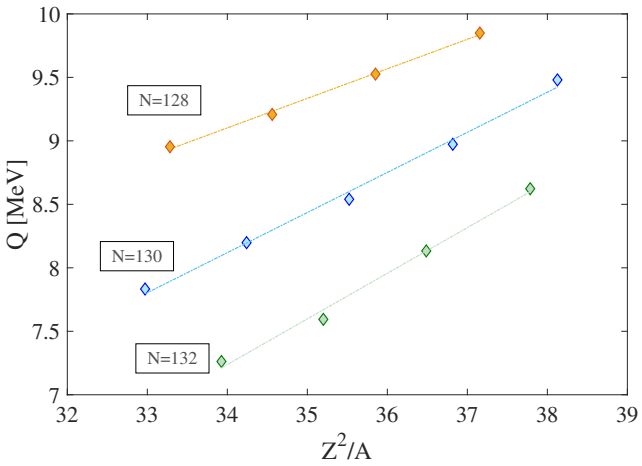

Figure 4.6: *The experimental Q-values of the three even-even isotone islands as a function of the Coulomb factor*

Determination and investigation of the properties of the tunneling widths

One of the main goals of this section is to justify the hypothesis (4.2) in the case of three appropriately chosen isotone groups by numerical calculations and analysis. An additional purpose is to validate the previously introduced [Szilvasi et al., 2024] and above-presented non-hermitian, mean-field cluster-core model for estimating the mean-field alpha cluster lifetime. The first goal can be accomplished by the approximation of the s_0 nuclear structure factor from the $\Gamma - \Gamma^{\text{decay}}$ plots after the numerical production of the mean-field widths. In order to attempt to validate the calculation framework for Γ, specific empirical trends present in the case of the three isotone groups (according to the experimental data available) shall be investigated in the case of the calculated mean-field widths. For the latter purpose, it is investigated whether the Geiger-Nuttal law is exhibited also by the calculated mean-field widths for all the three alpha-decaying isotone groups.

In order to numerically yield the complex spectra of the mean-field cluster-core Hamiltonians of all the nuclei under investigation and find the quasi-stationary eigenenergies, two different numerical approaches were used to calculate the matrix elements 2.22. In the first case the matrix elements were calculated using the symbolic toolbox of Matlab, while in the second case, a numerical process, written in Python provided the solutions.

The overall mean-field NHQM-model contains three tunable parameters (a, V_0, b). In order to identify the quasi-stationary alpha states (through their complex eigenenergy) in the spectrum of the Hamiltonians corresponding to each isotones, these parameters must be tuned. The mean-field nuclear potential (4.6) has two free parameters, a the diffusion parameter and V_0 the depth of the potential, the range of the possible values of which are dictated by experimental clues. There is an additional parameter due to the discretization of the problem: the harmonic oscillator basis parameter b. Provided that one is able to execute the numerical computation of the matrix elements up to high basis number (N), the basis parameter should only moderately influence the end results. However, in this case the computational performance limits the maximal basis number to $N = 30$, hence the appropriate choice of b is crucial [Szilvasi et al., 2022 ; Szilvasi et al., 2024]. Eliciting the complex energy requires precise numerical analysis on the basis of the three parameters.

The parameter tuning is primarily governed by the experimentally known alpha energies Q_α (Table 4.1) which are essentially used as input parameters for this model, and also by the premise that within an isotone chain the nuclear potential parameters shall differ slightly.

Relying on the latter assumption, in the case of each single isotone chain

the diffusion parameter and the oscillator parameter is fixed. In the manner of this, for each isotone groups one shall fit the real part of the quasi stationary alpha energies to the Q_α values, in order for this the V_0 depth parameter of the nuclear potential is migrated in the range of $[40 - 55]$MeV. Once the anticipated alpha energy is found, the corresponding Γ mean-field width can be calculated from the imaginary part of the eigenvalue. The computation of the mean-field width was performed for all three isotone groups, the numerical results are summerized in Tables 4.2, 4.3, 4.4.

After matching the calculated mean-field width to the experimentally known total decay widths the s_0 structure factor could be calculated for all single isotones, and is estimated by linear fitting to the $\Gamma - \Gamma^{\text{decay}}$ data, that is depicted in Figure 4.7. One can deduce from the data that the anticipated linear trend is present in the case of all series. Although, as illustrated on the figures, one can observe that the smallest mass-number nuclei of each series are quite distinct. This observation suggests to exclude these nuclei from the fitting, and a possible explanation for this feature could be that as the mass number decreases for an isotone series, the Z/N ratio also decreases, which signifies the increment of the relative neutron number. The higher relative number of neutrons generally implies stronger nuclear structural effect that, on the terms of this model, could result in the distinction of the hypothetical structure factor s_0.

Executing the linear fit on the three largest mass-number nuclei of the groups, one can conclude that for $N = 128$ the calculated data is well-fitting on a line with less than 4% relative error. This indicates the approximately constant nature of the structure factor for these isotones. However, in the case of $N = 130$, $N = 132$ isotone chains, the calculated mean-field widths do not fit as smoothly on a line as for the $N = 128$ group, although the anticipated trend is still clearly exhibited with the relative error of the slopes being less than 30%. An obvious explanation for the declining trend could be found by taking into account the numerical uncertainties of the mean-field width computation, that is certainly executed with a given systematic error. Decreasing the numerical error by more proper computational performance could increase the goodness of the solutions. It shall be noted that higher neutron-number isotone chains correspond to longer decay lifetimes.

Another demonstration of the calculation framework for the mean-field widths is provided in Figure 4.8. Here, the empirical Geiger-Nuttal law (which describes the observed linearity of the $\log(T) - \sqrt{Q_\alpha}$ relationship for alpha-decaying nuclei) is shown to be a good approximation for the calculated mean-field tunneling widths and the real alpha energies. From the perspective of quasi-stationary states (representing the state of the preformed alpha cluster within

the mean-field potential), this law can be interpreted as a special relationship between the real and imaginary parts of the complex eigenenergy.

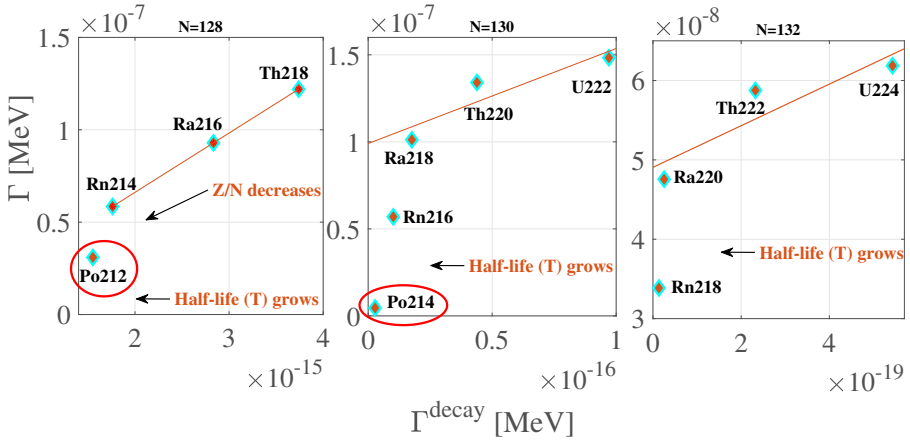

Figure 4.7: $\Gamma - \Gamma^{\text{decay}}$ *plots for all three isotone series. In this figure the calculated mean-field width* (Γ) *were produced by Python and the linear fit is performed by Matlab. During the calculations of the tunneling widths* $\theta = 0.03$ *scaling angle was used, and the nuclear radius was defined as:* $R = r_0 A^{1/3}$, *where* $r_0 = 1.3118\,fm$. *The linear trend is present for all series up to 30% relative error when the smallest mass-number isotones are excluded.*

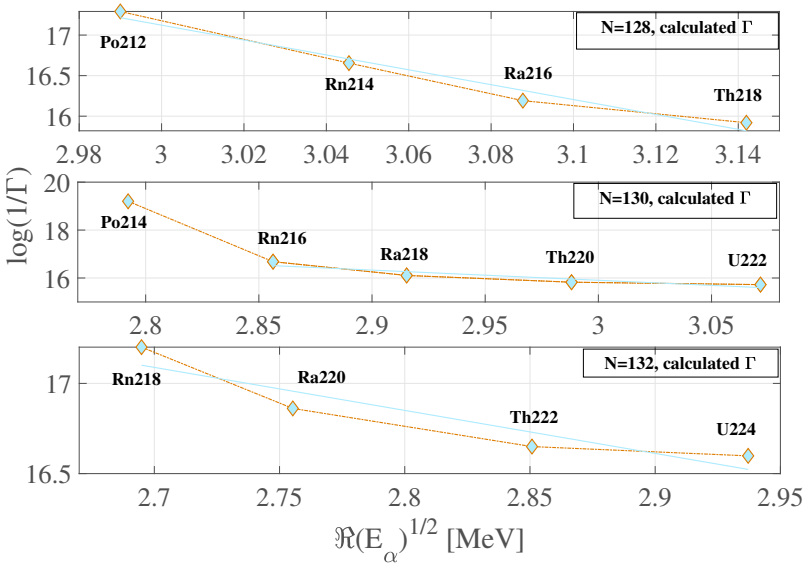

Figure 4.8: *Geiger-Nuttal law for all isotone groups with the mean-field tunneling widths and the computed real alpha energies.*

N=128								
	Matlab				Python			
	a=0.66 fm				a=0.66 fm			
	b=1.34 fm				b=1.34 fm			
Isotone	$\Re(E_\alpha)$ [MeV]	Γ [MeV]	V_0 [MeV]	Γ^{decay}/Γ	$\Re(E_\alpha)$ [MeV]	Γ [MeV]	V_0 [MeV]	Γ^{decay}/Γ
^{212}Po	8.94	$17 \cdot 10^{-9}$	51	$9.123 \cdot 10^{-8}$	8.949	$30.94 \cdot 10^{-9}$	51.38	$5.0162 \cdot 10^{-8}$
^{214}Rn	9.275	$53.5 \cdot 10^{-9}$	50.4	$3.29 \cdot 10^{-8}$	9.203	$58.49 \cdot 10^{-9}$	50.88	$3.0125 \cdot 10^{-8}$
^{216}Ra	9.534	$84.7 \cdot 10^{-9}$	49.9	$3.131 \cdot 10^{-8}$	9.520	$92.93 \cdot 10^{-9}$	50.30	$3.0496 \cdot 10^{-8}$
^{218}Th	9.872	$116.8 \cdot 10^{-9}$	49.3	$2.44 \cdot 10^{-8}$	9.843	$122 \cdot 10^{-9}$	49.72	$3.0656 \cdot 10^{-8}$

Table 4.2: *The applied parameters and the calculated alpha energies ($\Re(E_\alpha)$) and mean-field widths (Γ) of the isotones in group N=128.*

N=130								
	Matlab				Python			
	a=0.66 fm				a=0.66 fm			
	b=1.34 fm				b=1.34 fm			
Isotone	$\Re(E_\alpha)$ [MeV]	Γ [MeV]	V_0 [MeV]	Γ^{decay}/Γ	$\Re(E_\alpha)$ [MeV]	Γ [MeV]	V_0 [MeV]	Γ^{decay}/Γ
^{214}Po	7.841	$6.7 \cdot 10^{-9}$	52.05	$4.161 \cdot 10^{-10}$	7.797	$4.6 \cdot 10^{-9}$	52.49	$6.094 \cdot 10^{-10}$
^{216}Rn	8.136	$56.3 \cdot 10^{-9}$	51.4	$1.802 \cdot 10^{-10}$	8.158	$56.9 \cdot 10^{-9}$	51.86	$1.781 \cdot 10^{-10}$
^{218}Ra	8.549	$102.7 \cdot 10^{-9}$	50.8	$1.715 \cdot 10^{-10}$	8.499	$101.2 \cdot 10^{-9}$	51.25	$1.74 \cdot 10^{-10}$
^{220}Th	8.965	$135.2 \cdot 10^{-9}$	50.1	$3.244 \cdot 10^{-10}$	8.929	$134.1 \cdot 10^{-9}$	50.53	$3.271 \cdot 10^{-10}$
^{222}U	9.46	$149.4 \cdot 10^{-9}$	49.3	$6.497 \cdot 10^{-10}$	9.435	$148.4 \cdot 10^{-9}$	49.71	$6.543 \cdot 10^{-10}$

Table 4.3: *The applied parameters and the calculated alpha energies ($\Re(E_\alpha)$) and mean-field widths (Γ) of the isotones in group N=130.*

Prediction of unknown half-lives: estimating the half-life of $A = 220, Z = 92$ nucleus

A possible direction to exploit the estimation of the structure factor of the isotone series could involve the potential predictions about the widths and half-lives of certain experimentally not-yet-known nuclei. Such nucleus is the ($A = 220, Z = 92$) uranium for which no experimental data is present in the literature. According to our predictions, this nucleus could undergo alpha decay and belong to the N=128 isotone group, potentially having the shortest half-life. Based on this assumption, the structure factor estimation for the N=128 isotonic chain can be applied to predict the half-life of the U-220 nucleus. To achieve this, linear regression of the Γ-Γ^{decay} data will be performed. Initially, the mean-field width (Γ) of the ($A = 220, Z = 92$) nucleus needs to be determined from the complex spectrum. The complex eigenenergy of this nucleus will be determined by extrapolating the α-particle energy (Q_α) from experimental data shown in Figure 4.6 ($Q_\alpha = 10.14$ MeV), followed by tuning the potential depth parameter V_0 such that the real part of the complex energy ($\Re(E_\alpha)$) matches Q_α. The computed value of the mean-field tunneling width for U-220 is $\Gamma_U = 140.2 \times 10^{-9}$ MeV with $V_0 = 49.18$ MeV.

Accurate calculation of the mean-field widths in this series provides a solid

N=132								
	Matlab				Python			
	a=0.7 fm				a=0.7 fm			
	b=1.34 fm				b=1.34 fm			
Isotone	$\Re(E_\alpha)$ [MeV]	Γ [MeV]	V_0 [MeV]	Γ^{decay}/Γ	$\Re(E_\alpha)$ [MeV]	Γ [MeV]	V_0 [MeV]	Γ^{decay}/Γ
^{218}Rn	7.299	$34.7 \cdot 10^{-9}$	52.32	$3.9 \cdot 10^{-13}$	7.262	$33.86 \cdot 10^{-9}$	52.75	$3.99 \cdot 10^{-13}$
^{220}Ra	7.602	$47.86 \cdot 10^{-9}$	51.77	$5.3 \cdot 10^{-13}$	7.592	$47.56 \cdot 10^{-9}$	52.16	$5.33 \cdot 10^{-13}$
^{222}Th	8.155	$58.83 \cdot 10^{-9}$	51	$39.49 \cdot 10^{-13}$	8.127	$58.76 \cdot 10^{-9}$	51.31	$39.53 \cdot 10^{-13}$
^{224}U	8.625	$61.4 \cdot 10^{-9}$	50.14	$88.46 \cdot 10^{-13}$	8.627	$61.86 \cdot 10^{-9}$	50.51	$87.8 \cdot 10^{-13}$

Table 4.4: *The applied parameters and the calculated alpha energies ($\Re(E_\alpha)$) and mean-field widths (Γ) of the isotones in group N=132.*

basis for estimating the unknown decay width and half-life via linear regression, as the $\Gamma^{\text{decay}}(\Gamma)$ function exhibits linearity with less than 4% relative error for this series (indicating that the structure factor can be considered approximately constant). The result of the linear regression is shown in Figure 4.9, where the estimated half-life is $T_{\text{U}}^{\text{est}} = 141.7 \pm 5.3$ ns. The error reflects the standard error of the linear regression. It is noteworthy that the numerical values presented above were obtained using the Python algorithm; Matlab also produced $T_{\text{U}}^{\text{est}} = 139.6$ ns, falling within the estimated error interval, that is not surprising according to the conclusion of 4.3.2 drawn by analysing the two numerical approaches. From the obtained numerical results, the final estimate for the half-life can be given using the weighted average and its corresponding standard deviation: $T_{\text{U}}^{\text{est}} = 140.9 \pm 4.3$ ns.

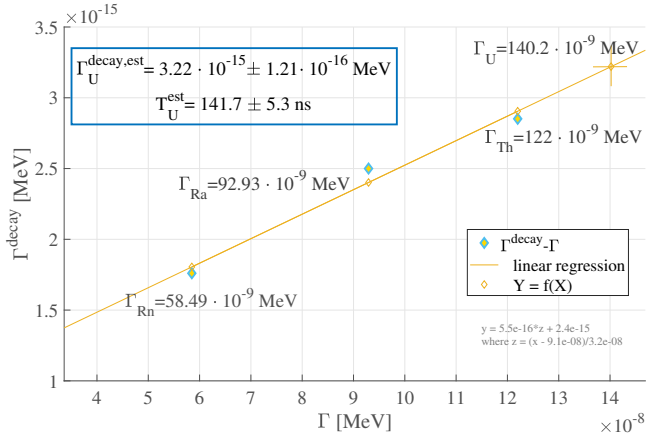

Figure 4.9: *Estimation of the half-life of U-220 nucleus from fitting on the three isotones with the largest mass number (A) of N=128 group. The mean-field tunneling widths used are produced by the Python algorithm, while the linear regression was executed by Matlab fitting. The predicted value of the half-life of U-220 is: $T_U^{\text{est}} = 141.7 \pm 5.3$ ns, where the error estimate involves the standard error of the linear regression. The predicted half-life using the mean-field widths computed by Matlab is* 139.6 ns *which falls within the estimated error interval.*

5

Super-intense laser-assisted alpha decay

This chapter addresses the primary objective of this thesis: the investigation of the coupled laser-nucleus system in the context of alpha decay. The previous chapters set the ground for the appropriate description of laser-assisted alpha decay. Drawing from these considerations, the task shall be reformulated as (or specified to): model how a super-intense laser field might influence the mean-field lifetime attached to an alpha cluster.

This chapter provides a thorough and careful exploration of the problem, starting with providing the appropriate conceptual framework of the super-intense laser and nucleus interaction that is examined in Section 5.1. This section focuses on the thorough discussion of the non-relativistic limit in strong-field interactions, particularly emphasizing the importance of the calculation of the ponderomotive potential. I underline the main concepts and present my corollaries in the matter.

Section 5.2 provides a brief insight to the investigation of laser-assisted alpha decay within the traditional Hermitian quantum-mechanical calculation scheme. I present my analytical and numerical results obtained for the interaction with continuous-wave laser. In Section 5.3 I explain how this approach is limited to time-periodic external drivings.

In Section 5.4 I turn to the approach established in the previous chapters, which aims to solve the problem using the non-hermitian quantum-mechanical framework, that is the natural framework for quasi-stationary states, the description of which is mathematically compatible with the (t,t')-formalism. In this section I demonstrate my numerical results obtained for the complex-energy shift. I investigate how the relative change of the mean-field tunneling width depends on the parameters of the laser pulse, and how this dependence can be addressed numerically in relation to the photon energy and intensity. Finally, I

intend to show the systematic behavior of the relative change of the lifetime for the nuclei in the $N = 128$ isotonic chain, based on my numerical analysis.

5.1 General properties of the interaction of alpha-decaying nuclei and super-intense lasers

There can be found voluminous literature exploring the theoretical possibilities of laser-assisted alpha decay [Mişicu et al., 2013a ; Mişicu et al., 2013b ; Misicu et al., 2016 ; Delion et al., 2017 ; Bai et al., 2018 ; J. Qi et al., 2019 ; Rehman et al., 2022]. Most of them follow similar line of concept when they provide the conceptual framework for the problem, especially for the description of the interaction. Naturally, the non-relativistic Schrödinger equation is solved within the dipole approximation that is legitimate considering that the relative size of the nucleus and the typical wavelength of the laser light is small enough. However, a great number of these studies operate with the length gauge that is conventionally used in electrodynamics and do not usually address the problem at the limit of the non-relativistic approximation that is closely related to the notion of the ponderomotive potential.

In this section I intend to set the conceptual grounds for the high-intensity laser and alpha-cluster interaction, exploring the limitations of the non-relativistic theory and accentuating the attributes of the many-photon strong-field interaction that manifests in the context of high-intensity laser-induced phenomena such as the complex-energy shift function of the alpha cluster to be presented later on.

5.1.1 Intense-laser driven alpha cluster: which part of the nuclear force is subjected to the laser?

The typical magnitude of alpha-cluster energy levels inside the nucleus are between $4 - 10$ MeV. The experimentally achievable photon energy magnitudes in the super-intense laser experiments planned for the near future are expected in the range of $1 - 1000$ eV. It is evident that a monochromatic field with such energy is not capable of altering the cluster energy enough to excite the alpha cluster to a higher energy level (or, in our model, to a different eigenstate). As a conclusion, the perturbative description of the interaction is justified.

It has already been referred to in 4 that inside the nucleus, considering the mean-field picture, the attractive part of the nuclear force dominates over the electric (Coulomb) part. Estimating the magnitude of the amplitude of the laser

(A_0) by using $E_0 = \frac{E_{\text{ph}}}{\hbar c} A_0$, where $E_0 = \sqrt{\frac{4\pi}{c}}\sqrt{I}$ with I denoting the intensity of the laser field, and compare it to the amplitude of the electric field inside the nucleus (E) at $r = R$, one finds that the amplitudes are comparable. Let the intensity of the laser field be $I = 10^{18} W/cm^2$:

$$E_0 = \sqrt{\frac{4\pi}{c}} \cdot \sqrt{I} \simeq 10^{12} \frac{\sqrt{MeV}}{cm}, \tag{5.1}$$

$$E \simeq 4.7 \cdot 10^{12} \frac{\sqrt{MeV}}{cm}. \tag{5.2}$$

Thus, by these estimations one can state that the effect the laser field has on the nuclear part of the potential can be neglected. Primarily the Coulomb-interaction is exposed to the laser. One might also conclude that a threshold peak-intensity value can be identified for laser-nuclei interaction happening via coupling to the Coulomb potential (influencing the Coulomb potential well). However, it is discussed in the next subsections that upon considering super-high intensity laser fields, one must pay attention to the relation between the intensity and photon energy when investigating problems in certain limits (for example the non-relativistic limit) since the strength of the high-intensity laser coupling depends on the ratio of the photon energy and intensity.

5.1.2 The ponderomotive potential

From the classical physical point of view, whenever charged particles are subjected to some electromagnetic field, during the interaction they experience a - generally nonlinear - force resulting in a harmonic "motion", characterized by a quiver energy, also known as the ponderomotive potential energy. Despite of the indisputable advantage of such an illustrative formulation, it has been established (see for more detail [Reiss, 2014]) that the proper and fundamental interpretation of this energy is the ponderomotive *potential* energy, not a type of kinetic energy.

Following the disciplines of the classical description of a charged particle in some electromagnetic field, the expression for the acquired ponderomotive energy can be derived by considering the force the particle undergoes and calculating the average energy of the particle over a time period. Historically, the ponderomotive potential energy was defined for an electron quivering in a homogeneous electric field. However, the major significance of this quantity appears in the description of interactions by strong-field quantum electrodynamics (SFQED). Phenomena requiring the strong-field model (such as interactions with high-intensity coherent plane-waves) typically start from a relativistic approach, hence entailing the relativistic generalization of the ponderomotive potential.

Originally, the ponderotomotive potential energy term arises from the *vector potential* A^ν [Reiss, 2014]:

$$U_\mathrm{p} = \frac{e^2}{2mc^2} \langle |A^\nu A_\nu| \rangle \,, \tag{5.3}$$

where m is the mass of the charged particle subjected to the high-intensity plane-wave field and the bracket denotes the cycle-average. Specifically, for the interaction of a free electron with a continuous plane-wave:

$$U_\mathrm{p} = \frac{I}{(2\omega)^2} \tag{5.4}$$

with ω photon energy and I (peak) intensity. An effective coupling constant can be defined for charged particle interaction with strong electromagnetic fields. This quantity is also referred to as intensity parameter and is practically the dimensionless expression of the ponderomotive potential energy. This coupling can be expressed in several ways depending on what one intends to measure. When expressing the non-relativistic limit of the strong-field interaction theory, the intensity parameter for a charged particle of mass m is given as:

$$z_\mathrm{f} = 2\frac{U_\mathrm{p}}{mc^2}. \tag{5.5}$$

When $z_\mathrm{f} = 1$ the interaction must be treated relativistically. It is evident from the expression of the ponderomotive potential with the intensity and photon energy that the relativistic limit may be approached from two distinct directions: when $I \to \infty$ obviously, and when $\omega \to 0$. (Note that the expressions in this section are given in atomic units, since they were invented in the theory of atomic electron interactions.)

This condition is further explored in the next section.

5.1.3 Discussion of the non-relativistic limit for an alpha cluster

Following from the previous section, since the interaction is realized through a strong-field coupling (z_f), the peculiarities arising from the strong-field must be addressed carefully. One such characteristic is the limit of the non-relativistic approximation, which, considering the interaction with a high-intensity laser field (transvers plane-wave field) has a high-intensity limit and also a low-frequency limit.

Accordingly, the typical values of the external control parameters of the laser field (I, E_ph) must be assigned carefully. In the present theoretical approach a classical description of the laser-matter interaction is given - considering a classical laser field and an alpha cluster in a mean-field potential -, neglecting

any relativistic effect, which has to be justified upon setting the intensity-photon energy values. There can be found considerable studies concerning the non-relativistic description of laser-electron interactions based on the calculation of ponderomotive potentials [Reiss, 2002 ; Reiss, 2008 ; Reiss, 2014 ; Reiss, 2019] which suggest that either the $E_{\mathrm{ph}} \to 0$ or the $I \to \infty$ limits leads to the relativistic domain. There exists a condition with regard to the non-relativistic treatment of a free electron in a (plane-wave) laser field which is detailed in [Reiss, 2008]. According to [Della Picca et al., 2016] the effect of a few-cycle laser pulse could be estimated from the maximum of a cycle-dependent ponderomotive potential energy, which is equal to the ponderomotive energy of a plane-wave laser.

In the situation of alpha-decay instead of a free electron a quasi-bound alpha particle is exposed to the laser, the rest mass of which ($\approx$ 4 GeV) is almost three orders of magnitude larger than the rest mass of the free electron ($\approx$ 0.5 MeV), which - according to the relativistic condition $\frac{I}{\omega^2} = 2m_{\mathrm{e}}c^2$ [Reiss, 2008] - guaranties that the limits defined for the electron can serve as a lower estimate to the limits for the alpha cluster. Based on this argument, Table I in Figure 5.3 summarizes the reasonable numerical values of the relative change of the lifetime obtained by the non-relativistic region of the laser parameter pairs.

It is essential to emphasize that this feature of strong laser fields restricts all the non-relativistic theoretical models to a maximal intensity and a minimal photon energy! The $E_{\mathrm{ph}} \to 0$ limit leads to the relativistic domain where our model is not predictive. According to this restrictive aspect of the framework of the model, an upper bound can be determined for the possible effect of the laser on the lifetime. Although, it is necessary to emphasize that this circumstance and the defined bounds on the intensity and photon energy values are the consequence of the fabricated model, they are not necessarily originated from the nature of the physical process.

5.2 Investigations within the Hermitian framework: laser-modified alpha-cluster potential in the Henneberger picture

I included this section in order to illustrate how, applying the decay width produced by the standard WKB approximation and operating within that framework, one can mathematically address the problem of the laser-coupled system in terms of time dependence. Several articles in the literature approach the laser-assisted alpha decay problem working within the WKB framework [Delion et al., 2017 ; J. Qi et al., 2019 ; Pálffy et al., 2020 ; Rehman et al., 2022]. Many are the studies that follows the below presented mathematical technique to treat the time-dependence (e.g. [Delion et al., 2017]) that reach similar conclusions as the authors in [D. Kis et al., 2018] (that is the basis of this section), however several results are reached by a different methodology which fails to carefully manage the aspect of time dependence in relation to the WKB form of the decay width.

This section is concerned with the presentation of an alternative approach serving to estimate the influence of a periodic laser field on the WKB decay width [Kalbermann, 2008] in zero-order, without stepping into the - otherwise necessary - realm of non-hermitian quantum theory. The ultimate purpose is to demonstrate that investigating the problem via a rather simple model in zero-order, the effect of the laser is such that it always seemed worthy to further explore the problem with more accurate and rigorous models such as the non-hermitian-based (t,t')-perturbation theory which is also suitable to study laser pulses.

In the following calculation scheme the influence of the laser on the lifetime (width) is mapped onto the alteration of the nuclear potential (notably the Coulomb barrier) through a mathematical technique. The alteration of the Coulomb barrier is manifested in the Gamow factor. The laser-modified Gamow factor is obtained through the special Henneberger transformation and is calculated for the ^{210}Po isotope.

5.2.1 The Henneberger transformation

As it is discussed in Chapter 4, the problem of α tunneling can be described by (special solutions of) the time-independent Schrödinger equation. Although, in the presence of an intense laser field, which is characterized by the vector potential, $\mathbf{A}(\mathbf{r}, t)$, the Hamiltonian is time-dependent. Following the discussion

presented in Subsection 3.2 and Section 3.4, considering the Schrödinger equation in radiation gauge

$$i\hbar\frac{\partial}{\partial t}\Psi(r,t) = \hat{H}(r,t)\Psi(q,t), \tag{5.6}$$

where

$$\hat{H} = \frac{1}{2M}\left(\mathbf{p} - \frac{e}{c}\mathbf{A}(t)\right)^2 + V(r), \tag{5.7}$$

where M is the reduced mass of the α-cluster. The dipole approximation can be used so the vector potential depends only on time $\mathbf{A}(\mathbf{r},t) = \mathbf{A}(t)$. In this framework this approximation is valid when the wave length λ of the radiation field is greater than the characteristic size of the nucleus, thus λ is greater than the characteristic length of tunneling ($r_3 - r_2$, denoting the region between the turning points of the nuclear potential). The potential energy term $V(r)$ refers to one of the typical nuclear potentials introduced and discussed in Chapter 4 and corresponds to a central, spherically symmetric problem.

In this subsection I investigate the time-dependent problem from a unique approach: the Henneberger transformation. By the Henneberger transformation the explicit time-dependence of the problem is rendered implicit. In the followings, I briefly present the main steps of such a transformation.

In order to simplify the calculations, let us take care of the $\mathbf{A}^2$-term in the Hamiltonian. Remember, that in this section, I intend to provide the laser-modified decay width through the traditional approach, without the non-hermitian quantum-mechanical toolkit (and hence, without the restrictions following from it in relation to the quadratic term of the vector potential in the Hamiltonian).

Considering the dipole-approximation *and* staying within the hermitian quantum-mechanical territory (remember Section 3.4), in this situation the $\mathbf{A}^2$-term can indeed be transformed out by a unitary transformation:

$$U_2 = \exp\left(\frac{\mathrm{i}}{\hbar}\frac{\mathrm{e}^2}{2Mc^2}\int^t \mathbf{A}^2(\tau)\,\mathrm{d}\tau\right). \tag{5.8}$$

The Henneberger transformation is the following special unitary transformation to be applied on the *total* Schrödinger equation

$$U_1 = \exp\left(-\frac{\mathrm{i}}{\hbar}\mathbf{S}(t)\,\mathbf{p}\right), \tag{5.9}$$

where

$$\mathbf{S}(t) = \frac{\mathrm{e}}{Mc}\int^t \mathbf{A}(\tau)\,\mathrm{d}\tau. \tag{5.10}$$

As a result, the time-dependence is carried by the quantity $\mathbf{S}(t)$ that appears only in the argument of the unperturbed time-independent potential energy

term: $V^{\mathrm{H}}(\mathbf{r},t) \equiv V\left(\mathbf{r}-\mathbf{S}(t)\right)$. This is the implicit time-dependence obtained by the Henneberger transformation.

After carrying out the transformations $\Phi = U_1 U_2 \Psi$ [Henneberger, 1968] to equation (5.6), the time-dependent Schrödinger equation transforms into this

$$i\hbar\frac{\partial\Phi}{\partial t} = \left[\frac{\mathbf{p}^2}{2M} + V\left(\mathbf{r}-\mathbf{S}(t)\right)\right]\Phi. \tag{5.11}$$

The interaction term containing the explicit time dependence disappears from the Hamiltonian, in exchange for the spatial coordinate being shifted by an oscillatory term that oscillates according to the period of the laser. The potential energy generated this way, with a shifted argument, now only implicitly carries the time dependence, and like the vector potential, this potential energy also becomes a periodic function $V^{\mathrm{H}}(\mathbf{r},t) \equiv V\left(\mathbf{r}-\mathbf{S}(t)\right)$ and $V^{\mathrm{H}}(\mathbf{r},t) = V^{\mathrm{H}}(\mathbf{r},t+T)$ with time period $T = 2\pi/\omega$ (where ω is the main frequency of the monochromatic electromagnetic field). This periodicity can be exploited, the periodic potential can be expanded in Fourier basis [Gilary et al., 2002], namely

$$V^{H}(\mathbf{r},t) = \sum_{n=-\infty}^{\infty} V_n(\mathbf{r})\,\mathrm{e}^{in\omega t}, \tag{5.12}$$

where

$$V_n(\mathbf{r}) = \frac{1}{T}\int_0^T \mathrm{e}^{-in\omega t} V^{\mathrm{H}}(\mathbf{r},t)\,\mathrm{d}t. \tag{5.13}$$

In the present study and also in the related paper of the author [D. Kis et al., 2018] the investigation only covers the zero-order problem, any higher-order terms in the Fourier-expansion are considered as a perturbation and are not taken into account in this work, their influence can only be assessed using time-dependent perturbation calculations, however such a procedure is not compatible with the WKB framework (this is a weakness of the model). Accordingly, the zero-order Hamiltonian yields

$$H_0(\mathbf{r}) = \frac{\mathbf{p}^2}{2M} + V_0(\mathbf{r}) = \frac{\mathbf{p}^2}{2M} + \frac{1}{T}\int_0^T V\left(\mathbf{r}-\mathbf{S}(t)\right)\mathrm{d}t. \tag{5.14}$$

It is important to notice that the periodic property of the vector potential is crucial to carry out the calculations. This also means that the calculation scheme presented here has a limitation to periodic external drivings.

The zero-order Hamiltonian (5.14) is already a time-independent operator, now it might be possible to define the zero-order laser-modified width (4.3). However, with the shift in the spatial coordinate due to the Henneberger transformation, the central symmetry of the potential energy is lost. Since

the core idea of this approach is to be able to define a modified decay width, within the WKB-approximation, for the laser-driven (ultimately time-dependent) system, it is essential to extract the spherical part of the total potential in order to obtain an isotropic Hamiltonian. For this purpose one shall expand $V_0(\mathbf{r})$ in series of the spherical harmonics

$$V_0(\mathbf{r}) = \sum_{\ell=0}^{\infty} \sum_{m=-\ell}^{\ell} \frac{2\ell+1}{4\pi} C_{\ell m}(r)\, Y_{\ell m}(\Omega) = V_{00}(r) + \sum_{m=-1}^{1} V_{01}^{m}(r) Y_{1m} + \ldots, \tag{5.15}$$

where $Y_{\ell m}(\Omega)$ is the (ℓ, m) order spherical harmonics [Bronshtein et al., 1985] and $\mathbf{r} = r \cdot \underline{\Omega}$. By this, in the Hamiltonian, an isotropic and anisotropic potential term can be distinguished:

$$H_0 = \frac{\mathbf{p}^2}{2M} + V_{00}(r) + \sum_{\ell=1}^{\infty} V_{0\ell}(\mathbf{r}), \tag{5.16}$$

where the central part is V_{00}

$$V_{00}(r) = \frac{1}{4\pi} \frac{1}{T} \int_0^T \int_{4\pi} V\left(\mathbf{r} - \mathbf{S}(t)\right) \mathrm{d}\Omega \mathrm{d}t. \tag{5.17}$$

Appendix C presents the validation of WKB approximation for the Hamiltonian (5.16).

This model is based on the density-dependent cluster model (DDCM) theory, so the deformation of the proton density caused by the external laser field shall be investigated in the calculations. The problem of the deformed density and deformed cluster potential is briefly discussed here.

The deformed (non spherical) charge density ρ_ℓ is derived from the $V_{0\ell}$ via the Maxwell equation. The numerical investigations show that if the laser intensity is $I < 10^{21}\mathrm{Wcm}^{-2}$ then the non-spherical potentials $V_{0\ell}$ and so the non-spherical charge densities are three orders of magnitude smaller than the spherical part of the potential and density in the cases $\ell = 1, 2$. Therefore the dipole ($\ell = 1$) and quadrupole ($\ell = 2$) deformations of the density are negligible, the leading term is indeed (5.17) in the Hamiltonian. In other words it means that the cluster potential can be considered as a spherical Fermi-function in the presence of the laser field in DDCM.

Ultimately, laser-modified α decay can be described by a time-independent, isotropic potential in zero-order approximation, so the Hamiltonian yields

$$H_{00} = \frac{\mathbf{p}^2}{2M} + V_{00}(r). \tag{5.18}$$

The Schrödinger equation which includes Hamiltonian H_{00} can be subdivided into three separate differential equations: one of them depends only on the

radial variable r, and the other part only depends on the angular variables $\underline{\Omega}$ or (θ, ϕ). As the potential V_{00} only depends on the radial variable, the angular part is substituted by the centrifugal potential $V_\ell^{\rm cp}(r)$. So the three dimensional Schrödinger equation becomes a one-dimensional equation which can be rewritten by introducing a new radial wave function $u \equiv \phi_0(r) \cdot r$

$$\frac{\mathrm{d}^2 u}{\mathrm{d}r^2} + \frac{2M}{\hbar^2}\left[E - V_{00}(r) - V_\ell^{\rm cp}(r)\right] u = 0. \tag{5.19}$$

Equation (5.19) has the same mathematical form as the laser-free case of α-decay has, thus the expressions (4.1) and (4.3) can be applied to calculate the laser-modified life-time. In s-wave approximation the centrifugal potential is negligible, the laser modified, zero-order width $\Gamma_0^{\rm las}$ of the quasi-bound state of the α-cluster can be written as

$$\Gamma_0^{\rm las} = PF^{\rm las}\frac{\hbar^2}{4M}\exp\left(-2\int_{r_2}^{r_3}\kappa\left(r\right)\mathrm{d}r\right), \tag{5.20}$$

where F^{las} is the laser modified normalization factor and

$$\kappa\left(r\right) = \sqrt{\frac{2M}{\hbar^2}\left[V_{00}\left(r\right) - Q\right]}, \tag{5.21}$$

where the potential V_{00} is defined by (5.17), and $V_{00} > Q$. In practice there is no need for the absolute calculation of the laser-modified processes, the introduction of the relative change due to the presence of the laser field is usually sufficient, this ratio $\mathfrak{R}$ is defined by

$$\mathfrak{R} = \frac{F^{las}}{F}\exp\left[-2\left(\int_{\hat{r}_2}^{\hat{r}_3}\kappa(r)\mathrm{d}r - \int_{r_2}^{r_3}k(r)\mathrm{d}r\right)\right], \tag{5.22}$$

where $\hat{r}_2$ and $\hat{r}_3$ are the laser-modified classical turning points, and in many cases $F^{\rm las} \approx F$.

5.2.2 The relative change of the widths with mean-field nuclear potentials: analytical and numerical results for a single isotope

In this subsection let us experiment how some continuous laser field effects a typical mean-field nuclear potential. Investigating a nuclear potential suggests that an additional turning point, r_2, might now be subject to potential modifications. Two different potential models are chosen to be subjected to the Henneberger transformation upon accounting for the interaction with some

continuous laser field. As the previous chapters formulated, each of these nuclear potential models strongly relies on the theory of the Shell Model, where we account for the mean field that each nucleon experiences due to the collective influence of the others. The ratio $\mathfrak{R}_{(i)}$, which describes the difference between the decay constants of the laser-modified and the laser-free cases, is derived for the two possible polarization states of the laser.

Calculations are performed using the already introduced Section 4.3 mean-field nuclear potential built up with the Woods-Saxon attractive part and a Coulomb-type repulsive part:

$$V(r) = -V_0 f(r) + V_c(1 - f(r)). \tag{5.23}$$

It has already been stated that the effect the laser field has on the nuclear part of the potential can be neglected. Hence, it is worth carrying out the Henneberger transformation only to the Coulomb part. Based on the previous section, one is able to define the laser-modified potential in zero-order approximation

$$\begin{aligned} V_{00}(r) &= \frac{1}{4\pi}\frac{1}{T}\int_0^T \int_{4\pi} \mathrm{d}\Omega \mathrm{d}t \frac{V_0}{1+\mathrm{e}^{(r-R)/a}} + \\ &+ \frac{2Ze^2}{r}\left[1 - \frac{2\mathbf{rS}(t)}{r^2} + \frac{S^2(t)}{r^2}\right]^{-1/2} \cdot \left(1 - \frac{1}{1+\mathrm{e}^{(r-R)/a}}\right). \end{aligned} \tag{5.24}$$

In this case both turning points ($\hat{r}_2$,$\hat{r}_3$) can only be calculated by solving the equation $\kappa(r) = 0$ numerically.

Following the method we have already showed using the simplified model, the calculations can be specified for the two polarization cases by the definition of $\mathbf{S}$.

At the linearly polarized case the zero-order potential can be written as:

$$\begin{aligned} V_{00}^{Ia}(r,\xi) &= \frac{1}{4\pi}\frac{1}{2\pi}\int_0^{2\pi} \int_{4\pi} \mathrm{d}\Omega \mathrm{d}t \frac{V_0}{1+\mathrm{e}^{(r-R)/a}} + \\ &+ \frac{2Ze^2}{r}\left[1 + \frac{2\xi\cos(\vartheta)\sin(x)}{r} + \frac{(\xi)^2\sin^2(x)}{r^2}\right]^{-1/2} \cdot \left(1 - \frac{1}{1+\mathrm{e}^{(r-R)/a}}\right) \end{aligned} \tag{5.25}$$

Considering a circularly polarized electromagnetic wave, one can obtain the below presented closed formula for the zero-order potential:

$$\begin{aligned} V_{00}^{Ib}(r,\xi) &= \frac{1}{4\pi}\frac{1}{2\pi}\int_0^{2\pi} \int_{4\pi} \mathrm{d}\Omega \mathrm{d}t \frac{V_0}{1+\mathrm{e}^{(r-R)/a}} \frac{2Ze^2}{r}\left(1 - \frac{1}{1+\mathrm{e}^{(r-R)/a}}\right) \cdot \\ &\left[1 + \frac{2\xi\sin(\vartheta)}{r}\left(\cos(\varphi)\sin(x) + \sin(\varphi)\cos(x)\right) + \frac{(\xi)^2}{r^2}\right]^{-1/2}. \end{aligned} \tag{5.26}$$

By computing these expressions numerically one is able to calculate the Gamow-factors and the ratio defined in the previous section.

In the following, we are using the model of the homogeneously charged sphere to represent the Coulomb potential of the remaining nucleus. It is derived from the Maxwell equations.

$$V(\mathbf{r}) = \begin{cases} \frac{2Ze^2}{|\mathbf{r}|} & r \geq R \text{ (outside)}, \\ \\ \frac{2Ze^2}{2R} \cdot \left(3 - \frac{|\mathbf{r}|^2}{R^2}\right) & r < R \text{ (inside)}, \end{cases} \tag{5.27}$$

Based on the idea of the previous subsection, one can also neglect the laser field's effect on the nuclear part of the potential, but the Henneberger transformation must be carried out to the Coulomb part, both inside and outside the sphere. Note that the fitting constants of the potential also change as an effect of the presence of the laser field. So, it is important to apply the Henneberger transformation before fitting the boundary conditions. By this method, the potential will surely be continuous at $r = R$. It is an important distinguishing property of this nuclear model. According to this, one shall note that this type of Coulomb potential model does not sufficiently describe the nuclear potential inside the nucleus. Certainly, it is not a problem from the viewpoint of studying the effect of the laser field, however, due to the Henneberger transformation inside the sphere, it induces the appearance of a stronger modifying effect inside the nucleus. This is only a consequence of the chosen Coulomb potential model.

The result of the Henneberger transformation always depends on the intensity of the laser field. Hence, these fitting parameters can only be calculated when one specifies the intensity. After applying the Henneberger transformation on the potential, we get directly from $\oint_{\partial V} \mathbf{E} \mathrm{d}\mathbf{A} = \int_V \rho \mathrm{d}V$ now without knowing exactly the fitting constants (C_1, C_2), the laser- modified potential under discussion will reach the below form taking into consideration the linearly polarized case: inside $(r < R)$

$$\begin{aligned} V_{00}^{IIa,\xi}(r) &= \frac{1}{4\pi}\frac{1}{2\pi}\int_0^{2\pi}\int_{4\pi} \mathrm{d}\Omega \mathrm{d}x V_0 \frac{1+\cosh(R/a)}{\cosh(r/a)+\cosh(R/a)} + C_2 - \frac{2Ze^2}{2R^3}r^2 \cdot \\ &\cdot \left[1 + \frac{2\xi\cos(\vartheta)\sin(x)}{r} + \frac{(\xi)^2\sin^2(x)}{r^2}\right] \end{aligned} \tag{5.28}$$

outside $(r \geq R)$

$$\begin{aligned} V_{00}^{IIa}(r,\xi) &= \frac{1}{4\pi}\frac{1}{2\pi}\int_0^{2\pi}\int_{4\pi} \mathrm{d}\Omega \mathrm{d}x V_0 \frac{1+\cosh(R/a)}{\cosh(r/a)+\cosh(R/a)} + \frac{2Ze^2}{r} \cdot \\ &\cdot \left[1 + \frac{2\xi\cos(\vartheta)\sin(x)}{r} + \frac{(\xi)^2\sin^2(x)}{r^2}\right]^{-1/2}. \end{aligned} \tag{5.29}$$

Considering circularly polarized state the zero-order potential has the form inside ($r < R$)

$$V_{00}^{IIb}(r,\xi) = \frac{1}{4\pi}\frac{1}{2\pi}\int_0^{2\pi}\int_{4\pi} \mathrm{d}\Omega \mathrm{d}x V_0 \frac{1+\cosh(R/a)}{\cosh(r/a)+\cosh(R/a)} + C_2 - \frac{2Ze^2}{2R^3}r^2 \cdot \cdot \left[1 + \frac{2\xi\sin(\vartheta)}{r}\left(\cos(\varphi)\sin(x)+\sin(\varphi)\cos(x)\right) + \frac{(\xi)^2}{r^2}\right] \quad (5.30)$$

outside ($r \geq R$)

$$V_{00}^{IIb}(r,\xi) = \frac{1}{4\pi}\frac{1}{2\pi}\int_0^{2\pi}\int_{4\pi} \mathrm{d}\Omega \mathrm{d}x V_0 \frac{1+\cosh(R/a)}{\cosh(r/a)+\cosh(R/a)} + \frac{2Ze^2}{r} \cdot \cdot \left[1 + \frac{2\xi\sin(\vartheta)}{r}\left(\cos(\varphi)\sin(x)+\sin(\varphi)\cos(x)\right) + \frac{(\xi)^2}{r^2}\right]^{-1/2} \quad (5.31)$$

The C_1 constant disappears as a consequence of fitting the boundary conditions. The other constant can only be computed numerically from the continuity condition. The ratio $\mathfrak{R}$ introduced in the previous subsection can be described as

$$\mathfrak{R}_{(j)} = \exp\left[-2\sqrt{\frac{2M}{\hbar^2}}\left(\int_{\widehat{r}_2}^{\widehat{r}_3}\sqrt{V_{00}^{j}(r,\xi)-Q}\mathrm{d}r - \int_{r_2}^{r_3}\sqrt{\frac{2Ze^2}{r}-Q}\mathrm{d}r\right)\right], \quad (5.32)$$

where $j = Ia, Ib, IIa, IIb$.

After obtaining the analytical formulas, the α-decay of ^{210}Po isotope is subject to numerical investigations in intense laser field by using the formula (5.32). The charge number is $Z = 84$, the alpha energy is 5.407 MeV [Firestone et al., 1996].

Figure 5.1. shows the shape of the spherically symmetric potential felt by the α-cluster with some pair of laser intensities and photon energies against the distance from the nucleus (the zero point denotes the point of the central of mass). Each figure belongs to the two different nuclear potential models in order: Fermi-type Wood-Saxon potential, homogeneous sphere potential. Both figures have the potential V_{00} depicted in the laser-free case, and with linearly polarized and circularly polarized electromagnetic wave in order with solid line, dashed line and dotted line. In Figure 5.1. **(a)** and **(b)** the intensity is $I = 5 \cdot 10^{19}$ W/cm^2 and the photon energy is $E_{ph} = 100$ eV. It can be seen that the effect of the presence of the laser field for the modified Coulomb potential strongly depends on the polarization state of the monochromatic electromagnetic field and on the field intensity.

Figure 5.2. shows the calculated Gamow-factors (the substraction of the laser-free and laser-modified Gamow factors) plotted against certain values of

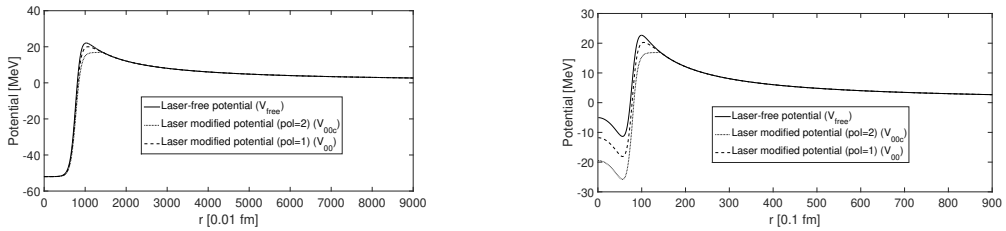

Figure 5.1: *The computed V_{00} potential as a function of the distance measured from the nuclear radius (r) with laser intensity of $I = 5 \cdot 10^{19}$ W/cm^2 and photon energy of $E_{ph} = 100$ eV. Subfigure* ***(a)*** *shows the deformation of the Fermi-type nuclear mean-field potential, while subfigure* ***(b)*** *displays the modification in the nuclear potential represented by a Coulomb term based on the uniformly charged sphere model, both setting having $V_0 = -52$ MeV and $a = 0.65$ fm as the nuclear potential parameters. Three different cases are represented: solid line stands for the laser-free case; dashed line stands for the linearly polarized case; dotted line stands for the circularly polarized case.*

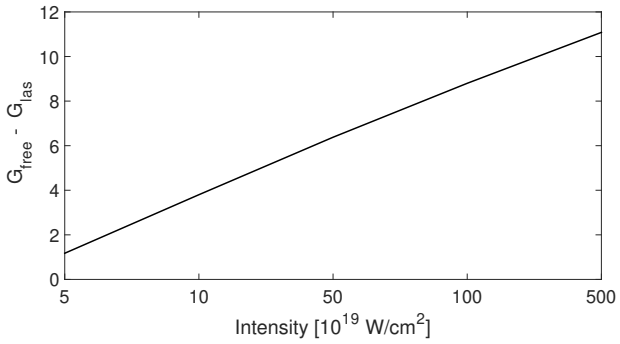

Figure 5.2: *The difference between the laser-free and laser-modified Gamow factors plotted against a narrow range of intensity values using the Fermi-type potential model choosing the free parameters as $a = 0.65$ fm and $V_0 = -52$ MeV.*

the intensity. It is clearly seen from Figure 5.2. that by the increase of the intensity the subtraction of the Gamow-factors increase approximately linearly in the given intensity region. So the results are more notable when a higher intensity laser field is applied (with fixed photon energy). Based on paper [Misicu et al., 2016] more greater ratio values are expected by applying laser pulse than in the case of plane wave laser field.

The applied realistic nuclear potentials has their own free parameters (a [fm], V_0 [MeV]). So we investigated what happens to our results if we change them. Thus the ratio (R_{ij}) was calculated in some specific cases of the values of the mentioned free parameters, for example one of the $V_0 - a$ pairs comes from [Buck et al., 1992].

It is clearly seen again from the above table that the effect the laser field has

Model (j), Polarization (i)	Intensity (W/cm^2)	a(fm)	V_0(MeV)	$\mathfrak{R}_{(ij)}$
$(j = 1), (i = 1)$	$5 \cdot 10^{19}$	0.65	−52	8.4015
$(j = 1), (i = 1)$	$5 \cdot 10^{19}$	0.7	−141.9	3.9414
$(j = 1), (i = 1)$	$5 \cdot 10^{19}$	0.76	−137.7	3.3319
$(j = 1), (i = 2)$	$5 \cdot 10^{19}$	0.65	−52	123.2366
$(j = 1), (i = 2)$	$5 \cdot 10^{19}$	0.7	−141.9	48.1420
$(j = 1), (i = 2)$	$5 \cdot 10^{19}$	0.76	−137.7	29.1531
$(j = 2), (i = 1)$	$5 \cdot 10^{19}$	0.65	−52	3.3129
$(j = 2), (i = 1)$	$5 \cdot 10^{19}$	0.76	−137.7	3.8796
$(j = 2), (i = 1)$	$5 \cdot 10^{19}$	0.7	−141.9	2.7542
$(j = 2), (i = 2)$	$5 \cdot 10^{19}$	0.65	−52	34.9973
$(j = 2), (i = 2)$	$5 \cdot 10^{19}$	0.7	−141.9	84.4423
$(j = 2), (i = 2)$	$5 \cdot 10^{19}$	0.76	−137.7	18.6598

Table 5.1: *The computed values of the ratio $R_{(ij)}$ with the two possible polarization state of the laser field denoted by* i *while j encoding the two applied potential models.* j = 1 *stands for the uniquely parameterized Woods-Saxon and Coulomb potential, while* j = 2 *indicates the homogeneously charged sphere model for the electrostatic repulsion of the nucleons.* i = 1 *symbolizes the linear polarization state, while* i = 2 *connotes the circularly polarized field. The photon energy is set to 100* eV*. a and V_0 are the free parameters of nuclear mean-field potential model.*

on the static potential strongly depends on the polarization. Table 1. shows that in the cases of circularly polarized state the ratio $\mathfrak{R}_{(ij)}$ (which is proportional to the laser modified decay probability) is one or two orders of magnitude greater than in the cases of the linearly polarized state. It can also be inferred that the parameters of the applied nuclear potential can influence the final results.

Based on these numerical results it is concluded that the derived expression (5.32) give non-zero laser modified physical effects in a very narrow range of values of the intensity and the photon energy. When the theoretical steps were introduced it was remarked that during the calculations only the zero-order spherical harmonics ($\ell = 0$) potential energy term is taken into account. Nevertheless, the $\ell = 1$ cases were also checked, which gave some rather insignificant additions to the already presented results.

5.3 The limitations of the Henneberger-transformation-based approach

The above-presented model of laser-assisted alpha decay proved to be suitable for describing the remaining nucleus and alpha cluster system in the mean-field approximation, coupled to the laser field characterized by a periodically time-dependent classical vector potential, with respect to the WKB decay lifetime, under a non-relativistic approximation and considering the zeroth-order Fourier series expansion of the time-dependent interaction. Such a description and the zeroth-order expression of the laser-modified width serves as a checkpoint in the theory of laser-assisted alpha decay: the performed numerical computations provided results showing that the effect of the laser (at a given intensity and photon energy) is non-negligible even at zeroth order, thus laying the foundation for further research.

As elegant as the Henneberger-transformation-based model is in addressing the problem of laser-driven alpha decay, it has some serious limitations in its application. The time-independent formulation of the interaction Hamiltonian is the exclusive consequence of the Fourier expansion of the Henneberger-transformed potential energy and the identification of a time-independent zeroth-order interaction term. Any higher-order - hence time-dependent - terms of the Henneberger-transformed potential energy cannot be considered while working within the WKB approximation. The property of the potential that allows for such an expansion is the periodicity of the vector potential representing the external laser field. For non-periodic drivings, such as laser pulses, the

extraction of a time-independent term is not this straightforward. The core of this approach is to manipulate the time-dependence of the coupled-laser system in order to arrive at a Schrödinger equation that is consistent mathematically in the WKB-framework, hence allowing for the derivation of a laser-modified decay width. However, the production of the decay width is more natural and most importantly quantum-mechanically accurate in the natural coordinate system of decay that requires the non-hermitian formulation of quantum mechanics.

However, it was proved in [Pfeifer et al., 1983] that the special (t,t')-formalism (originally Floquet-formalism) is extendable to problems with general, not only periodic time-dependence [Sambe, 1973]. This result naturally lays the groundwork for the direction of further research from the perspective of the model framework. As it was already discussed in Chapter 2, the appliance of the (t,t')-formalism requires a wave-function centered description, hence the demand for the non-hermitian extension of the alpha-decay problem is evident. The next section summarizes the numerical results obtained within this framework.

5.4 Results within the non-hermitian framework: the laser-induced shift of the complex energy-eigenvalue of the alpha cluster

In this chapter I present my numerical results of laser-assisted alpha decay obtained within the non-hermitian framework. Chapter 3 sets the conceptual ground and the mathematical framework for the description of the laser-coupled system in the non-hermitian formalism as well as the derivation of the complex-energy shift formulae. Building upon this and the concepts of Section 5.1 on the subject of the properties of super-intense laser interacting with an alpha cluster, conclusive findings of the matter are formulated.

Let us return to the previously discussed (see Subsection 3.1 specification of the external coherent electromagnetic field in the context of interacting with non-hermitian systems. As it was already introduced and explained, we specify $\hat{H}_I^\theta(\mathbf{r},t)$ by a non-relativistic, classical vector potential ($\mathbf{A}(\mathbf{r},t)$) characterizing the external laser field by minimally coupling the vector potential to the kinetic part of the Hamiltonian operator. The problem is considered in Coulomb gauge ($\nabla\mathbf{A}=0$) and within the Long Wave Approximation; and according to 3.4 exclusively the velocity gauge is adoptable, in which case the interaction Hamiltonian of the laser-assisted decaying system has the form:

$$\hat{H}_I^\theta(\mathbf{r},t)=\frac{-e}{Mc}\mathbf{p}^\theta\mathbf{A}^\theta(t)+\frac{e^2}{2Mc^2}\left(\mathbf{A}^\theta(t)\right)^2. \tag{5.33}$$

where e is the elementary charge and c is the speed of light. Later on the fine structure constant α is indicated in the analytic formulas instead of the elementary charge, according to the relation: $e^2 = \alpha \cdot \hbar \cdot c$.

The vector potential is specified for two different polarization cases (p = l, c): results are presented for linearly (l) and circularly (c) polarized laser fields. In both cases the vector potential contains a Gaussian-envelope function accounting for the effect of laser pulses. For linear polarization the vector potential is built up as

$$\mathbf{A}^{(\mathrm{l})}(t) = A_0 \mathbf{e}_z \cos\left(\frac{E_{\mathrm{ph}}}{\hbar} t + \gamma\right) \mathrm{e}^{-\left(\frac{E_{\mathrm{ph}} t}{\hbar\sigma}\right)^2}, \tag{5.34}$$

while for circular polarization $\mathbf{A}(\mathbf{r}, t)$ is expressed as

$$\mathbf{A}^{(\mathrm{c})}(t) = A_0 \left(\mathbf{e}_x \cos\left(\frac{E_{\mathrm{ph}}}{\hbar} t + \gamma\right) + \mathbf{e}_y \sin\left(\frac{E_{\mathrm{ph}}}{\hbar} t + \gamma\right)\right) \mathrm{e}^{-\left(\frac{E_{\mathrm{ph}} t}{\hbar\sigma}\right)^2},$$

where $\mathbf{e}_x$, $\mathbf{e}_y$, $\mathbf{e}_z$ are the unit vectors in Cartesian coordinate system, $\frac{E_{\mathrm{ph}}}{\hbar}$, γ are the frequency and the phase of the laser field, respectively and σ is the width of the Gaussian envelope function. A_0 can be expressed with the amplitude of the corresponding electric field $E_0 = \frac{E_{\mathrm{ph}}}{\hbar c} A_0$, where $E_0 = \sqrt{\frac{4\pi}{c}}\sqrt{I}$ with I denoting the peak intensity of the laser field in the unit of $\frac{\mathrm{MeV}}{\mathrm{s \cdot fm^2}}$. Due to the circumstance that in this calculation scheme expectation values are computed rather than transition matrix elements, upon performing integrals over the whole coordinate space in the extended Hilbert space to get the correction from the (t,t')-expectation value in equation (2.41), only the quadratic vector potential term (second term in equation (5.33)) gives non-zero contribution.

Computing this expectation value $\varepsilon^{(1,\mathrm{p})} = (\langle\tilde{\Phi}^{\theta}(\mathbf{r}, t)| \frac{e^2}{2Mc^2} \left(\mathbf{A}^{\theta(\mathrm{p})}(\mathbf{r}, t)\right)^2 |\tilde{\Phi}^{\theta}(\mathbf{r}, t)\rangle)$, the already introduced closed-form expressions are achieved for the complex energy correction of the (preformed) quasi-stationary alpha cluster. According to this the complex energy correction of the alpha cluster in the case of linear polarization (with the condition $\frac{\Gamma}{E_{\mathrm{ph}}} << \sigma$ which is justified by the typical order of magnitude of nuclear decay widths ($\Gamma^{\mathrm{decay}}_{\mathrm{exp}} < 10^{-14}$ MeV), for *laser* photon energies within the non-relativistic limit):

$$\begin{aligned} \varepsilon^{(1,\mathrm{l})} &= \mathcal{N}^2 \mathcal{K} \frac{I\hbar}{E^3_{\mathrm{ph}}} \sqrt{\frac{\pi}{2}} \left(\frac{1}{4\sigma} \mathrm{e}^{\frac{\Gamma^2}{8E^2_{\mathrm{ph}}\sigma^2}} f(\sigma, \Gamma, E_{\mathrm{ph}}) + \right. \\ &+ \left. h(\sigma) \left[\mathrm{e}^{-2\mathrm{i}\frac{\Gamma\sigma^2}{8E_{\mathrm{ph}}}} \mathrm{e}^{2\mathrm{i}\gamma} g(\sigma) + \mathrm{e}^{2\mathrm{i}\frac{\Gamma\sigma^2}{8E_{\mathrm{ph}}}} \mathrm{e}^{-2\mathrm{i}\gamma} g^*(\sigma) \right] \right), \end{aligned} \tag{5.35}$$

where the function $g(\sigma) = \left(1 + \mathrm{i} \cdot \mathrm{erfi}\left(\frac{\sigma}{\sqrt{2}}\right)\right)$ and $g^*(\sigma)$ is its complex conjugate. The function $f(\sigma, \Gamma, E_{\mathrm{ph}})$ is expressed as $f(\sigma, \Gamma, E_{\mathrm{ph}}) = \left[1 - \mathrm{erf}\left(\frac{\Gamma}{\sqrt{8}E_{\mathrm{ph}}\sigma}\right)\right]$, and function $h(\sigma) = \frac{\sigma}{16}\mathrm{e}^{\left(\frac{\Gamma^2}{E_{\mathrm{ph}}^2} - 4\right)\frac{\sigma^2}{8}}$. Physical constants are encompassed by $\mathcal{K} = \frac{\alpha 2\pi(\hbar c)^3}{\mu c}$, where $\mu = Mc^2$. The width Γ is also implicitly present in the complex normalization factor $\mathcal{N}^2$. Using the same symbols, the energy correction for circular polarization is determined as:

$$\varepsilon^{(1,\mathrm{c})} = \mathcal{N}^2\mathcal{K}\frac{I\hbar}{E_{\mathrm{ph}}^3}\sqrt{\frac{\pi}{8}}\frac{1}{\sigma}\mathrm{e}^{\frac{\Gamma^2}{8E_{\mathrm{ph}}^2\sigma^2}} f(\sigma, \Gamma, E_{\mathrm{ph}}). \tag{5.36}$$

In practice it is reasonable to determine the relative change of the width, which is inversely proportional to the relative change of the lifetime (τ):

$$\frac{\tau}{\tau^{\mathrm{las}}} = \frac{\Gamma^{\mathrm{las}}}{\Gamma} = 1 + \frac{\varepsilon^{(1,\mathrm{p})}}{\Gamma}. \tag{5.37}$$

Although the above formulae suggest a sole intensity and photonenergy-dependent function, however it is not reasonable to look at the complex energy correction formula as a clear function of the intensity and the photon energy. Because taking the divergent $E_{\mathrm{ph}} \to 0$ and $I \to \infty$ limits leads us to false conclusions that typically arise in the description of many-photon strong-field phenomena that shall be discussed in terms of the ponderomotive potential energy along with the non-relativistic approximation as is suggested in [Reiss, 2019 ; Reiss, 2021] and that are detailed in Section 5.1.

It is clearly seen from equation (5.35) and (5.36) that the *correction* $\varepsilon^{(1,\mathrm{p})}$ is proportional to the intensity, which is consonant to the intensity-dependence of the ponderomotive potential energy typically obtained in calculations concerning laser-matter interactions with plane waves.

The photon-energy dependence, though, significantly alters from that of the ponderomotive energy, which is due to the fact that now laser impulses are studied which are mathematically represented by a photon-energy dependent Gaussian envelope function (the pulse length is measured in $\frac{\sigma\hbar}{E_{\mathrm{ph}}}$, where σ is a dimensionless quantity). The shape of $\frac{\Gamma^{las}}{\Gamma}$ is presented in Figure 5.5 for the appropriate intensity-photon energy range which is to be quantitatively given in the next subsection.

5.4.1 The relative change of the lifetime as a function of the laser control parameters

In this subsection demonstrative calculations are presented for the laser-modified lifetime of the alpha cluster formed in the ^{212}Po isotope, by means of exploring the external control-parameter-dependence of the relative change of the width of the quasi-stationary state $\frac{\Gamma^{las}}{\Gamma} = 1 + \frac{\epsilon^{(1,p)}}{\Gamma}$.

The quantitative limit of the non-relativistic approximation for laser-assisted alpha-decay in the non-hermitian framework is depicted in Figure 5.3 considering typical photon energy values and the super-high-intensity regime. The relative change of the width of the quasi-stationary state $\frac{\Gamma^{las}}{\Gamma} = 1 + \frac{\epsilon^{(1,l)}}{\Gamma}$ is calculated for the different intensity-photon energy pairs (fixing the laser phase γ and the width of the laser pulse σ and considering linearly polarized laser field). The dark red area of the table contains those pairs that exceeds the numerical limit of the non-relativistic approximation. All the values below the gradient are obtained within the non-relativistic approximation, thus are the only considerable results of our model (light purple cells).

E_{ph} \ Intensity [W/cm^2]	10^{19}	10^{20}	10^{21}	10^{22}	10^{23}	10^{24}	10^{25}	10^{26}	10^{27}	10^{28}	10^{29}	10^{30}
1 eV	451,5	*4506*	$4{,}5{\cdot}10^{4}$	$4{,}5{\cdot}10^{5}$	$4{,}5{\cdot}10^{6}$	$4{,}5{\cdot}10^{7}$	$4{,}5{\cdot}10^{8}$	$4{,}5{\cdot}10^{9}$	$4{,}5{\cdot}10^{10}$	$4{,}5{\cdot}10^{11}$	$4{,}5{\cdot}10^{12}$	$4{,}5{\cdot}10^{13}$
10 eV	1,451	5,505	46,05	*451,5*	4506	$4{,}5{\cdot}10^{4}$	$4{,}5{\cdot}10^{5}$	$4{,}5{\cdot}10^{6}$	$4{,}5{\cdot}10^{7}$	$4{,}5{\cdot}10^{8}$	$4{,}5{\cdot}10^{9}$	$4{,}5{\cdot}10^{10}$
100 eV	1	1,005	1,045	1,451	5,505	*46,05*	451,5	4506	$4{,}5{\cdot}10^{4}$	$4{,}5{\cdot}10^{5}$	$4{,}5{\cdot}10^{6}$	$4{,}5{\cdot}10^{7}$
1 keV	1	1	1	1	1,005	1,045	1,451	*5,505*	46,05	451,5	4506	$4{,}5{\cdot}10^{4}$
10 keV	1	1	1	1	1	1	1	1,005	1,045	*1,451*	5,505	46,05

Figure 5.3: *The quantitative limit of the non-relativistic approximation. The table contains the numerical values of the complex-energy shift that are obtained by different peak intensity and photon energy settings.*

The appropriate intensity-photon energy region, posed in the table in Figure 5.3, is encircled by an ellipse in Figure 5.4 in order to highlight the distinct parameter domains that corresponds to the relativistic and non-relativistic limits of the many-photon strong field interaction.

Turning to the examination of the additional laser parameters, it can be deduced from Figure 5.5 that the maximal effect (highest Γ^{las}, smallest τ^{las}) is obtained for $\sigma = 1$ (when the pulse length is equal to $\tilde{T} = \frac{\hbar}{E_{ph}}$) and the effect is more pronounced for phase-shifts around $\gamma = n\pi$ ($n = 0, 1, 2...$). It could be stated that as a result of this wavefunction-centered computational technique, a circularly or linearly polarized laser pulse could produce an evident increment in the width of the quasi-stationary state, thus the lifetime of the alpha-cluster in a mean-field nuclear potential could decrease. As an illustrative example,

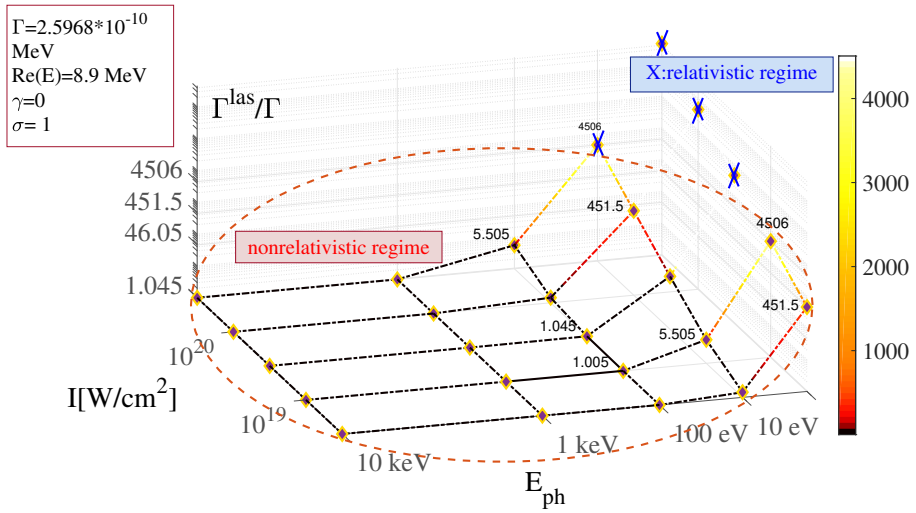

Figure 5.4: *The diagram indicate the increment in the width of the alpha-cluster (decrement in the lifetime) in log scale for a laser pulse with a typical range of peak intensity and photon energy. It is also shown that the complex energy shift indeed grows linearly with the intensity, although due to the relative width formula ($\frac{\Gamma^{\text{las}}}{\Gamma} = 1 + \frac{\epsilon^{(1,p)}}{\Gamma}$), for relatively small intensity values paired with higher photon energies the linearity of the function is spoiled.*

setting the peak intensity of the laser pulse $I = 10^{24}\ \frac{W}{cm^2}$ and the photon energy $E_{\text{ph}} = 100$ eV along with $\gamma = 0$ and $\sigma = 1$ the decrement in the lifetime is around $\frac{1}{70}\tau$ for linearly polarized laser, although for a significantly lower peak intensity value, $I = 10^{21}\ \frac{W}{cm^2}$, there is still a few percent decrease predicted in the lifetime for the relatively high photon energy $E_{\text{ph}} = 100$ eV.

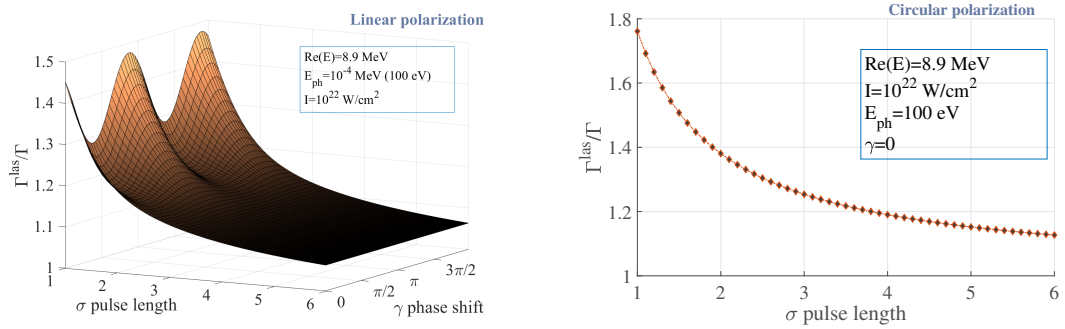

Figure 5.5: *The relative change of the width of the quasi-stationary state representing the alpha-particle $\frac{\Gamma^{\text{las}}}{\Gamma} = 1 + \frac{\epsilon^{(1,l)}}{\Gamma}$, for both circular and linear polarization cases of the laser field, fixing the photon energy $E_{\text{ph}} = 100$ eV and field intensity $I = 10^{22}\ \frac{\text{W}}{\text{cm}^2}$. The effect of the external laser field decreases with the width of the Gaussian envelope function σ in the same fashion for both polarization cases.*

With respect to the quantitative limit of the photon energy and peak intensity

pairs induced by the non-relativistic requirement, for an appropriately chosen intensity range for 100 eV photon energy, the first-order relative energy correction $\epsilon^{1,l}$ as a function of the peak intensity is depicted in Figure 5.6 regarding a laser field in linearly polarized state.

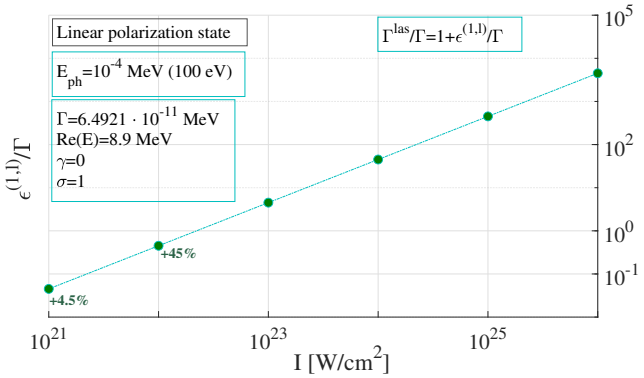

Figure 5.6: *The relative imaginary energy correction of the quasi-stationary alpha cluster* $\frac{\epsilon^{(1,l)}}{\Gamma}$ *as a function (setting a logarithmic scale) of the peak intensity I of the external propagating laser pulse in linear polarization state, fixing the photon energy* $E_{\text{ph}} = 100$ eV. *The effect of the external laser field increases with the peak intensity. Note that axis y is in logarithmic scale.*

5.4.2 Numerical results for the N=128 isotonic chain

In Chapter 4 I determined the mean-field tunneling widths (Γ) of special alpha-decaying isotonic nuclei in the cluster-remaining nucleus picture from the complex energy. The investigation of the relationship between the calculated mean-field tunneling widths (Γ) and the total decay widths (Γ^{decay}) known from experiments for the $N = 128$ isotonic chain confirmed the hypothesis with high accuracy that the variation in the Coulomb barrier of the heavy, alpha-decaying nuclei composing the studied isotonic series predominantly determines the differences in their decay lifetimes. In the case of these nuclei, the nuclear structure remains nearly constant (expressed via the previously introduced factor s_0), while the variation in the number of protons (Z) primarily affects the Coulomb barrier, the alteration of which is what determines the mean-field tunneling lifetime.

This hypothesis and these findings suggest that the effect of any external driving that alters the Coulomb barrier can be traced via the change in the mean-field tunneling width. In Section 5.1, it was shown that an intense laser field with the typical peak intensities and photon energies predominantly influence the Coulomb barrier of the nucleus.

According to these observations and knowledge, it is worth to investigate the complex energy shifts and calculate the relative change of the mean-field tunneling widths of nuclei in the context of isotonic series with neutron number N=128.

The investigated isotones and their mean-field tunneling widths along width the relative change of the widths $\frac{\Gamma^{\text{las}}}{\Gamma}$ are displayed in Table 5.2.

	Γ [MeV]	$\Gamma^{\text{las}}/\Gamma$
^{212}Po	$30.94 \cdot 10^{-9}$	**1.633**
^{214}Rn	$58.49 \cdot 10^{-9}$	**1.711**
^{216}Ra	$92.93 \cdot 10^{-9}$	**1.79**
^{218}Th	$122 \cdot 10^{-9}$	**1.871**

Table 5.2: *The relative change of the mean-field widths of the quasi-stationary cluster states in nuclei from the N=128 isotonic series. The laser control parameters are set to:* $I = 10^{22}$ $\frac{\text{W}}{\text{cm}^2}$, $E_{\text{ph}} = 100$ eV, *the pulse length* $\sigma = 1$ *and the phase shift is* $\gamma = 0$.

Table 5.2 shows a slight difference in the effect of the laser pulse with $I = 10^{22}$ $\frac{\text{W}}{\text{cm}^2}$, $E_{\text{ph}} = 100$ eV, despite of the mean-field tunneling widths (and so the total decay widths according to Chapter 4) being more distinct (relatively). The largest mean-field width belonging to ^{218}Th is 4 times larger than the smallest width

belonging to ^{212}Po, while the difference between the relative changes is at most 2.4.

Nevertheless, one can observe a systematic in $\frac{\Gamma^{\text{las}}}{\Gamma}$ as a function of the lifetime (or decay width). Note, that there is an inverse relation between the lifetime of the alpha cluster (τ) and the corresponding decay width (Γ), hence ^{212}Po has the largest lifetime (and the smallest alpha energy E_α or decay energy Q_α) and ^{218}Th has the smallest one (hence the largest alpha energy). The relative change of the lifetime is the most significant for ^{218}Th (the higher the ratio of $\frac{\Gamma^{\text{las}}}{\Gamma}$ the shorter the lifetime gets due to the laser field). In this series Th has the smallest neutron to proton ratio ($Z = 90$), although the alpha-energy level is the highest for this nuclei (see Table 4.2). In an intuitive picture, this refers to the thorium isotope with the shortest lifetime being closest to the peak of the Coulomb barrier, where the barrier is also narrowest (the probability of tunneling depends on both the height and width of the barrier); which circumstance could potentially enhance the effect of the external laser field.

Moreover, a similar systematics can be observed in the relative change of the lifetime as in the dependence of decay widths and alpha energies on Z^2/A. The ratios ($\frac{\Gamma^{\text{las}}}{\Gamma}$) form an arithmetic series as a function of the relative number of protons. The underlying systematics is preserved. This observation could potentially facilitate the extrapolation of the anticipated relative change of the lifetime to other (even-even) nuclei within the isotonic series. However, caution must be exercised here, as increasing the number of neutrons relative to protons strengthens the effects arising from the nuclear structure, which extends beyond the scope of the current model framework.

6

Summary and conclusion

In this thesis I set my primary task to examine the issue of laser-assisted alpha decay by studying the lifetime of the alpha cluster formed in radioactive alpha-decaying isotopes, and by investigating the possible modifications to the lifetime induced by the influence of some external laser field: continuous plane wave or laser pulse.

In this study I considered alpha decay as a two-step process which is composed of the formation of the alpha cluster (clustering) and the interaction between the preformed alpha cluster and the residual nucleus; the latter resulting in the tunneling through the Coulomb barrier. I discussed that, in leading order, the most pronounced effect of the laser field is displayed in the potential alteration of the Coulomb barrier, primarily influencing the tunneling process; the impact on the nuclear structure is not significant due to the strength of the nuclear forces. In this dissertation, therefore, I investigated the tunneling phase of alpha decay in the case of heavy alpha-decaying isotone nuclei, concentrating on the alpha cluster in the mean-field potential of the surrounding nucleons.

I investigated the problem within the non-relativistic and dipole approximation, taking into account that the validity of these approximations depends on the intensity and photon energy jointly and this dependence is expressed through the ponderomotive potential of the alpha cluster. According to this, I determined those photon energy and intensity pairs that do not exceed the validity of the approximations. The external laser field was represented as a classical vector potential and the interaction was realized through minimal coupling and considered as a perturbation.

As a first step I performed demonstrative calculations, wherein the tunneling process is interpreted within the conventional quantum mechanical framework using the expression for the decay width (Γ^{decay}) derived in WKB-approximation, with the Gamow factor representing the tunneling. I examined the effect of the laser field through the alteration of the Coulomb barrier in the nuclear potential

(that manifests in the change of the Gamow factor) due to the interaction with a *periodically* time-dependent vector potential. In this case I rendered the time-dependence of the external laser field implicit through the *Henneberger transformation*, which allows for the determination of the zeroth-order, laser-modified decay width in the case of periodic vector potentials. The goal was to show that, even under significantly simplified conditions—considering a plane-wave laser and calculating the laser-modified decay width in a zeroth-order approximation—the effect of the laser is non-negligible. I performed numerical calculations for ^{210}Po isotope and drew the main conclusion that the ratio of the laser-modified and laser-free widths ($\mathcal{R} = \frac{\Gamma^{las}}{\Gamma}$) is largest upon considering circularly polarized laser.

The model based on the Henneberger transformation is consistently applicable only in the case of laser fields with periodic time-dependence. To investigate further and to be able to study the effects of laser pulses an alternative modeling framework was required.

In this framework I identified the alpha cluster as a quasi-stationary state with complex energy, the imaginary part of which yields the decay width. I studied the interaction of the alpha cluster with a super-intense laser pulse within the (t,t')-formalism, that provides an appropriate framework for the analytical and perturbative investigation of time-dependent, non-periodic potentials (by regarding the time parameter as an extra coordinate in an extended Hilbert space). To perform the perturbative investigation, the non-hermitian quantum-mechanical framework - and specifically the Complex-scaling transformation of the Schrödinger equation - was necessary which provides the natural environment for the consistent treatment of quasi-stationary states. The complex energy of the quasi-stationary state was obtained by the complex spectral calculation that is based on the diagonalization of the complex-scaled Hamiltonian. I derived a first-order (t,t')-perturbative, analytical formula within the non-hermitian framework, that gives the shift in the complex energy due to some external, not necessarily time-periodic driving of the system in a quasi-stationary state.

I specifically investigated the limitations of applying characteristic gauges (the rE length-gauge and the pA radiation-gauge) in the interaction between intense coherent electromagnetic fields and matter, when examining a system characterized by quasi-stationary states within a non-Hermitian quantum mechanical framework. I found that upon describing quasi-stationary states in non-Hermitian quantum theory the phase transformation of the wave function that connects the different gauges cannot be performed due to the use of the c-product that is the non-hermitian inner product. Hence the radiation and length gauges could not be applied in the presented theoretical framework, the

physical gauge is the velocity gauge.

The super-intense laser-induced first-order (t,t')-perturbative correction to the decay width of the alpha cluster was calculated for the alpha-decaying isotones ^{212}Po, ^{214}Rn, ^{216}Ra, and ^{218}Th, considering different polarization states of the external Gaussian laser pulse. From numerical computations it was found that the relative change of the lifetime is non-zero for at least $I = 10^{20}$ $\frac{W}{cm^2}$ peak-intensity with small enough photon energy, e.g $E_{\mathrm{ph}} = 100$ eV, and is largest for ^{212}Po among the four isotones, while a similar systematics could be observed in the relative change of the lifetime as in the dependence of decay widths and alpha energies on Z^2/A. It was also found that the pulse length exerts a dominant influence on the shift in the imaginary energy, which decreases with an increasing number of cycles, while the effect is greater when considering circularly polarized laser field. It can be stated that, according to this non-hermitian quantum theory based model, the influence of some external laser pulse might produce decrement in the lifetime of an alpha-cluster.

The determination of the decay width of the quasi-stationary alpha cluster state through complex spectral calculations does not yield the total decay width, only that which is associated with the tunneling process. Thus, an important objective was the validation of the calculations, using the experimentally known decay lifetimes of specific isotone series. For this purpose, I investigated the even-even N=128, 130 and 132 isotonic chains with several nuclei and computed the mean-field tunneling widths by the complex spectral calculation method through numerical analysis. By fitting to experimental data, I proved that for the studied isotonic chains, the complex alpha cluster energy characterizing the mean-field tunneling is suitable to trace empirical trends that is manifested in the fulfillment of the Geiger-Nuttal law by the real and imaginary parts of the complex cluster energy. Hence, in this case, the decay is properly depicted by a non-perturbatively derived, single quantity.

As the final conclusion, the main scientific yield of my analysis is that by representing the alpha cluster as a quasi-stationary state with complex energy eigenvalue, a quantum-mechanically consistent description of the decay phenomenon can be given by means of applying the apparatus of non-hermitian quantum theory, which is naturally extendable to the analytical, perturbative mathematical treatment of the interaction of the alpha cluster with time-dependent laser pulses, by the (t,t')-formalism.

As a future direction, the developed framework is readily adaptable to study super-intense laser-induced modifications to, for example, spontaneous fission or nuclear compound reaction rates; and could also serve as a fundament to investigate laser-assisted alpha decay in even-odd deformed isotones, and

potentially longer lifetime nuclei (for which advanced numerical precision and the more nuanced description of clustering is required).

7

Theses of the dissertation

Thesis 1

I investigated the theoretical possibility of laser-assisted alpha decay in the presence of an intense laser field ($I \geq 10^{19}$ W/cm^2) assuming a plane-wave laser. In the non-relativistic and long-wavelength approximation, using mean-field nuclear models, I calculated the relative change ($\mathcal{R} = \frac{\Gamma^{\text{las}}}{\Gamma}$) in the decay width ($\Gamma$) valid in the Wentzel-Kramers-Brillouin (WKB) approximation for the alpha-decaying isotope ^{210}Po in the Henneberger picture. I examined the dependence of $\mathcal{R}$ on the frequency (ω) and intensity (I) of the external laser field for both circularly and linearly polarized laser fields. I demonstrated that, for circularly polarized lasers, depending on the free parameters of the Woods-Saxon nuclear potential, the estimated zero-order value of the ratio lies between $\mathcal{R} = 30$ and $\mathcal{R} = 123$, indicating that the effect of the intense laser field on the decay width is already significant at the zeroth order of the Fourier expansion.

Related publication: [D. Kis et al., 2018]

Thesis 2

I developed a general method suitable for determining the change in the complex spectrum of a quasi-bound system in the leading order of perturbation theory in the presence of a non-periodic time-dependent potential. By combining the (t, t')-formalism with a numerical discretization method for determining the complex energy spectrum, I derived an analytical, closed formula for the Floquet-type energy eigenvalue correction $\left(\epsilon^{(1)}\right)$ in the leading order of perturbation theory, which can be trivially projected onto the actual energy correction. As a result of the method, I determined the change in the imaginary energy, interpreted as the change in the lifetime of the state, caused by different time-dependent Gaussian-type perturbing potentials.

Related publication: [Szilvasi et al., 2022]

Thesis 3

I investigated the perturbative effect of an intense laser pulse, represented by a minimally coupled classical vector potential characterized by a Gaussian envelope function, on a quasi-bound system described by a special Gaussian-type potential barrier, in terms of the complex energy eigenvalue of the decaying system. Using the (t, t')-perturbation theory, I derived a general analytical formula for the first-order complex-energy correction, applicable to decaying systems described by continuous analytical potentials, in the field of either linearly or circularly polarized laser pulses. I established that, in the calculation of the first-order (t, t')-perturbative complex-energy correction, the non-zero matrix element contribution arises from the quadratic term in the vector potential $\left(\mathbf{A}^2\right)$ instead of the term proportional to $\mathbf{pA}$ that regularly appears in electromagnetic interactions.

Related publication: [R. Szilvási et al., 2023]

Thesis 4

I demonstrated that the non-Hermitian description of quasi-bound states interacting with an intense laser field, characterized by a classical vector potential, and specifically the application of the c-product, excludes the validity of the special ($\mathbf{pA}$) and ($\mathbf{rE}$) gauges for this problem. Furthermore, the "velocity-gauge" can be considered a physical gauge, consistent with the general description of systems interacting with intense laser fields under specific approximations (LWA and non-relativistic). I showed that the mathematical reason behind this is the requirement to apply the c-product on the complex-scaled system, which leads to a violation of the phase symmetry of the wave function. Consequently, the phase transformations of the wave function, as required by the full gauge symmetry, are only valid to a limited extent.

Related publication: [R. Szilvási et al., 2023]

Thesis 5

I performed an approximation of the complex energy spectrum of the Hamiltonian describing the quasi-stationary alpha-cluster state and the residual nucleus system, considering different mean-field nuclear potentials—specifically, the Woods-Saxon potential coupled to a Coulomb barrier and a Woods-Saxon corrected harmonic oscillator potential. Through a detailed analysis of the harmonic oscillator basis functions and the nuclear potential parameters, I identified the alpha energy (E_α) of the ^{212}Po alpha-decaying isotope with a numerical precision

of approximately 1%. Furthermore, I determined the decay width characterizing the quasi-stationary state and demonstrated its relation to the total decay width of alpha decay.

Related publication: [Szilvasi et al., 2024]

Thesis 6

I employed the analytical, complex Floquet type, first-order perturbative, non-relativistic energy-correction formula derived to laser pulses for the alpha-decaying isotones ^{212}Po, ^{214}Rn, ^{216}Ra, and ^{218}Th. I explored the dependence of the relative change of the lifetime on the key control parameters of the laser pulse, including peak intensity, photon energy, pulse duration, and phase shift. It was found that the pulse length exerts a dominant influence on the shift in the imaginary energy, which decreases with an increasing number of cycles. Additionally, the combined values of peak intensity and photon energy jointly determine the magnitude of this change. I provided an estimate of the boundaries of the non-relativistic approximation's validity in the context of alpha-cluster interactions with super-intense laser pulses. The results indicate that, at a photon energy of 100 eV, a peak intensity of 10^{24} W/cm^2 is still permissible, and the computed relative change of the lifetime is largest for ^{212}Po among the four isotones.

Related publication: [Szilvasi et al., 2024]

Thesis 7

In the non-Hermitian model framework I developed, I determined the complex energy eigenvalue, with particular emphasis on the imaginary part, Γ, for short lifetime nuclei in the isotone series with $N = 128$, 130, and 132. I demonstrated that for the $N = 128$ isotone series, the ratio of the calculated Γ values to the experimentally known total decay widths (Γ^{decay}) is constant within 4% accuracy. This consistency confirms that for these isotonic nuclei, the dominant contribution to the difference in the decay widths, in the alpha-cluster and residual nucleus system is due to changes in the Coulomb barrier induced by the protons. Based on this, I provided an estimate for the half-life of the yet unobserved uranium isotope with $Z = 92$, $A = 220$, yielding $T = 141.7 \pm 5.3$ ns. I concluded that for alpha-decaying isotones, the empirical nature of the Geiger-Nuttall law can be adequately described by a single, non-perturbatively calculated quantity, the complex energy of the quasi-bound state describing the alpha cluster.

Related publication: [Réka Szilvási et al., 2025]

This page intentionally left blank.

Bibliography

Aguilar, J. and J. M. Combes (1971). "Comm. Math. Phys." In: *Comm. Math. Phys.* 22, p. 269.

Bai, D., D. Deng, and Z. Ren (2018). "Charged particle emissions in high-frequency alternative electric fields". In: *Nuclear Physics A* 976, pp. 23–32. DOI: 10.1016/j.nuclphysa.2018.05.003.

Balslev, E. and J. M. Combes (1971). "Comm. Math. Phys." In: *Comm. Math. Phys.* 22, p. 280.

Basu, D. N. (2003). "Nuclear alpha decay half-lives and barrier tunneling". In: *Phys. Lett. B* 566, p. 90.

Bengtsson, J., E. Lindroth, and S. Selsto (2008a). "Phys. Rev. A". In: *Phys. Rev. A* 78, p. 032502.

Bengtsson, J., E. Lindroth, and S. Selstø (Sept. 2008b). "Time-dependent approach to resonances in the hydrogen negative ion". In: *Phys. Rev. A* 78.3, p. 032502. DOI: 10.1103/PhysRevA.78.032502.

Biswas, S. (1949). "Title of the article". In: *Phys. Rev.* 75, p. 530.

Bronshtein, I. N. and K. A. Semendyayev (1985). *Handbook of Mathematics*. Leipzig: Verlag Harri Deutsch.

Brown, B. A. (1992). "Title of the article". In: *Phys. Rev. C* 46, p. 811.

Buck, B., A. C. Merchant, and S. M. Perez (1992). "Phys. Rev. C". In: *Phys. Rev. C* 45.4.

Chu, S. I. and D. A. Telnov (Jan. 2004a). "Beyond the Born-Oppenheimer approximation: Multidimensional potential energy surfaces and nuclear quantum dynamics". In: *Phys. Rep.* 390.1, pp. 1–102. DOI: 10.1016/j.physrep.2003.10.001.

— (2004b). "Phys. Rep." In: *Phys. Rep.* 390, p. 1.

Csótó, A. et al. (Apr. 1990). "Back-rotation of the wave function in the complex scaling method". In: *Phys. Rev. A* 41.4, pp. 3469–3473. DOI: 10.1103/PhysRevA.41.3469. URL: https://doi.org/10.1103/PhysRevA.41.3469.

Delion, D. S. (2010). *Theory of Particle and Cluster Emission*. Springer.

Delion, D. S. and S. A. Ghinescu (2017). "Phys. Rev. Lett." In: *Phys. Rev. Lett.* 119, p. 202501.

Della Picca, R. et al. (2016). "Phys. Rev. A". In: *Phys. Rev. A* 93, p. 023419.

Duarte, S. B. et al. (2002). "Nuclear decay data for alpha emissions". In: *At. Data Nucl. Data Tables* 80, p. 235.

Dumitrescu, A. and D. S. Delion (2023). "Phys. Rev. C". In: *Phys. Rev. C* 107, p. 024302.

Elander, N. and E. Yarevsky (1998). "Phys. Rev. A". In: *Phys. Rev. A* 57, p. 3119.

Extreme Light Infrastructure (ELI) (2011). www.eli-np.org; www.eli-hu.hu. ELI-ALPS Research Institute.

Faisal, F. H. and G. Schlegel (2005). "J. Phys. B". In: *J. Phys. B* 38, p. L223.

— (2006). "J. Mod. Opt." In: *J. Mod. Opt.* 53, p. 207.

Firestone, R. B. and V. S. Shirley (1996). *Table of Isotopes*. 8th. New York: Wiley.

Froman, P. O. (1957). "Title of the article". In: *Mat. Fys. Medd. K. Dan. Vidensk. Selsk.* 1, p. 3.

Gambhir, Y. K., A. Bhagwat, and M. Gupta (2005). "Alpha decay half-lives of heavy and superheavy nuclei". In: *Phys. Rev. C* 71, p. 037301.

Gamow, G. (1928). "Z. Phys." In: *Z. Phys.* 51, p. 204.

El-Ganainy, R., K. Makris, M. Khajavikhan, et al. (2018). "Non-Hermitian physics and PT symmetry". In: *Nature Physics* 14, pp. 11–19. DOI: 10.1038/nphys4323. URL: https://doi.org/10.1038/nphys4323.

Gilary, I. and N. Moiseyev (2002). "Phys. Rev A". In: *Physical Review A* 66, p. 063415.

Gupta, R. K., S. Kumar, and W. Greiner (2002). "Alpha-decay chains of superheavy elements". In: *Phys. Rev. C* 65, p. 024601.

Gurvitz, S. A. and G. Kalbermann (1987). "Phys. Rev. Lett." In: *Phys. Rev. Lett.* 59, p. 262.

Hatsukawa, Y., H. Nakahara, and D. C. Hoffman (1990). "Title of the article". In: *Phys. Rev. C* 42, p. 674.

Henneberger, W. C. (1968). "Phys. Rev. Lett." In: *Physical Review Letters* 21, p. 838.

Horn, H. M. Van and E. E. Salpeter (1966). "Equation of State and Crystallization of Stellar Matter". In: *Physical Review* 157, pp. 751–758.

Horner, D. A. et al. (2007). "Phys. Rev. A". In: *Phys. Rev. A* 76, 030701(R).

Jolicard, G. and E. Austin (1985). "Chem. Phys. Lett." In: *Chem. Phys. Lett.* 121, p. 106.

Kalbermann, G. (2008). "Phy. Rev. C". In: *Phys. Rev. C* 77, 041601(R).

Kalman, P. (1991). "Phys. Rev. A". In: *Phys. Rev. A* 43, p. 2603.

Kalman, P. and J. Bergou (1986). "Phys. Rev. C". In: *Phys. Rev. C* 34, p. 1024.

Keller, K. A. and H. Münzel (1972). "Title of the article". In: *Z. Phys.* 255, p. 419.

Kis, D. and R. Szilvasi (2018). "J. Phys. G: Nucl. Part. Phys." In: *J. Phys. G: Nucl. Part. Phys.* 45, p. 045103.

Kis, D. et al. (2010). "Phys. Rev. A". In: *Phys. Rev. A* 81, p. 013421.

Kis, Dániel Péter (2013). "Magfizikai folyamatok intenzív lézertében doktori értekezés". Ph.D. thesis. Budapest, Hungary: Budapesti Műszaki és Gazdaságtudományi Egyetem.

Lovas, R. G. et al. (1998). "Phys. Rep." In: *Phys. Rep.* 294, p. 265.

M. Sargent, M. O. Scully and W. E. Lamb (1974). *Laser Physics*. Addison-Wesley Publishing Company Inc., pp. 15–16. ISBN: 0-201-06904-0.

McCurdy, C. W., T. N. Rescigno, and D. Byrum (1997). "Phys. Rev. A". In: *Phys. Rev. A* 56, p. 1958.

Messiah, A. (1966). *Quantum Mechanics*. 5th. Vol. 1. New York: Wiley.

Misicu, S. and M. Rizea (2016). "Open Phys." In: *Open Phys.* 14, pp. 81–7.

Mişicu, Ş. and M. Rizea (2013a). "Study on nuclear structure effects in α-decay". In: *Journal of Physics G: Nuclear and Particle Physics* 40, p. 095101. DOI: 10.1088/0954-3899/40/9/095101.

— (2013b). "-decay in ultra-intense laser fields". In: *Journal of Physics G: Nuclear and Particle Physics* 40, p. 095101. DOI: 10.1088/0954-3899/40/9/095101.

Mohr, P. (2006). "Alpha decay of deformed nuclei". In: *Phys. Rev. C* 73, 031301(R).

Moiseyev, N. (2011). *Non-Hermitian Quantum Mechanics*. Cambridge University Press.

Moiseyev, Nimrod (2011). "Non-Hermitian Quantum Mechanics". In: Cambridge: Cambridge University Press. Chap. 6, p. 182.

Morales, F., C. W. McCurdy, and F. Martin (2006). "Phys. Rev. A". In: *Phys. Rev. A* 73, p. 014702.

Moshammer, R. et al. (2003). "Phys. Rev. Lett." In: *Phys. Rev. Lett.* 91, p. 113002.

Muga, J. G. et al. (2004). "Phys. Rep." In: *Phys. Rep.* 395, p. 357.

Myo, T. and K. Kato (2020a). "Prog. Theor. Exp. Phys". In: *Prog. Theor. Exp. Phys* 2015, p. 36.

— (2020b). "Prog. Theor. Exp. Phys." In: *Prog. Theor. Exp. Phys.* 2015.

Pálffy, A. and S. V. Popruzhenko (2020). "Laser-assisted decay in intense laser fields". In: *Phys. Rev. Lett.* 124.21, p. 212505. DOI: 10.1103/PhysRevLett.124.212505.

Peskin, U. and N. Moiseyev (Sept. 1993). "The solution of the time-dependent Schrödinger equation by the (t,t') method: Theory, computational algorithm and applications". In: *J. Chem. Phys.* 99.6, pp. 4590–4598. DOI: 10.1063/1.465635.

Pfeifer, P. and R. D. Levine (Dec. 1983). "Analysis of dynamical properties in phase space: Time evolution of the Wigner distribution for classically chaotic systems". In: *J. Chem. Phys.* 79.12, pp. 5512–5524. DOI: 10.1063/1.445684.

Poenaru, D. N., R. A. Gherghescu, and W. Greiner (2011). "Phys. Rev. C". In: *Phys. Rev. C* 83, p. 014601.

Poenaru, D. N., M. Ivascu, and D. Mazilu (1980). "Title of the article". In: *J. Phys. Lett.* 41, pp. L–589.

Qi, C. et al. (2009). "Phys. Rev. Lett." In: *Phys. Rev. Lett.* 103, p. 072501.

Qi, J. et al. (2019). "Alpha decay in intense laser fields: calculations using realistic nuclear potentials". In: *Physical Review C* 99, p. 044610. DOI: 10.1103/PhysRevC.99.044610.

Rehman, Z. U., N. Shabbir, S. Shafiq, et al. (2022). "Laser-assisted alpha decay in hydrogen-like Po-212". In: *European Physical Journal A* 58, p. 60. DOI: 10.1140/epja/s10050-022-00720-2.

Reiss, H. R. (2002). "Spectra of atoms at nonperturbative laser intensities". In: *Physical Review A* 65, p. 055405. DOI: 10.1103/PhysRevA.65.055405.

— (2008). "Phys. Rev. Lett." In: *Phys. Rev. Lett.* 101, p. 043002.

— (Feb. 2014). "Theoretical foundations of strong-field ionization". In: *Phys. Rev. A* 89.2, p. 022116. DOI: 10.1103/PhysRevA.89.022116.

— (2019). "Phys. Rev. A". In: *Phys. Rev. A* 100, p. 052105.

— (2021). "Eur. Phys. J. D". In: *Eur. Phys. J. D* 75, p. 158.

Rescigno, T. N. et al. (1997). "Phys. Rev. A". In: *Phys. Rev. A* 55, p. 4253.

Rowley, N., G. D. Jones, and M. W. Kermode (1992). "Deformation and alpha-decay anisotropies". In: *J. Phys. G* 18, p. 165.

Royer, G. (2000). "Title of the article". In: *J. Phys. G* 26, p. 1149.

Royer, G. and R. A. Gherghescu (2002). "Alpha emission and spontaneous fission through quasi-molecular shapes". In: *Nucl. Phys. A* 699, p. 479.

Sambe, H. (1973). "Phys. Rev. A". In: *Phys. Rev. A* 7, p. 2203.

Siegert, A. J. (1939). "Phys. Rev." In: *Phys. Rev.* 56, p. 750.

Szilvasi, Reka and Daniel P. Kis (2022). “J. Phys. A: Math. Theor.” In: *J. Phys. A: Math. Theor.* 55, p. 275301.

— (2024). “J. Phys. G: Nucl. Part. Phys.” In: *J. Phys. G: Nucl. Part. Phys.* 51, p. 055101.

Szilvási, R. and D. P. Kis (2023). “Laser-Assisted Reactions in Nuclear Systems”. In: *Results in Physics* 54, p. 107080.

Szilvási, Réka, István Andorfi, and Dániel P. Kis (2025). “Nucl. Phys. A”. In: *Nuclear Physics A* 1053. Published online in October 2024, p. 122968.

Taagepera, R. and M. Nurmia (1961). “Title of the article”. In: *Ann. Acad. Sci. Fenn., Ser. A, VI* 78, p. 1.

Varga, K., R. G. Lovas, and R. J. Liotta (1992). “Microscopic description of alpha decay”. In: *Phys. Rev. Lett.* 69, p. 37.

Viola, V. E. and G. T. Seaborg (1966). “Title of the article”. In: *J. Inorg. Nucl. Chem.* 28, p. 741.

Wapstra, A. H., G. J. Nijgh, and R. van Lieshout (1959). *Nuclear Spectroscopy Tables*. Amsterdam: North-Holland, p. 37.

Wickenhauser, M. et al. (2006). “Phys. Rev. A”. In: *Phys. Rev. A* 74, 041402(R).

Wiehle, R. et al. (2003). “Phys. Rev. A”. In: *Phys. Rev. A* 67, p. 063405.

Xu, C. and Z. Ren (2006). “Nucl. Phys. A”. In: *Nucl. Phys. A* 760, p. 303.

This page intentionally left blank.

Appendices

This page intentionally left blank.

A

Appendix A: Mathematical grounds of the complex scaling transformation

One can show that the general properties of the scaling operator have some crucial significance. Generally the scaling operator is unitary:

$$\hat{S}_\theta^{-1} = \hat{S}_{-\theta} = \hat{S}_\theta^*, \tag{A.1}$$

$$\hat{S}_\theta^{-1}\hat{S}_\theta = \hat{S}_\theta^*\hat{S}_\theta = \hat{I}. \tag{A.2}$$

By the use of a basis of square integrable functions (Φ, ϕ), it is straightforward to show that $\hat{S}_\theta$ is also self adjoint:

$$\int dq\Phi(q)\hat{S}_\theta^+\phi(q) = \int dq\phi(q)\hat{S}_\theta^*\Phi(q) = \int dq\Phi(q)\hat{S}_\theta\phi(q), \tag{A.3}$$

where the effect of the scaling function as the rotation into the complex plane on an eigenfunction of the Hamiltonian is written as:

$$\hat{S}_\theta\Psi(q) = e^{i\frac{\theta}{2}}\Psi(qe^{i\theta}). \tag{A.4}$$

As a consequence of the properties of the scaling operator, it is quite straightforward to prove that a Hermitian Hamilton operator ($\hat{H} = \hat{H}^+$) stops being self-adjoint after the complex scaling transformation has been performed, and this feature appears explicitly in the scaling angle:

$$\hat{H}_\theta = \hat{S}_\theta\hat{H}\hat{S}_\theta^{-1}, \tag{A.5}$$

$$\hat{H}_\theta = \hat{S}_\theta\hat{H}\hat{S}_{-\theta}. \tag{A.6}$$

Respectively $\hat{H}_{-\theta}$ can be written as:

$$\hat{H}_{-\theta} = \hat{S}_{-\theta}\hat{H}\hat{S}_\theta. \tag{A.7}$$

Utilizing the self-adjoint property of the scaling operator, one gets the followings for the adjoint of the complex scaled Hamiltonian:

$$\hat{H}_\theta^+ = (\hat{S}_\theta \hat{H} \hat{S}_{-\theta})^+ = \hat{S}_{-\theta}^+ \hat{H}^+ \hat{S}_\theta^+ = \hat{S}_{-\theta} \hat{H}^+ \hat{S}_\theta. \tag{A.8}$$

Since the unscaled Hamiltonian is considered to be self-adjoint ($\hat{H}^+ = \hat{H}$), this expression is exactly equals $\hat{H}_{-\theta}$, hence the non-Hermiticity of the scaled Hamiltonian is proved:

$$\hat{H}_\theta^+ = \hat{H}_{-\theta}. \tag{A.9}$$

One can ask how the complex scaled Hamiltonian, which is - according to the above proof - not self adjoint ($\hat{H}_\theta^+ = \hat{H}_{-\theta}$), operates on any square integrable functions - complex scaled resonance ($\Phi(q), \phi(q)$) and bound states (f, g) also. First, it is important to remember that for a complex scaled but otherwise Hermitian Hamiltonian the left and right (also complex scaled) eigenfunctions are the same. In this case the c-product is equivalent to the standard scalar product having the complex conjugate of the eigenfunctions as the bra state:

$$\langle \Phi(q)^* | \Phi(q) \rangle = \int_{allspace} dV \Phi(q) \Phi(q) = \left(\Phi(q) | \Phi(q) \right). \tag{A.10}$$

Again, this is only true for $\Phi(q), \phi(q)$ having complex eigenvalues, for bound states (f, g) that have real eigenenergies the standard scalar product applies. However, by complex scaling these bound states, it is essential to pay attention to the complex conjugation operation. Analytical continuation suggests that the complex conjugation operation must only be taken on terms which are complex regardless of the complex scaling of the coordinates! Once this operation is taken care of properly, the complex scaled bound states remain orthonormal with respect to the standard scalar product N. Moiseyev, 2011 :

$$\langle f | g \rangle = 1 \tag{A.11}$$

$$\langle f | g \rangle_\theta = 1. \tag{A.12}$$

These considerations are meticulously explicated in the referred monograph of Moiseyev N. Moiseyev, 2011 , throughout my work I do not deal with stationary bound states, only decaying quasi-stationary states. Deducing from the above arguments, one can simply define the effect of the complex-scaled Hamiltonian on the complex-scaled resonance eigenfunctions by the use of the standard norm:

$$\langle \Phi(q)^* | \hat{H}_\theta | \Phi(q) \rangle = \int_{allspace} dV \Phi(q) \hat{H}_\theta \Phi(q) = \left(\Phi(q) | \hat{H}_\theta | \Phi(q) \right), \tag{A.13}$$

$$\langle \Phi(q)^* | \hat{H}_\theta^+ | \phi(q) \rangle = \langle \phi(q)^* | \hat{H}_\theta^* | \Phi(q) \rangle , \tag{A.14}$$

recall that since the unscaled Hamiltonian - in our case - is Hermitian, the following $\hat{H}_\theta^* = \hat{H}_{-\theta}$ equality applies, for $\theta \to -\theta$:

$$\langle \Phi(q)^* | \hat{H}_\theta | \phi(q) \rangle = \langle \phi(q)^* | \hat{H}_\theta | \Phi(q) \rangle . \tag{A.15}$$

B

Appendix B: Brief explanation of the stationary solutions of the Floquet-type equation

The statement:

$$\chi(t;q,t')|_{t\equiv t'} = \Psi(q,t'), \tag{B.1}$$

where $\chi(t;q,t')$ is the solution of the following Schrödinger-like equation:

$$i\hbar\frac{\partial}{\partial t}\chi(t;q,t') = \hat{H}_F\chi(t;q,t'), \tag{B.2}$$

the operator $\hat{H}_F$ is a Floquet-type operator, and is the generator of the (B.2) t time evolution in the extended Hilbert space:

$$\hat{H}_F(q,t') = \hat{H}(q,t') - i\hbar\frac{\partial}{\partial t'}. \tag{B.3}$$

Projection (B.1) is a many-to-one projection, many solutions of equation (B.2) yield the same Ψ upon projecting. But the general t-dependent solution of equation (B.2) for a t'-dependent Hamiltonian can be written as the below t-evolution:

$$\chi(t;q,t') = \mathcal{T}exp\left(-\frac{i}{\hbar}\int_{t'-t}^{t'}\hat{H}(q,\tau)\mathrm{d}\tau\right)\chi(0;q,t'-t), \tag{B.4}$$

where $\mathcal{T}$ is the time-ordering operator. This reduces to the simple form for t'-independent Hamiltonians:

$$\chi(t;q,t') = exp\left(-\frac{i}{\hbar}\hat{H}(q,t')t\right)\chi(0;q,t'-t) = exp\left(-\frac{i}{\hbar}\hat{H}(q,t')t - t\frac{\partial}{\partial t'}\right)\chi(0;q,t'), \tag{B.5}$$

which shows that upon projecting $\chi(t;q,t')|_{t\equiv t'}$ is generated from the state $\chi(0;q,0)$ by a time evolution driven by the original Hamiltonian $\hat{H}$, and that this solution is actually t-independent! Thus $\chi(0;q,t')$, the stationary solution of the t-progress equation with $\hat{H}_F$ must satisfy the original Schrödinger equation with t' and $\hat{H}$ in order for it to give the required $\Psi(q,t')$, which is what we wanted!

C

Appendix C: The validation of the WKB approximation for Γ_0^{las}

One of the possible methods to calculate the imaginary part of the complex energy of the quasi-stationary state is the WKB approximation, which assumes purely central potential. For example the problem of alpha-decay is solved with complex energy method in WKB approximation in Kalbermann, 2008 . The derived Hamiltonian (5.16) which describes the laser modified barrier has non-central potential also, but basically it cannot be a problem, because the WKB approximation method in three dimensions was discussed by Horn and Salpeter Horn et al., 1966 for problems with an axis of symmetry, but the potentials need to be separable functions of the coordinates.

Naturally the derived formula for Γ_0^{las} is only valid if the WKB approximation is valid, respectively. To check this validity let us consider the following inequality Messiah, 1966

$$\frac{|m\hbar V'|}{|2m\,(V-E)\,|^{3/2}} << 1. \tag{C.1}$$

where V' is derived from V. In our case the potential is the laser-modified potential $V = V_{00}$, which has a transformed argument: $\mathbf{r} \rightarrow \mathbf{r} - \mathbf{S}(t)$. It can be seen that the argument is shifted by the space-dependent vector $\mathbf{S}$, that means the derived $V'(\mathbf{r} - \mathbf{S}(t))$ is the same as the original (laser-free) derived potential, $V'(\mathbf{r} - \mathbf{S}(t)) = V'(\mathbf{r})$. Because V_{00} is defined by the equation (5.17) the validity of the inequality requires numerical computations which show that $|V_{00} - E|$ is smaller than that of the laser-free case, furthermore V_{00} is less sharp than the laser-free potential V around the location of maximum (see Fig. 2), so $V'_{00} < V'$. Both actions overall lead to the inequality (C.1) remaining also valid in the presence of the laser field.